



15th ICRSS 2018

Polar Regions in Transformation -

Climatic Change and Anthropogenic Pressures

BOOK OF ABSTRACTS

Edited by Frank Günther, Guido Grosse, and Benjamin Jones

15th International Circumpolar Remote Sensing Symposium
10 – 14 September 2018, Potsdam, Germany

15th International Circumpolar Remote Sensing Symposium
Polar Regions in Transformation - Climatic Change and Anthropogenic Pressures

Book of Abstracts

Edited by Frank Günther, Guido Grosse and Benjamin M. Jones

Alfred Wegener Institute Helmholtz Centre for Polar and Marine Research

Recommended citation

Günther, F., Grosse, G., and Jones, B. M. (Eds.) (2018): 15th International Circumpolar Remote Sensing Symposium – Book of Abstracts, 10–14 September 2018, Potsdam, Germany. Bibliothek Wissenschaftspark Albert Einstein. doi:[10.2312/GFZ.LIS.2018.002](https://doi.org/10.2312/GFZ.LIS.2018.002).

Disclaimer and Copyright

Each author is responsible for the content of his or her abstract and has the copyright for his or her figures.

Imprint**Publisher**

Bibliothek Wissenschaftspark Albert Einstein
Telegrafenberg
14473 Potsdam
Published in Potsdam, Germany

Editors

Frank Günther
Guido Grosse
Benjamin M. Jones



Preface

Dear ICRSS Participant,

We are delighted to welcome you to Potsdam and present the conference proceedings of the 15th International Circumpolar Remote Sensing Symposium (ICRSS). This ICRSS conference series deals specifically with remote sensing applications in the polar environments, both Arctic and Antarctic. After being born in Yellowknife, Canada in 1990 it has alternated between North America and Europe on a biennial basis and now for the first time reaches Germany. The theme of the 15th ICRSS is “Polar Regions in Transformation – Climatic Change and Anthropogenic Pressures”. Earth’s Polar Regions, including high mountain regions outside the high latitudes, feature cold-climate environments characterized by unique landscapes, biota, and processes. Many of these features and dynamics are Cryosphere-driven and either are already subject to or have the potential for fundamental and rapid changes in a warming world. The myriad of Earth observation technologies provide crucial tools to understand and quantify these changes.

The 15th ICRSS in Potsdam is the largest in the conference series to date: About 100 registered participants come from 16 countries, demonstrating the true international character of this otherwise intimate but focused polar symposium. Together, with an engaged Local Organizing Committee and the International Scientific Committee, we organized 10 scientific sessions with 61 oral and 38 poster presentations, covering nearly all fields of Cryosphere research as well as research on northern vegetation and polar oceanography. The symposium program will be headlined by an exciting set of 7 keynote speakers highlighting the scientific frontiers in our research fields. About half of this year’s participants are early career scientist (graduate students or within 3 years following PhD completion) who will enjoy this symposium for the first time, while many of the senior participants have been frequent visitors to previous ICRSS. It is

great to see that this research community is growing with an influx of young researchers – we believe the future of remote sensing in Polar Regions is bright and exciting.

In Potsdam, as with previous ICRSS, we will strive to provide a platform for the exchange of current applied research and best practices, the presentation of new technology and further innovation, and the advancement of international co-operation in the circumpolar regions of the world. New to this ICRSS is the facilitation of several workshops at the end of the conference week that will involve discussions on some of the cutting edge research topics (polar ocean color, Arctic vegetation dynamics) as well as hands-on technical training for new and rapidly evolving remote sensing methods (InSAR subsidence measurements, point cloud data processing, Big Data processing infrastructure and approaches).

Without the help of many individuals the organization of this symposium would not have been possible: Big Thanks to Gabriela Schlaffer from AWI, everyone in the LOC and SOC, Marla Hood and Mary Whalen from the USGS for hosting the website, all the student assistants, our AWI administration folks, and the partners for the symposium event locations, logistics, and catering! We also wish to acknowledge the strong financial support by AWI and the important in-kind contributions by all our partners. We further thank all the external sponsors that helped making this event possible.

We are looking forward to providing you with a very positive and memorable event in a magical setting on the shores of the Havel River in Potsdam, Germany.

Guido Grosse & Benjamin M. Jones
Conference Chairs, 15th ICRSS 2018
Potsdam, Germany



Partners

The 15th ICRSS is made possible with the help and support from many national and int. partners.

 <p>ALFRED-WEGENER-INSTITUT HELMHOLTZ-ZENTRUM FÜR POLAR- UND MEERESFORSCHUNG</p> <p>Alfred Wegener Institute Helmholtz Centre for Polar and Marine Research</p>		
 <p>USGS</p>	 <p>University of Potsdam, Institute of Earth and Environmental Science</p>	 <p>German Research Centre for Geosciences</p>
 <p>proWissen Potsdam e.V.</p>	 <p>Geo.X</p>	



Local Organizing Committee

Sofia Antonova, U Heidelberg	Birgit Heim, AWI	Ingmar Nitze, AWI
Alison Beamish, AWI	Anna Irrgang, AWI	Alexandra Runge, AWI
Bodo Bookhagen, U Potsdam	Bennet Juhls, FU Berlin	Torsten Sachs, GFZ
Matthias Fuchs, AWI	Soraya Kaiser, AWI	Gabriela Schlaffer, AWI
Guido Grosse, AWI (<i>Conference Chair</i>)	Katrin Kohnert, GFZ	Lydia Stolpmann, AWI
Frank Günther, AWI	Sebastian Laboor, AWI	

Technical Support

Astrid Feuster, AWI (<i>payments</i>)	Dyke Scheidemann, AWI (<i>registration desk</i>)
Frank Günther, AWI (<i>proceedings</i>)	Gabriela Schlaffer, AWI (<i>technical organisation, registration desk</i>)
Marla Hood, USGS (<i>ICRSS website</i>)	Mary Whalen, USGS (<i>ICRSS website</i>)
Sebastian Laboor, AWI (<i>logos, graphics, signs, and maps; abstract submission and registration site</i>)	

International Scientific Committee

Annett Bartsch, bgeos	Daniel Hayes, U Maine
Astrid Bracher, AWI	Birgit Heim, AWI
Matthias Braun, U Erlangen-Nürnberg	Angelika Humbert, AWI
Bodo Bookhagen, U Potsdam	Benjamin Jones, UAF (<i>Conference Co-Chair</i>)
Gerald "JJ" Frost, ABR Inc.	Achim Roth, DLR
Guido Grosse, AWI (<i>Conference Chair</i>)	Torsten Sachs, GFZ
Antonie Haas, AWI	



Contents

Preface	i
Partners	ii
SPONSORS	1
PLENARIES	6
Progress in remote sensing reveals new insights on the impact of climate change on glaciers and rock glaciers on the Third Pole <i>T. Bolch</i>	7
TanDEM-X: Contribution to a better understanding of cryospheric applications <i>I. Hajnsek</i>	8
From Shelf Seas to Fram Strait: A changing Transpolar Drift System <i>T. Krumpen</i>	10
Ocean color of the Arctic Ocean <i>A. Matsuoka</i>	11
The 2017 Arctic Boreal Vulnerability Experiment (ABOVE) Airborne Campaign <i>C. E. Miller, P. C. Griffith, S. J. Goetz, L. Hoy, N. Pinto, I. McCubbin, A. Thorpe, M. Hofton, D. Hodkinson, C. Hansen, J. Woods, E. Larson, E. S. Kasischke, & H. A. Margolis</i>	12
A new raster version of the Circumpolar Arctic Vegetation Map (CAVM) <i>M. K. Reynolds & D. A. Walker</i>	13
Changing Polar Coasts and Deltas	15
Temporal variability of coastal retreat at Kharasavey area, Western Yamal Peninsula, the Kara Sea <i>N. G. Belova, A. V. Baranskaya, A. V. Novikova, N. N. Shabanova, & S. A. Ogorodov</i>	16
The spatial extent of Arctic river deltas: Version 1.0 of the Arctic river delta data set <i>M. Fuchs, I. Nitze & G. Grosse</i>	17
Impacts of coastal dynamics on the socio-economic component of the Yukon coast, western Canadian Arctic <i>A. M. Irrgang, H. Lantuit, R. R. Gordon, A. Piskor, & G. K. Manson</i>	18
High temporal and spatial resolution satellite image observations for the past decade highlight complexities associated with permafrost coastal bluff erosion in the Arctic <i>B. M. Jones, D. L. Bull, L. M. Farquharson, C. A. Baughman, C. D. Arp, G. Grosse, F. Günther, M. Kanevskiy, G. Iwahana, A. Bondurant, R. M. Buzard, T. Sachs, I. Nitze, J. L. Kasper, J. M. Frederick, M. Thomas, A. Mota, C. Jones, J. Roberts, S. Dallimore, C. Tweedie, C. Maio, D. H. Mann, B. Richmond, A. Gibbs, M. Xiao, & V. E. Romanovsky</i>	19



Coastal destruction in the western and eastern-most occurrence of tabular ground ice in the Eurasian Arctic
A. I. Kizyakov, F. Günther, M. V. Zimin, A. V. Sonyushkin, & S. Wetterich 20

Dynamics of permafrost coasts of Baydaratskaya Bay (Kara Sea) based on multi-temporal remote sensing data
A. Novikova, N. Belova, A. Baranskaya, A. Maslakov, D. Aleksyutina, N. Shabanova, E. Zelenin, & S. Ogorodov 21

Floating Ice: Sea, River, and Lake Ice 22

Influence of lake ice formation and break-up on ASCAT backscatter
H. Bergstedt, A. Bartsch, B. M. Jones, & C. Duguay 23

Eighteen-year MODIS detection of ice breakup on Alaskan rivers wider than 150 m
W. Dolan, T. Pavelsky, S. Zhang, & X. Yang 24

Remote sensing; a key tool for understanding change in carbon storage on polar seabeds
C. Held, A. Fleming, D. K. A. Barnes, C. J. Sands, B. Moreno, R. Downey, M. Paulsen, C. Moreau, & N. Bax 25

Remote Sensing of Arctic Sea Ice Thickness with Radar Altimeters
S. Hendricks, R. Ricker, S. Paul, & C. Haas 26

Microwave emission of sea ice – variability of permittivity and transmissivity at interfaces
M. Huntemann & G. Spreen 27

Towards a reliable method for measuring arctic sea ice thickness from satellite radar altimetry during summer months
J. Landy, A. Komarov, & C. Haas 29

Satellite-derived changes of ice-free period in the Barents and Kara Seas coastal zones
N. Shabanova & P. Shabanov 31

Operational Synthetic Aperture Radar based sea ice classification
S. Singha 32

Glaciers and Ice Sheets 33

Detecting and monitoring ice-shelf basal mass balance in Dronning Maud Land, East Antarctica
S. Berger, V. Helm, N. Neckel, N. Dörr, R. Drews, F. Pattyn, & O. Eisen 34

Sub-glacial bedrock topography of Austfonna, Svalbard derived from potential field modeling
M.-A. Dumais & M. Brönnner 35

Decadal changes of glacial extents and snowline altitude of the Batura Glacier, Karakoram: Classification and spectral unmixing of remote sensing data
A. Muetting, B. Bookhagen, & T. Smith 36

Multi-temporal analysis of the Greenland Ice Sheet based on TanDEM-X DEM data between 2010 and 2017
C. Wohlfart, S. Abdullahi, B. Wessel, M. Huber, T. Leichtle, & A. Roth 37



New Sensors and Operational Services	38
A webcam network, open data and free toolbox for monitoring phenology and snow cover <i>A. N. Arslan, C. M. Tanis, & M. Peltoniemi</i>	39
Circumpolar to global remote sensing of permafrost – contributions of ESA DUE GlobPermafrost to a permafrost information system <i>A. Bartsch, G. Grosse, A. Kääb, S. Westermann, T. Strozzi, A. Wiesmann, C. Duguay, F. M. Seifert, J. Obu, I. Nitze, B. Heim, A. Haas, S. Laboor, S. Muster, & B. Widhalm</i>	40
FireBIRD- High Dynamic Range Thermal Infrared Satellite Systems for hot and cold temperature environments <i>C. Fischer, T. Bucher, T. Säuberlich, & W. Halle</i>	41
A customized airborne optical remote sensing system for polar environments <i>T. Bucher, J. Brauchle, & D. Steinhage</i>	42
PerSys – WebGIS-based permafrost data visualisation system for ESA GlobPermafrost <i>A. Haas, A. Walter, B. Heim, G. Grosse, S. Muster, S. Laboor, A. Immerz, C. Schäfer-Neth, A. Bartsch, & F. M. Seifert</i>	43
Remote sensing the ocean-induced magnetic field in polar regions <i>C. Irrgang, J. Saynisch, J. Petereit, M. Thomas</i>	44
The Data Catalogue of the Permafrost Information System PerSys – An Open Access geospatial data dissemination and visualization portal for products from ESA DUE GlobPermafrost <i>S. Laboor, G. Grosse, S. Muster, B. Heim, A. Haas, C. Schäfer-Neth, I. Nitze, A. Bartsch, & K. Elger</i>	45
From basic research to application – technology transfer from AWI <i>E. J. Sauter, L. Rabenstein, B. Heim, & E. Precht</i>	47
The EUMETSAT Network of Satellite Application Facilities (SAF Network): Operational data and software products for polar regions <i>L. Schüller</i>	49
The role of satellite-based information to inform change in arctic ecosystems at the Canadian High Arctic Research Station, Nunavut <i>J. Wagner & D. McLennan</i>	50
Observing Permafrost State and Changes	51
Thaw subsidence of a yedoma landscape in northern Siberia, measured <i>in situ</i> and estimated from TerraSAR-X interferometry <i>S. Antonova, H. Sudhaus, T. Strozzi, S. Zwieback, A. Kääb, B. Heim, M. Langer, N. Bornemann, & J. Boike</i>	52
Predicting potential permafrost distribution based on land surface variables and remote sensing data in Southern Carpathians (Romania) <i>F. Sîrbu, F. Ardelean, & A. Onaca</i>	53



The impact of exceptional warming conditions in 2016 on central Yamal – observations in situ and from space
A. Bartsch, T. Strozzi, M. Leibman, B. Widhalm, A. Khomutov, D. Mullanurov, & A. Gubarkov . 54

Large-scale monitoring of rapid permafrost thaw with satellite radar Interferometry
P. Bernhard, S. Zwieback, & I. Hajnsek 55

Global-scale mapping of periglacial landforms on Earth and Mars using deep convolutional networks
L. Fanara, E. Hauber, R. Hänsch, K. Gwinner, J. Oberst, A. Morgenstern, & G. Grosse 57

Multi-model assessment of climate change impacts on Arctic infrastructure
A. Gädeke, K. Thonicke, J. Boike, E. J. Burke, J. Chang, P. Ciais, M. Langer, S. Ostberg, S. Schaphoff, H. Müller-Schmied, S. Seneviratne, & W. Thiery 58

Polarimetric D-InSAR for ground deformation estimation over permafrost environment
F. Garestier, S. Guillaso, E. Zakharova, A. Kouraev, & R. Desyatkin 59

Remote sensing of drained thermokarst lake basin successions
G. Grosse, I. Nitze, B. M. Jones, J. Wolter, A. Runge, M. Fuchs, Frank Günther, A. Veremeeva, & S. Westermann 60

Spatial analysis of periglacial processes and landforms on Hurd Peninsula, Livingston Island, Antarctica, using advanced SAR techniques
S. Guillaso, T. Schmid, & J. López-Martínez 61

Repeat terrestrial LiDAR for quantification of extensive thaw subsidence within different tundra vegetation groups
F. Günther, G. Grosse, G. T. Maximov, A. Veremeeva, A. Fricke, M. Haghshenas Haghghi, & A. I. Kizyakov 62

Measuring elevation change in arctic permafrost landscape using SAR interferometry
M. H. Haghghi, F. Günther, B. Heim, & M. Motagh 63

Linking tundra landscapes with its disturbance history. A ThawTrendr pilot study in Nome, Alaska.
W. Hantson, S. Serbin, J. Kilbride, & D. Hayes 64

Thawtrendr: Characterizing patterns of disturbance history in permafrost landscapes using Landsat time-series segmentation algorithms
D. J. Hayes, W. Hantson, R. E. Kennedy, B. M. Jones, S. Serbin, & G. Grosse 65

Thermokarst lake monitoring on the Bykovsky Peninsula using high-resolution remote sensing data
T. Henning, F. Günther, A. I. Kizyakov, & G. Grosse 66

Identifying erosional hot spots around thermokarst lakes using RapidEye imagery
S. Kaiser, T. Schneider von Deimling, S. Jacobi, R. Mommertz, & M. Langer 68

Representation of mean annual ground temperature by satellite derived surface status
C. Kroisleitner, A. Bartsch, & H. Bergstedt 69

Relief modification caused by formation of gas-emission craters, remote-sensing and field studies
M. O. Leibman, A. I. Kizyakov, M. V. Zimin, E. A. Babkina, Yu. A. Dvornikov, R. R. Khairullin, & A. V. Khomutov 70



Remote-sensing based global map of permafrost <i>J. Obu, S. Westermann, A. Kääh, & A. Bartsch</i>	71
Ground displacement in permafrost terrain from Sentinel-1 time-series SAR interferometry <i>K. Teshebaeva & Ko J. van Huissteden</i>	72
UAS remote sensing in detection of the rapid decay of palsa mires <i>M. Verdonen, T. Kumpula, & P. Korpelainen</i>	73
Analyzing tundra vegetation characteristics for terrestrial LiDAR surveys of permafrost thaw subsidence <i>A. Veremeeva, F. Günther, A. Kizyakov, & G. Grosse</i>	74
Sensitivity of soil freezing process to snow cover changes and permafrost active layer dynamics in Arctic Alaska <i>Y. Yi, J. S. Kimball, R. H. Chen, M. Moghaddam, & C. Miller</i>	76
Investigating the decadal changes of frozen ground at Resolute Bay in the Canadian High Arctic through surface elevation changes measured by GPS Interferometric Reflectometry <i>J. Zhang, L. Liu, & Y. Hu</i>	78
Oceanography of Polar Seas	79
Validation of ocean colour products for the Arctic Ocean <i>A. Bracher, Y. Liu, R. Goncalves-Araujo, I. Peeken, & T. Dinter</i>	80
Analyzing arctic seasonal phytoplankton dynamics with MERIS satellite fluorescence <i>J. R. El Kassar, B. Juhls, R. Preusker, & J. Fischer</i>	82
Measuring bio-optical properties in coastal waters of the Laptev Sea and Lena River for the improvement of Ocean Color algorithms <i>B. Juhls, P. P. Overduin, & J. Fischer</i>	83
Assessing nearshore sediment and sea surface temperature dynamics using Landsat satellite imagery at Herschel Island, western Canadian Arctic <i>K. P. Klein, H. Lantuit, B. Heim, F. Fell, D. J. Jong, & J. E. Vonk</i>	84
Highly resolved data set on different phytoplankton pigments and functional types retrieved from underway spectrophotometry in the Fram Strait <i>Y. Liu, E. Boss, A. Chase, Y. Pan, H. Xi, E. Nöthig, S. Wiegmann, & A. Bracher</i>	85
Phytoplankton diversity in the Southern Ocean retrieved from hyperspectral satellite observations <i>J. Oelker, S.N. Losa, M.A. Soppa, T. Dinter, V.V. Rozanov, A. Richter, J.P. Burrows, & A. Bracher</i>	86
First steps towards assessing the radiation budget in the shelf areas of the Laptev Sea by remote sensing and radiative transfer modelling <i>V. Pefanis, M. A. Soppa, S. Hellmann, J. Hölemann, M. A. Janout, F. Martynov, B. Heim, V. Rozanov, S. Loza, T. Dinter, & A. Bracher</i>	87
Spatio-temporal patterns of the carbon-to-chlorophyll ratio of natural phytoplankton communities in the Southern Ocean <i>C. M. Robinson, N. Schuback, T. J. Ryan-Keogh, W. Moutier, S. J. Thomalla, & D. Antoine</i> . . .	88
Reassessing satellite algorithms for phytoplankton in the Southern Ocean <i>C. M. Robinson, N. Schuback, T. J. Ryan-Keogh, W. Moutier, S. J. Thomalla, & D. Antoine</i> . . .	89



Polar Lake Dynamics	91
Terrestrial CDOM in lakes of Yamal Peninsula: Connection to lake and lake catchment properties – a remote sensing study <i>Y. Dvornikov, M. Leibman, B. Heim, A. Bartsch, U. Herzschuh, T. Skorospekhova, I. Fedorova, A. Khomutov, B. Widhalm, A. Gubarkov, & S. Rößler</i>	92
Detection of recent permafrost region disturbances across the Arctic and Subarctic with Landsat time-series and machine-learning classification <i>I. Nitze, G. Grosse, B. M. Jones, V. E. Romanovsky, & J. Boike</i>	93
Towards understanding the contribution of permafrost waterbodies to methane emissions on a regional scale using aircraft measurements and remote sensing data <i>K. Kohnert, B. Juhls, S. Muster, S. Antonova, A. Serafimovich, S. Metzger, J. Hartmann, & T. Sachs</i>	94
Decadal time-scale controls on catastrophic lake drainage in northern Alaska <i>M. J. Lara, B. M. Jones, & H. Genet</i>	95
Using Google Earth Engine to examine water and permafrost <i>E. D. Trochim & G. Donchyts</i>	96
Polar Land Cover and Vegetation	97
Estimation of forest properties in the treeline zone using TanDEM-X and airborne laser scanning data <i>S. Antonova, C. Thiel, B. Höfle, S. Marx, K. Anders, & J. Boike</i>	98
Evaluation of a Metop ASCAT derived surface soil moisture product in the Lena Delta <i>E. Högström, B. Heim, A. Bartsch, H. Bergstedt, & G. Pointner</i>	99
Influence of litter and non-vascular components on the spatial aggregation of hyperspectral data in a low-Arctic ecosystem <i>A. Beamish, M. Brell, S. Chabrillat, N. Coops, & B. Heim</i>	100
ArcticDEM terrain roughness and Structure from Motion for forest structure analysis and biomass quantification in the tundra-taiga ecotone (Siberia) <i>F. Brieger, S. Kruse, B. Heim, B. Bookhagen, I. Shevtsova, & U. Herzschuh</i>	101
Ecosystem functional diversity of the circumpolar arctic tundra <i>H. Epstein, A. Armstrong, D. Alcaraz-Segura, E. Montefiori, A. Castro, M. Reynolds, & Q. Yu</i>	102
Retrospective remote sensing reveals accelerating rates of permafrost degradation on Alaska's Yukon-Kuskokwim Delta: Bellwether of the future Arctic, or black sheep? <i>G. V. Frost, M. J. Macander, M. T. Jorgenson, M. A. Whitley, & D. Dissing</i>	104
Analysis of permafrost taiga by means of X/C-Bands SAR imagery <i>S. Guillaso & F. Garestier</i>	106



Spatial and temporal variability at the Toolik Lake vegetation grid (Alaska) <i>B. Heim, A. Beamish, D. A. Walker, H. E. Epstein, U. Herzschuh, T. Sachs, S. Chabrillat, M. Brell, S. Rößler, & M. Buchhorn</i>	107
Viability of interferogram stacking for change detection in arctic environments using ESA Sentinel-1 Data <i>M. Hovemyr & I. A. Brown</i>	108
Morphostratigraphy investigation of alas on Kurungnakh Island (the Lena River Delta) by means of remote sensing UAV data and field studies <i>A. A. Kartoziia</i>	109
Progress towards pan-arctic shrub mapping using spectral, radar, and stereo metrics <i>M. J. Macander, G. V. Frost, P. M. Montesano, C. S. R. Neigh, & P. R. Nelson</i>	110
Urban heat island effects in the northern high latitudes as revealed by remote sensing <i>V. Miles & I. Esau</i>	112
Quantifying patterns of forest structure across a circumpolar biome boundary <i>P. M. Montesano & C. S. R. Neigh</i>	113
3D satellite observations North American boreal forest growth <i>C. S. R. Neigh, P. M. Montesano, J. O. Sexton, M. Feng, S. Channan, N. Carvalhais, M. Forkel, L. Calle, & B. Poulter</i>	114
Mapping vegetation in a north-boreal fen in very-high and ultra-high spatial resolution <i>A. Räsänen, S. Juutinen, & T. Virtanen</i>	115
Comparing spectral characteristics of Landsat-8 and Sentinel-2 data for Arctic permafrost regions <i>A. Runge & G. Grosse</i>	116
Changes in land cover classes of north-eastern Siberia between 2001 and 2016 inferred from combining field data with Landsat spectral ratio indices <i>I. Shevtsova, B. Heim, S. Kruse, & U. Herzschuh</i>	117
Zackenbergl Valley seen by TerraSAR-X – land cover and moisture conditions <i>J. Sobiech-Wolf, T. Ullmann, A. Roth, & W. Dierking</i>	119
More lightning in the high latitudes: implications for fire and carbon <i>S. Veraverbeke, Y. Chen, B. M. Rogers, M. L. Goulden, R. R. Jandt, C. E. Miller, E. B. Wiggins, & J. T. Randerson</i>	120
Remote Sensing of the Polar Atmosphere	121
A new algorithm for cloud identification over the Arctic using AATSR/SLSTR and its application for ACLOUD/PASCAL campaigns <i>S. Jafariserajehlou, L. Mei, M. Vountas, V. V. Rozanov, & J. P. Burrows</i>	122
Understanding of polar atmospheric dynamics by measurements of surface air pressure using O2-band differential absorption radar <i>B. Lin, Q. Min, S. Harrah, Y. Hu, & R. Lawrence</i>	123



Characteristics and genesis conditions of January polar lows: Microwave satellites, radiative transfer simulations and arctic system reanalysis
A. Radovan, S. Crewell, M. Mech, & A. Rinke 124

Snow Trends 125

Quantifying spring snow cover evolution on Kurungnakh Island, North Siberia
T. Hainbach, A. Morgenstern, & B. Heim 126

Fractional snow cover area from terrestrial photography in Svalbard Islands (Norway)
R. Salzano & R. Salvatori 127

Local and regional trends in snow cover from a 34-year time series of satellite observations
R. Solberg, Ø. Rudjord, A.-B. Salberg, M. A. Killie, S. Eastwood, & L.-A. Breivik 128

TerraSAR-X time series fills a gap in high spatiotemporal monitoring of snowmelt in small Arctic catchments
S. Stettner, H. Lantuit, B. Heim, B. Rabus, J. Eppler, A. Roth, & A. Bartsch 129

Author Index 130

Picture Credits 133

Appendix 134

Helmholtz Climate Initiative Regional Climate Change (REKLIM)
. 135

IEEE Geoscience and Remote Sensing Society
. 137

EUMETSAT
. 138



SPONSORS



The 15th ICRSS is made possible through the financial and in-kind support of sponsors.

Ice Shelf Sponsors



Alfred Wegener Institute Helmholtz Centre for Polar and Marine Research

As the Helmholtz Centre for Polar and Marine Research, the Alfred Wegener Institute is primarily active in the cold and temperate regions of the world. Working together with numerous national and international partners, we are actively involved in unravelling the complex processes at work in the “Earth System”. Our planet is undergoing fundamental climate change; the polar regions and the oceans, which play central roles in the global climate system, are in flux. How will planet Earth evolve? Do the phenomena we’re observing represent short-term fluctuations or long-term trends? Polar and marine research has always been a fascinating scientific challenge; today it is also research into the future.

www.awi.de



Helmholtz Climate Initiative - Regional Climate Change: REKLIM

Helmholtz Climate Initiative Regional Climate Change (REKLIM) is a consortium of nine German Research Centres of the Helmholtz Association. REKLIM combines regional observations and process studies coupled with model simulations to improve regional and global climate models, providing a more solid basis for climate-related decision support. Among the eight research themes especially one topic focuses on the Arctic and its permafrost regions. REKLIM places a major emphasis on knowledge transfer and dialogue processes between science and society.

www.reklim.de



Ice Berg Sponsors



The **AWI Geosciences Department** explores the evolution of the polar regions, past climatological and environmental states, as well as recent reaction of the Earth system to climate change. Research fields include geophysics, glaciology, marine geology, marine geochemistry, permafrost, and polar terrestrial ecology.

www.awi.de/en/science/geosciences.html



The **IEEE Geoscience and Remote Sensing Society** interests are the theory, concepts, and techniques of science and engineering as they apply to the remote sensing of the earth, oceans, atmosphere, and space, as well as the processing, interpretation and dissemination of this information. www.grss-ieee.org



The **German Society of Polar Research (DGP)** promotes science and research in the polar regions. For that, DGP organizes meetings on a regular basis, publishes the journal "Polarforschung" (Polar Research), and organizes working groups engaged with specific research themes and aspects of communication and outreach.

www.polarforschung.de



EUMETSAT is an intergovernmental organization with the purpose to supply weather and climate-related satellite data, images and products – 24 hours a day, 365 days a year – to the National Meteorological Services of our Member States in Europe, and other users worldwide.

www.eumetsat.int



The **Institute of Earth and Environmental Science at University of Potsdam** conducts research on topics on the Earth and it's environment around the globe, using a broad range of techniques from the natural sciences complemented with interdisciplinary networks.

<http://www.geo.uni-potsdam.de>



RUS-Copernicus is the Copernicus Research and User Support, a "New Expert Service for Sentinel Users" funded by the European Commission, managed by the European Space Agency, and operated by CS SI and its partners. The main objectives of the RUS Service are to promote the uptake of Copernicus data and to support the scaling up of R&D activities with Copernicus data. <https://rus-copernicus.eu>



Deltares is an independent institute for applied research in the field of water and subsurface with five areas of expertise. www.deltares.nl



Ice Floe Sponsors



The **USGS Alaska Science Center** provides timely data, information, and research findings about the earth and its flora and fauna to Federal, State, and local resource managers and the public to support sound decisions regarding natural resources, natural hazards, and ecosystems in Alaska and circumpolar regions.

www.usgs.gov/centers/asc



The **Climate and Cryosphere (cliC)** project is one of the core projects of the World Climate Research Programme, serving as the focal point for climate science related to the cryosphere, its variability and change, and interaction with the broader climate system. www.climate-cryosphere.org



The **Geo.X** research network brings together geoscientific partners from universities and non-university research institutions in Berlin and Potsdam. The key motivation is to foster close cooperation in research, teaching, joint infrastructure use, internationalisation and transfer into society and industry. www.geo-x.net



The **International Permafrost Association** fosters the dissemination of knowledge concerning permafrost and promotes cooperation among persons and national or international organizations engaged in scientific and engineering work on permafrost. The IPA Action Group on Permafrost Thaw Subsidence is hosting a workshop during the ICRSS and supports travel for ECR to the ICRSS. <https://ipa.arcticportal.org>



Copernicus Publications publishes open access journals covering remote sensing and polar sciences

https://publications.copernicus.org/remote_sensing.html



MDPI Remote Sensing is a peer-reviewed open access journal about the science and application of remote sensing technology, and is published monthly online by MDPI.

www.mdpi.com/journal/remotesensing



The **Association of Friends and Sponsors of the AWI** aims to financially support the activities of the Institute and to increase our knowledge of climate and marine systems for the benefit of humankind. www.awi.de/en/about-us/organisation/friends-association.html



Ice Crystal Sponsors



Springer is a leading global scientific, technical and medical portfolio, providing researchers in academia, scientific institutions and corporate R&D departments with quality content through innovative information, products and services. www.springer.com



The **German Research Centre for Geosciences (GFZ)** is the national research centre for Earth sciences. Research focuses on the geosphere within the highly complex System Earth with its further subsystems, its interacting subcycles, and its wide network of cause-and-effect chains. www.gfz-potsdam.de



The **International Society for Photogrammetry and Remote Sensing (ISPRS)** is a non-governmental organization devoted to the development of international cooperation for the advancement of photogrammetry and remote sensing and their applications. www.isprs.org

A photograph of the Aurora Borealis (Northern Lights) in a snowy landscape. The sky is a deep blue-green, filled with numerous stars and the vibrant green and blue bands of the aurora. The foreground shows a vast, snow-covered field with some tracks or indentations in the snow. The overall scene is serene and majestic.

PLENARIES



Progress in remote sensing reveals new insights on the impact of climate change on glaciers and rock glaciers on the Third Pole

T. Bolch

Mountain Cryosphere Research Group, Department of Geography, University of Zurich, Switzerland

High Mountain Asia (also called the “Third Pole”) is one of the most heavily glacierised areas outside the Polar regions ($\approx 90,000 \text{ km}^2$). The area affected by permafrost is about ten times as high and numerous rock glaciers and other forms of subsurface ice in permafrost conditions exist. Until recently, our knowledge of glacier characteristics and glacier change was limited; estimates of glacier area strongly deviated, and almost nothing was known about rock glacier occurrence and their response to climate change in the Himalayas, Pamir and Tibetan mountains. This can be mainly attributed to the remoteness and ruggedness of most of the mountain areas making field investigations very difficult.

Recent progress in processing of various kinds of remote sensing imagery, and the availability of high spatial and temporal resolution imagery has allowed unprecedented information about glacier changes to be obtained, and to detect and understand relevant processes such as glacier surges, melt of debris-covered glaciers and the evolution of rock glaciers.

The gradual release of archived aerial imagery and high resolution declassified satellite imagery from the 1960s and 1970s provide important insights into the longer-term changes.

This talk will provide a glimpse of the challenges of identifying and mapping glaciers, rock glaciers and other forms of subsurface ice, will provide an overview about the current knowledge of glacier and rock glacier occurrence and characteristics, followed by information about glacier mass changes on the entire Third Pole since the 1970s. Special emphasis will be given to the use of satellite imagery to

- understand why debris-covered glaciers have lost ice mass at a rate similar to clean ice glaciers, despite the insulating effect of debris cover, and
- to investigate the evolution of rock glaciers, their similarity and differences to debris-covered glaciers and their response to climate in specific study regions.

TanDEM-X:

Contribution to a better understanding of cryospheric applications

Irena Hajnsek^{1,2}

¹*ETH Zurich, Institute of Environmental Engineering, Zurich, Switzerland;*

²*DLR German Aerospace Center, Microwaves and Radar Institute, Department of Radar Concepts, Research Group: Pol-InSAR, Wessling, Germany*

The subsurface structure of snow and ice bodies is one of the critical unknowns for assessing their current condition and temporal change. The ability of microwaves to penetrate into or even through snow and ice layers and the sensitivity to geometric and dielectric characteristics make SAR configurations a unique tool for snow, firn and ice monitoring. Today, already some applications like the monitoring of retreat and surface velocity of glaciers have advanced to be used quasi operationally with satellite sensors. There exist also several regional examples for glacier mass balance calculations - a derived product from radar digital elevation model changes - which is an important knowledge for freshwater storage and climate relates changes. In addition regional thermokarst features can be detected happening due to abrupt changes in the order of 1–3 m per year in permafrost areas. All this applications have been demonstrated with TanDEM-X and will be presented.

In the last years, the evolution of snow and ice applications performed important development steps. The first was initiated by advances in understanding the interaction of polarized electromagnetic waves with the micro-structure of snow, firn and ice volumes. Triggered by new laboratory results indicating the anisotropic structure of snow and ice, the experimental demonstration by means of polarimetric SAR measurements of dielectric anisotropy in snow and firn as a result of temperature gradient metamorphism was an important result [Leinss et al., 2014]. This, together with a better description of the internal structure of snow and firn layers provided by field measurements, was essential for the interpretation of the scattering signature at different frequencies and for the development of new retrieval algorithms.

Based on the new understanding, conventional polarimetric scattering and decomposition models have been reviewed and improved. Multi-layer snow, firn and ice models have been developed and validated including the anisotropy (i.e. orientation distribution) and density of the ice grains as well as enclosed ice lenses as they develop by the refreezing of melt water [Parrella et al., 2016a]. Using these new models it was possible to estimate (and validate) the thickness and structural anisotropy of snow and firn layers by means of polarimetric phase differences at different frequencies in alpine as well as polar glaciers and ice sheets [Parrella et al., 2016b]. At the same time the separation of different glacier zones and the estimation of the equilibrium and firn line, i.e. the transition between the individual ice zones and their annual variation has been demonstrated (Fig. 1) [Parrella et al., 2018].

The second important development step was facilitated by a number of multi-baseline or tomographic Pol-InSAR data sets acquired in the frame of airborne experiments on Alpine and Polar glaciers [Pardini et al., 2016]. The tomographic reconstruction of the 3D radar reflectivity at different polarizations and frequencies critically improved the understanding of the penetration and of the 3D scattering processes occurring in firn and ice sheets. Accordingly, access to the 3D reflectivity enables to separate scattering at the snow-ice interface from subsurface scattering occurring in the underlying ice volume and to detect air, water and/or firn bodies embedded in the ice volume as well as surface like layers at different depths. Examples to the new development in the understanding of microwave remote sensing and cryosphere applications will be presented.

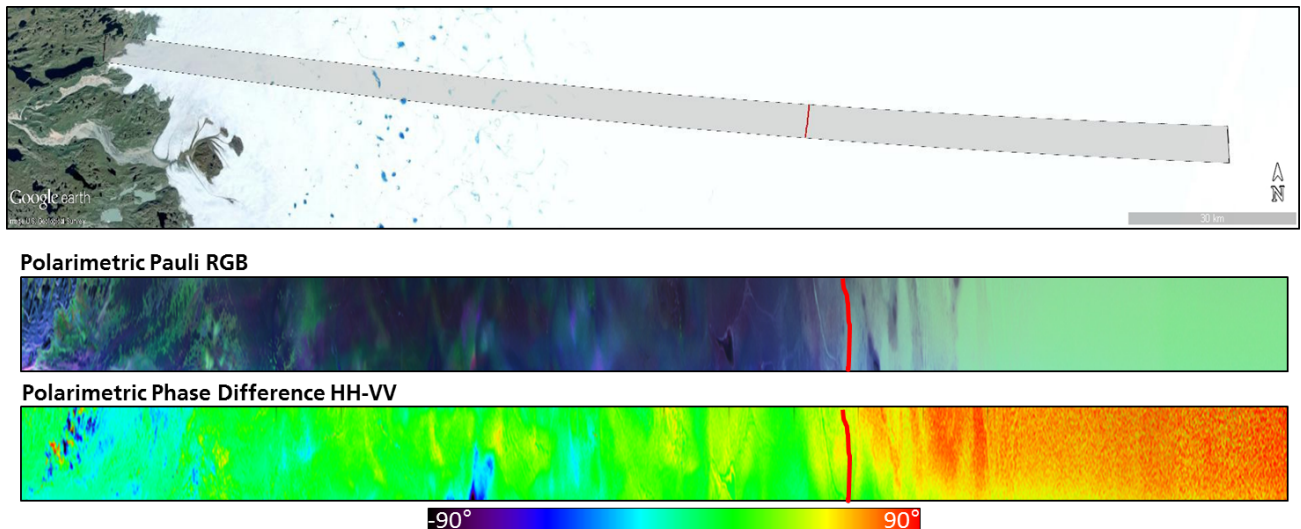


Figure 1: Quad-polarimetric transect acquired at L-band during the ARCTIC15 campaign with a length of 200 km starting on Greenland's west coast at an altitude of 300 m (left) until the inner part of the ice sheet at an altitude of 2100 m (right). The red line indicates the equilibrium line, located at about 1700 m, which separates the ablation from the accumulation (firn) zone. The polarimetric Pauli RGB composite image is shown in the middle. On the bottom the polarimetric HH-VV phase difference is shown.

References

- Leinss S., Parrella G., & I. Hajnsek [2014]: Snow height determination by polarimetric phase differences in X-band SAR data. *IEEE JSTARS*, 7(9): 3794–3810. doi:[10.1109/JSTARS.2014.2323199](https://doi.org/10.1109/JSTARS.2014.2323199).
- Parrella G., Hajnsek I., & K. Papathanassiou [2016a]: Polarimetric decomposition of L-band PolSAR backscattering over the Austfonna ice cap. *IEEE TGRS*, 54(3): 1267–1281. doi:[10.1109/TGRS.2015.2477168](https://doi.org/10.1109/TGRS.2015.2477168).
- Parrella G., Hajnsek I., & K. Papathanassiou [2016b]: On the interpretation of polarimetric phase differences in SAR data over land ice. *IEEE GRSL*, 13(2): 192–196. doi:[10.1109/LGRS.2015.2505172](https://doi.org/10.1109/LGRS.2015.2505172).
- Parrella G., Fischer G., Hajnsek I., & K. Papathanassiou [2018]: Mapping the Ice Zones of West Greenland using Multi-Frequency Polarimetric SAR Data. in: *Proc. of EUSAR2018*, 4–7 June 2018, Aachen, Germany.
- Pardini M., Parrella G., Fischer G., & K. Papathanassiou [2016]: A Multi-Frequency SAR Tomographic Characterization of Sub-Surface Ice Volumes. in: *Proc. of EUSAR2016*, 6–9 June, Hamburg, Germany.



From shelf seas to Fram Strait: A changing transpolar drift system

Thomas Krumpen

AWI

The Transpolar Drift System serves as a conveyor belt carrying sea ice from the Siberian shelves towards Fram Strait where it leaves the Arctic Ocean and melts. It plays an important role for the Arctic sedimentary budget and biogeochemical cycles, since ice carries gaseous, dissolved and particulate matter from one place to another.

A warming Arctic and declining sea ice cover in summer have a profound effect on the Transpolar Drift System. Changes are determined not only by changes in the energy balance of the coupled ice–ocean–atmosphere system but also by the increasing influence of dynamic effects. Observations in Fram Strait give insight into the magnitude of changes taking place further upstream. Airborne observations carried out between Greenland and Svalbard show

a substantial thinning of the ice cover and satellite observations indicate that thinning is accompanied by an increase in ice drift velocity and deformation and a reduction of ice age in Fram Strait. Similar changes can be observed at the other end of the Transpolar Drift System: Sea ice export from the Laptev Sea towards central Arctic Ocean has increased significantly. An enhanced offshore advection of sea ice leads to a thinner ice cover that melts more rapidly once temperatures rise above freezing and preconditions anomalies in summer ice extent. Enhanced advection of ice and intensified melt in the marginal ice zones are expected to change biogeochemical fluxes and ecological processes in the Central Arctic. Quantitative assessments along the Transpolar Drift will be carried out during the MOSAiC drift campaign.



Ocean color of the Arctic Ocean

A. Matsuoka

Takuvik Joint International Laboratory (CNRS-Ulaval)

Climate change is affecting a broad spectrum of marine and terrestrial environments in high northern latitudes. Satellite records reveal that Arctic sea ice area and thickness have been decreasing almost over the last four decades due to ongoing global warming and ice-albedo feedback. The newly opened area now plays an important role in dissolution of atmospheric CO₂. In terms of additional CO₂ uptake, depending on nutrient availability and physical conditions (e.g., mixing), studies using ocean colour data showed that primary production of the Arctic Ocean (AO) is likely to increase, mainly because of increased light availability associated with the increase in open water area. On land, an increase in river discharge has been observed in both North American and Siberian sides of the Arctic region particularly since the late 20th century, which is likely related to recent decreases in Arctic sea ice. A significant amount of organic carbon originating from permafrost thaw is now anticipated to be delivered by river discharge into the AO. A portion of this organic carbon that was previously sequestered in the permafrost may be actively utilized by microbes, which may accelerate CO₂ release back to the atmosphere. Whether the AO is a sink or

source of atmospheric CO₂ is still not clear.

To address the changing carbon cycle, I have worked on ocean colour remote sensing together with other sensors in the near-infrared, microwave, and L-band. My recent research includes investigation of a trend in the flux of dissolved organic carbon observed in major Arctic river mouths by developing a semi-analytical algorithm for estimating DOC flux with known uncertainty. To examine the influence of river input on coastal marine ecosystems, I have also developed an objective algorithm for discriminating different surface water sources using remote sensing data alone. Broader application of this algorithm may lead to the discrimination of water sources in the surface layer in a variety of environments, which may be useful to improving our understanding of physical and biogeochemical processes related to each water source.

While ocean colour is a powerful tool for tracing organic matter temporally and geographically, there are some limitations (e.g., frequent cloud cover). In my talk, I will present the strengths and the limitations of ocean colour remote sensing for addressing Arctic Ocean carbon cycling and discuss possibility to overcome these issues.



The 2017 Arctic Boreal Vulnerability Experiment (ABoVE) Airborne Campaign

C. E. Miller¹, P. C. Griffith², S. J. Goetz³, L. Hoy⁶, N. Pinto¹, I. McCubbin¹, A. Thorpe¹, M. Hofton⁴, D. Hodkinson², C. Hansen⁴, J. Woods², E. Larson², E. S. Kasischke⁵, & H. A. Margolis⁵

¹*Jet Propulsion Laboratory, California Institute of Technology, Pasadena CA, USA;*

²*NASA Goddard Space Flight Center / SSAI, Greenbelt Maryland, USA;*

³*Northern Arizona University, Flagstaff AZ, USA;*

⁴*NASA Goddard Space Flight Center, Greenbelt MD, USA;*

⁵*Earth Science Directorate, NASA Headquarters, Washington DC, USA;*

⁶*NASA Goddard Space Flight Center / GST, Greenbelt Maryland, USA*

The 2017 Arctic Boreal Vulnerability Experiment Airborne Campaign (AAC) was one of the largest, most complex airborne science experiments conducted by NASA's Earth Science Division. Between April and November, the AAC involved ten aircraft in more than 200 science flights that surveyed over 4 million km² in Alaska and northwestern Canada. Many flights were coordinated with same-day ground-based measurements to link process-level studies with geospatial data products derived from satellite sensors. The AAC collected data spanning the critical intermediate space and time scales that are essential for a comprehensive understanding of scaling across the ABoVE Study Domain and ultimately extrapolation to the pan-Arctic using satellite data and ecosystem models. The AAC provided unique opportunities to validate satellite and airborne remote sensing data and data products for northern high latitude ecosystems.

The 2017 AAC science strategy coupled domain-wide sampling with L-band and P-band synthetic aperture radar (SAR), imaging spectroscopy (AVIRIS-NG), full waveform lidar (LVIS) and atmospheric carbon dioxide and methane with more spatially and

temporally focused studies using Ka-band SAR (Ka-SPAR) and solar induced chlorophyll fluorescence (CFIS). Additional measurements were coordinated with the NEON Airborne Observing Platform, the ASCENDS instrument development suite, and the ATOM EV-S2 investigation. Targets of interest included the array of field sites operated by the ABoVE Science Team as well as the intensive sites operated by the DOE NGEE-Arctic team on the Seward Peninsula and in Barrow, NSF's LTER sites at Toolik Lake (North Slope) and Bonanza Creek (Interior Alaska), NEON sites across Alaska, the Canadian Cold Regions Hydrology sites in the Arctic tundra near Trail Valley Creek NT, the Government of the Northwest Territories Slave River/Slave Delta watershed time series, carbon and energy flux sites at Scotty Creek NT and Daring Lake NT, and numerous forest and fire disturbance plots maintained by the Alaskan and Canadian Forestry Services.

We will present an overview of the 2017 AAC, highlight some key results, and present preliminary looks at limited time series data acquired during 2018.

A new raster version of the Circumpolar Arctic Vegetation Map (CAVM)

M. K. Raynolds & D. A. Walker

Institute of Arctic Biology, University of Alaska Fairbanks

The Circumpolar Arctic Vegetation Map (CAVM) is a vector (polygon) map showing the dominant physiognomy of the vegetation of the Arctic [CAVM Team, 2003]. The legend has 15 vegetation types, glacier, saline water, freshwater, and non-arctic land. It was published in 2003, and has been cited over 700 times. The main value of the map was that it mapped the vegetation of the whole Arctic using a consistent legend, at a level of detail appropriate for global or circumpolar analyses [Walker et al., 2005].

Although the CAVM has proved to be a very useful tool, there has been interest in a raster version of the map. The raster format better matches environmental data such as climate and substrate data from satellite sensors and other sources. Many researchers have used a simple rasterized version of the vector CAVM in their models. This project created a 1-km resolution raster CAVM using the same legend categories as the original CAVM (Fig. 1).

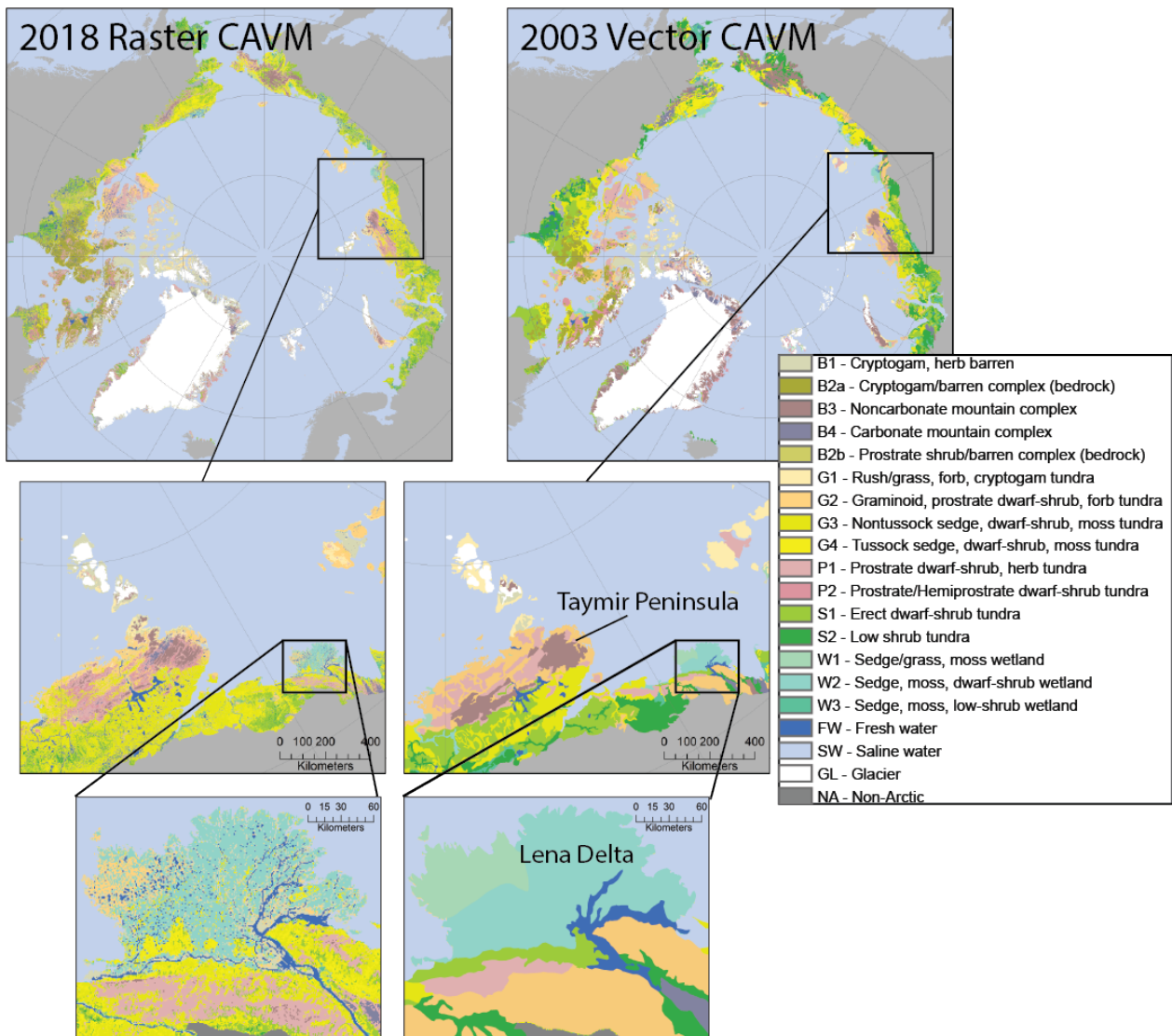


Figure 1: Top left: New Raster Circumpolar Arctic Vegetation Map (CAVM). Top right: original vector CAVM. Left/right sides – zoom into northern Russia and Lena River Delta, raster/vector versions, respectively.



The raster map provides greater resolution (1-km pixels vs. the 14-km minimum polygon diameter), while maintaining the same consistent vegetation legend (though the barren complex used to map the Canadian Shield was split into two sub-types). The greater spatial resolution of the raster format allows more detailed mapping of water bodies and mountainous areas. It portrays coastal-inland gradients, and better reflects the heterogeneity of vegetation type distribution.

The new map is based on unsupervised classifications of seventeen geographic/floristic sub-sections of the map using AVHRR and MODIS data (band and NDVI) and elevation data. The units resulting from the classification were modeled to the CAVM types using a wide variety of ancillary data: the original CAVM map, climate data, substrate data, existing regional vegetation maps and ground studies. The map was reviewed by experts familiar with their particular region, including many of the original authors of the CAVM from the U.S., Canada, Greenland (Denmark), Iceland, Norway (including Svalbard), and Russia.

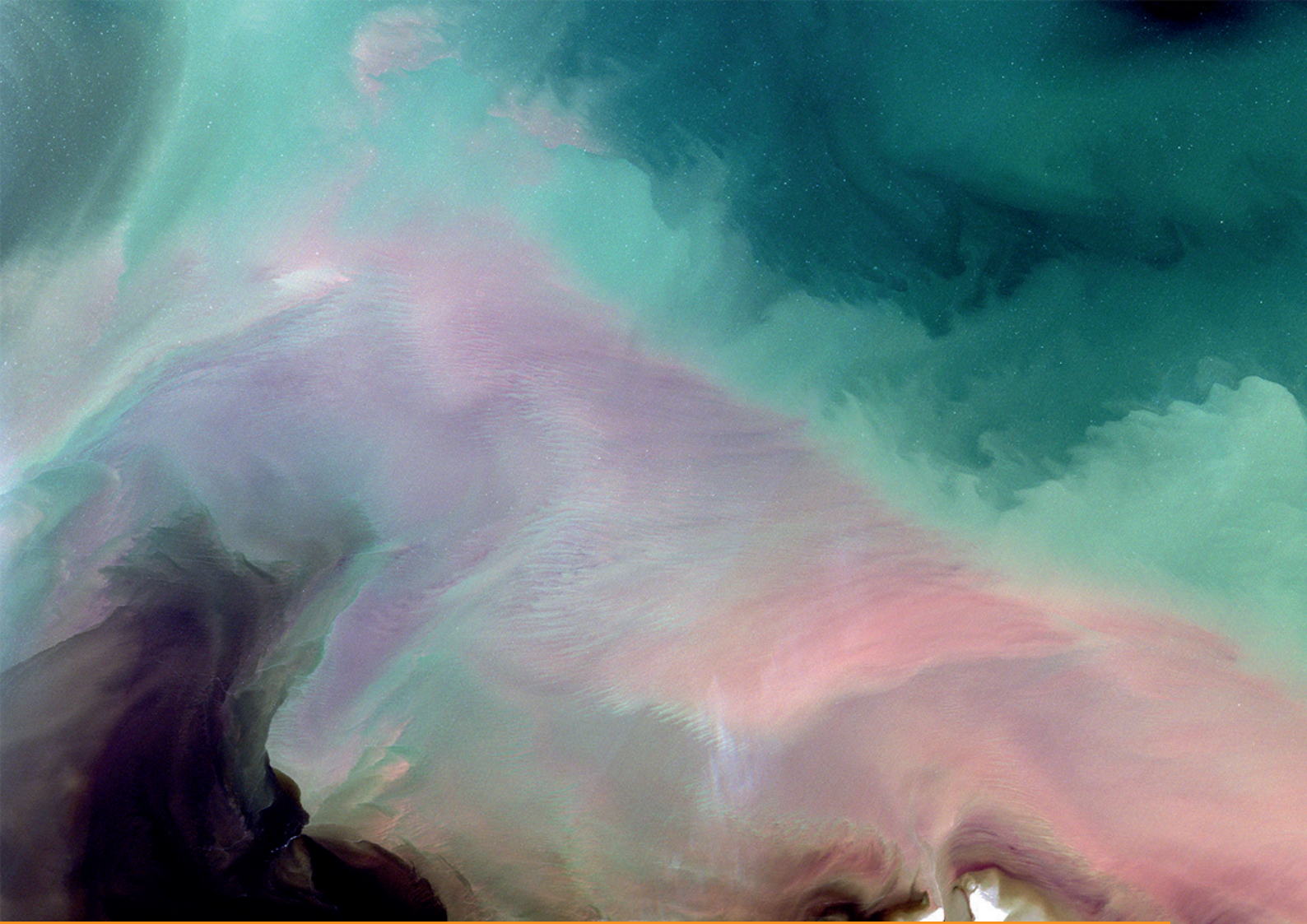
The proportions of the land cover units on the new Raster Circumpolar Arctic Vegetation Map (Raster CAVM) and the original vector CAVM differ mostly due to the resolution of the two maps (Fig. 1). There is four times as much water on the raster map (4.0 %) compared to the vector map (0.9 %), since many waterbodies smaller than the vector minimum polygon

size were mapped. It was also possible to map mountainous areas in much greater detail on the raster map, leaving much less in the mountain complex types (2.4 vs. 9.5 %). Differences in interpretation can be seen in the reduction in low shrub tundra (1.7 vs. 8.6 %). Unlike the original vector map, which showed low shrub tundra as the dominant type of large areas, the Raster CAVM shows it as occurring mostly in narrow bands along river valleys, and as the main land cover type only in hilly areas close to the southern treeline boundary.

The final product is available from the authors, and will be posted on the Alaska Arctic GeoEcological Atlas hosted by GINA at the University of Alaska Fairbanks <http://arcticatlas.geobotany.org/>.

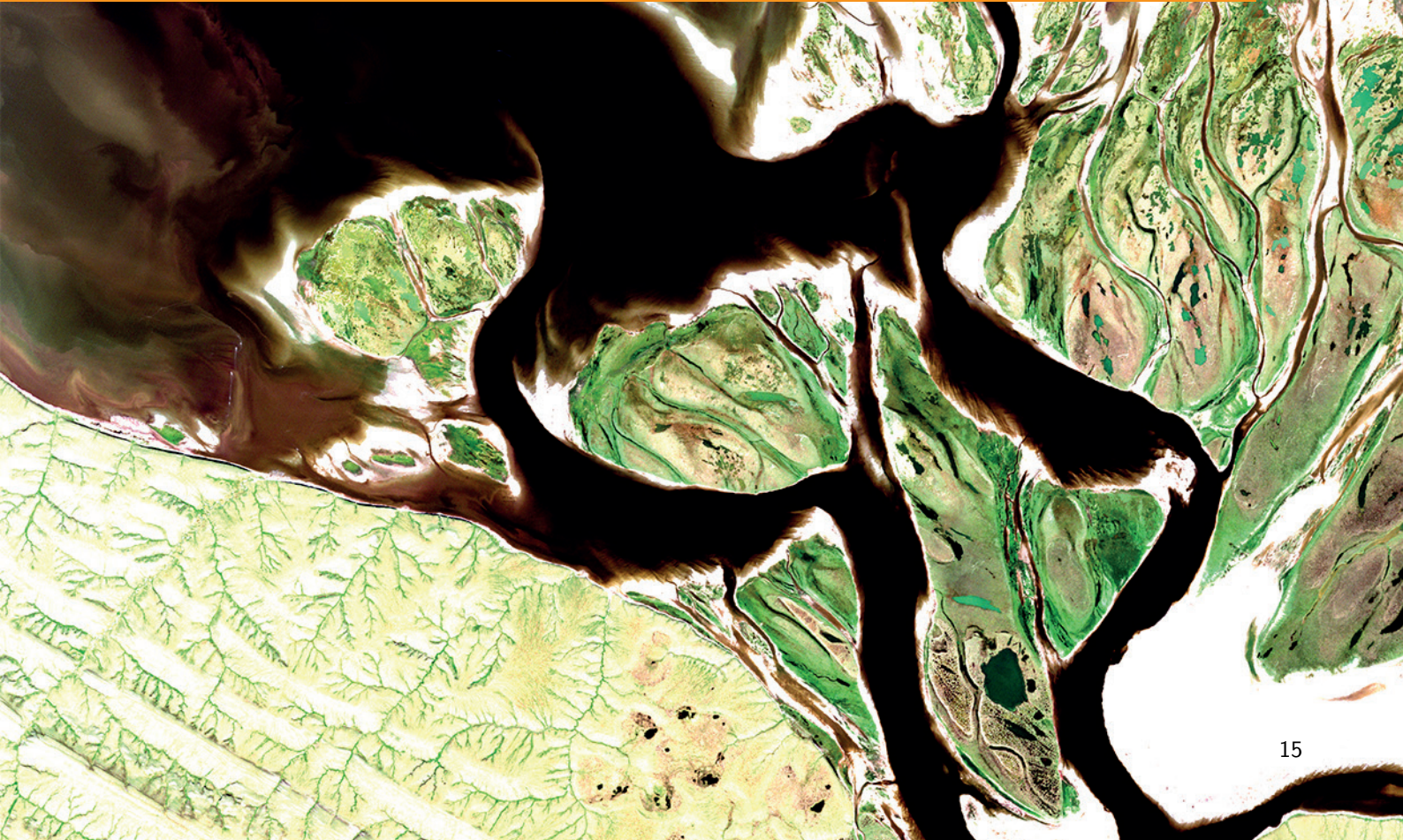
References

- CAVM Team [2003]: *Circumpolar Arctic Vegetation Map, scale 1:7 500 000*. Conservation of Arctic Flora and Fauna (CAFF) Map No. 1. U.S. Fish and Wildlife Service, Anchorage, Alaska.
- D. A. Walker, M. K. Raynolds, F. J. A. Daniels, E. Einarsson, A. Elvebakk, W. A. Gould, A. E. Katenin, S. S. Kholod, C. J. Markon, E. S. Melnikov, N. G. Moskalenko, S. S. Talbot, B. A. Yurtsev, and CAVM Team [2005]: The Circumpolar Arctic Vegetation Map. *Journal of Vegetation Science*, 16, p. 267–282. doi:[10.1111/j.1654-1103.2005.tb02365.x](https://doi.org/10.1111/j.1654-1103.2005.tb02365.x).



SESSION

Changing Polar Coasts and Deltas



Temporal variability of coastal retreat at Kharasavey area, Western Yamal Peninsula, the Kara Sea

N. G. Belova, A.V. Baranskaya, A.V. Novikova, N.N. Shabanova, S.A. Ogorodov

Lomonosov Moscow State University, Faculty of Geography, Moscow, Russia

Coasts of the Kara Sea retreat at a mean annual rate of 0.7 m/yr [Lantuit et al., 2012]. At the Kharasavey gas condensate field in Western Yamal the development takes place from the 1970s and archival aerial photographs are available for 1977 and 1988 yrs. Together with multitemporal satellite imagery (1964, 2006, 2016), this allows us to trace in detail the temporal variability of permafrost coasts' destruction rates. Field data on the coastal sediments composition and ice content made it possible to clarify the reasons for the high rates of coastal segments retreat in certain periods. At 9-km section coastal cliffs of 7-12 m height retreat at a mean rate of 1.1 m/yr during 52-year period, while on certain segments it reaches 2-3 m/yr [Belova et al., 2017]. For icy coasts, acceleration of destruction rates in warm periods is noted, while increased rates of retreat of segments with low ice content often indicate an anthropogenic pressure (sediment excavation from beach and coastal bluff, dredging in the nearshore zone, etc.).

References

- H. Lantuit, P.P. Overduin, N. Couture, S. Wetterich, F. Aré, D. Atkinson, J. Brown, G. Cherkashov, D. Drozdov, D.L. Forbes, A. Graves-Gaylord, M. Grigoriev, H.-W. Hubberten, J. Jordan, T. Jorgenson, R.S. Ødegård, S. Ogorodov, W.H. Pollard, V. Rachold, S. Sedenko, S. Solomon, F. Steenhuisen, I. Streletskaia & A. Vasiliev [2011]: The Arctic Coastal Dynamics database: a new classification scheme and statistics on Arctic permafrost coastlines. *Estuaries and Coasts*, 35, 383–400. doi:10.1007/s12237-010-9362-6.
- N.G. Belova, N.N. Shabanova, S.A. Ogorodov, A.M. Kamalov, D.E. Kuznetsov, A.V. Baranskaya & A.V. Novikova [2017]: Erosion of permafrost coasts of Kara Sea near Kharasavey Cape, Western Yamal. *Earth's Cryosphere*, 21(6): 85–96. doi:10.21782/KZ1560-7496-2017-6(85-96).



The spatial extent of Arctic river deltas: Version 1.0 of the Arctic river delta data set

M. Fuchs, I. Nitze & G. Grosse

Alfred Wegener Institute Helmholtz Centre for Polar and Marine Sciences, Potsdam, Germany

Arctic river deltas are highly dynamic environments at the land-ocean interface and are underlain by permafrost. They are not only affected by fluvial and coastal processes but also by permafrost and thermokarst related processes. Here we present the first version of the Arctic river delta data set, which includes the subaerial extent of 269 deltas. This data set is based on a simple hands-on digitizing approach which will be combined with additional parameters (catchment size, water area coverage) from different remote sensing based products like a pan-arctic digital elevation model [Santoro & Strozzi, 2012] and the global water data set [Pekel et al., 2016] to further characterize Arctic river deltas. We are further analyzing Landsat-based trends of multispectral indices for all Arctic deltas allowing a detailed insight into the dynamics in deltas over the 1999–2014 period, when strong changes in sea ice over the Arctic Ocean started to affect coastal dynamics. Multispectral indices considered include NDVI, NDMI, NDWI, and Tasseled Cap Brightness, Greenness, and Wetness.

In this first version of the data set, Arctic river

deltas cover in total an area of 112 000 km² whereof the two mega deltas (Lena and Mackenzie River delta) already cover 39 % of this area. Medium and small deltas cover an area of 36 500 km² and cover therefore ≈33 % of the entire area covered by Arctic river deltas. This entire delta data set also allows better characterizing and scaling deltaic soil carbon storage in these highly vulnerable permafrost environments in the Arctic.

References

- J.-F. Pekel, A. Cottam, N. Gorelick & A. S. Belward [2016]: High-resolution mapping of global surface water and its long-term changes. *Nature*, 540, p. 418–422. doi:[10.1038/nature20584](https://doi.org/10.1038/nature20584).
- M. Santoro & T. Strozzi [2012]: Circumpolar digital elevation models > 55° N with links to geotiff images, ESA data user element – permafrost. *PANGAEA, Data Publisher for Earth and Environmental Science*. doi:[10.1594/PANGAEA.779748](https://doi.org/10.1594/PANGAEA.779748).

Impacts of coastal dynamics on the socio-economic component of the Yukon coast, western Canadian Arctic

Anna M. Irrgang^{1,2}, Hugues Lantuit^{1,2}, Richard R. Gordon³, Ashley Piskor⁴, & Gavin K. Manson⁵

¹*Department of Permafrost Research, Alfred Wegener Institute Helmholtz Centre for Polar- and Marine Research, Telegrafenberg A43, 14473 Potsdam, Germany;*

²*Institute of Earth and Environmental Science, University of Potsdam, Karl-Liebknecht-Strasse 24/25, 14476 Potsdam, Germany*

³*Department of Environment, Qikiqtaruk-Herschel Island Territorial Parks, Box 1129 Inuvik, Canada, X0E 1L0*

⁴*Western Arctic Field Unit, Parks Canada, PO Box 1840, 187 Mackenzie Road, Inuvik, Canada*

⁵*Geological Survey of Canada-Atlantic, 1 Challenger Drive, Dartmouth, NS B3B 1A6, Dartmouth, Canada*

The Yukon coast has a vivid history reaching back to the pre-historic time of the Thule Inuit. It also archives the diverse story of the Inuvialuit and their traditional and modern lifestyle, and the influences of western cultures. These cultural sites, as well as infrastructure and boating routes, which are nowadays used by the local population, are particularly vulnerable to coastal erosion. To assess this threat, shoreline change dynamics were analyzed along a 210 km long stretch of the Yukon coast by means of geo-coded aerial imagery from the 1950s, 1970s and 1990s, as well as Geo Eye 1 and World View 2 satellite images from 2011. The calculated rates of shoreline change were used to create a conservative (S1) and a dynamic (S2) scenario for possible shoreline positions for the year 2100. The future shoreline positions were then compared to locations of cultural features obtained from a Parks Canada database, the Yukon Archaeological

Program and derived from existing literature, as well as from aerial photographs and videos. In total 168 features were mapped, 26 % have been already lost due to coastal erosion and further 20 % (S1) to 26 % (S2) are expected to get lost due to future shoreline retreat, summing up to a total of 46 % (S1) to 52 % (S2) of lost cultural features by 2100. Under both scenarios, the sparse infrastructure in the form of two landing strips will be severely damaged by 2100, considerably restricting its usage. Expected higher sedimentation rates will likely lead to increasing difficulties in navigating the Workboat Passage, which is an important boating route for local travelers. Thus, expected future coastal erosion and sedimentation processes will lead to the disappearance of various cultural sites and impede travelling along the Yukon coast.

High temporal and spatial resolution satellite image observations for the past decade highlight complexities associated with permafrost coastal bluff erosion in the Arctic

Benjamin M. Jones¹, Diana L. Bull², Louise M. Farquharson³, Carson A. Baughman¹, Christopher D. Arp³, Guido Grosse⁴, Frank Günther⁴, Mikhail Kanevskiy³, Go Iwahana³, Allen Bondurant³, Richard M. Buzard³, Torsten Sachs⁵, Ingmar Nitze⁴, Jeremy L. Kasper³, Jennifer M. Frederick², Matthew Thomas⁶, Alejandro Mota², Craig Jones⁷, Jesse Roberts², Scott Dallimore⁸, Craig Tweedie⁹, Christopher Maio³, Daniel H. Mann³, Bruce Richmond¹⁰, Ann Gibbs¹⁰, Ming Xiao¹¹, & Vladimir E. Romanovsky³

¹Water and Environmental Research Center, Institute of Northern Engineering, University of Alaska Fairbanks, Fairbanks, AK, USA;

²Sandia National Laboratories, Albuquerque, NM, USA;

³University of Alaska Fairbanks, Fairbanks, AK, USA;

⁴Alfred Wegener Institute, Potsdam, Germany;

⁵GFZ German Research Centre for Geosciences, Potsdam, Germany;

⁶U.S. Geological Survey, Golden, CO, USA; ⁷Integral Consulting, Santa Cruz, CA, USA;

⁸Geological Survey of Canada, Sidney, BC Canada; ⁹University of Texas El Paso, Texas, USA;

¹⁰U.S. Geological Survey, Santa Cruz, CA, USA; ¹¹Penn State University, State College, PA, USA

Eroding permafrost coasts in the Arctic are potentially valuable indicators for accumulating impacts of changes in the Arctic System. Decline in sea ice extent and an increase in open water duration, combined with more frequent and effective storms, sea level rise, and warming permafrost, make them increasingly susceptible to increased rates of erosion. However, few observation sites in the Arctic have yet to firmly link erosion rates with changing environmental conditions due to broad temporal gaps in suitable observations necessary to address the relative role of potential drivers of change. Here, we use high spatial resolution optical satellite imagery acquired at high temporal resolution between 2008 and 2017 to explore potential environmental forcing factors responsible for rapid erosion events. We quantify annual erosion magnitude and environmental forcing factors for a 9 km segment of permafrost coastline at Drew Point, Beaufort Sea Coast, Alaska. We then place our observations in the context of decadal scale observations between 1955 and 2007. Mean annual erosion for the decade, 2007 to 2016, was 17.2 m yr⁻¹, which is 2.5 times faster than between 1955 and 1979. Annually, mean erosion along the length of the study coast varied from 6.7 m in 2010 to more than 20 m in 2007, 2012, and 2016. We quantified the open water season using satellite remote sensing time series observations available from the NSIDC. We then correlated mean

open water season erosion on an annual basis with the number of storms in a given erosion season, open water period, sea surface temperature, thawing degree day sums, near-surface permafrost temperature, and average storm power values. Multiple linear regression, forward stepwise regression, and best subsets regression of our annual erosion time series at Drew Point did not reveal any statistically significant relations. The lack of significant correlations between mean annual erosion and the suite of environmental variables compiled in this study means we are likely not accurately capturing all of the environmental forcing factors at adequate resolutions or accuracies, or that other not yet considered factors may be responsible for the increased erosion occurring at Drew Point. During a drilling campaign conducted in April 2018, we encountered a cryopeg at Drew Point that ranged in elevation from 0.3 m asl to > 2.3 m bsl. Ground temperature at this depth was ≈ -8 °C yet the material was unfrozen. It is conceivable that the 4 °C permafrost warming in the region over the past several decades has increased the erodibility of the saline permafrost deposits located at this critical elevation where thermo-mechanic erosional niches actively develop during periods of elevated water levels. This, combined with changes occurring in the marine system, are likely driving the well documented increase in erosion at Drew Point, Alaska, USA.

Coastal destruction in the western and eastern-most occurrence of tabular ground ice in the Eurasian Arctic

A. I. Kizyakov¹, F. Günther², M. V. Zimin³, A. V. Sonyushkin⁴, & S. Wetterich²

¹*Department of Cryolithology and Glaciology, Faculty of Geography, Lomonosov Moscow State University, Moscow, Russia;*

²*Alfred Wegener Institute Helmholtz Centre for Polar and Marine Research, Potsdam, Germany;*

³*Research and Development Center ScanEx, Moscow, Russia;*

⁴*OpenWeatherMap, Inc., NY, USA*

Destruction of arctic permafrost coasts occurs as a result of a complex suite of processes, predominantly thermal abrasion and denudation. Activation of these processes can be particularly observed in case of massive ground ice bodies (ice wedges or tabular ground ice) that become exposed on high bluffs along the coastline. Tabular ground ice is a widespread geological feature on Arctic plains.

Thermo-denudation of exposed ground ice includes ice ablation, thaw of enclosed frozen deposits and the development of retrogressive thaw slumps with thermo-cirques or thermo-terraces formation. Due to its high self-enforcing process intensity thermo-denudation can be referred to as one of the most hazardous processes of permafrost degradation.

We are study the current coastal destruction dynamics in the western (Kolguev Island) and eastern-most (Novaya Sibir' Island) occurrence of tabular ground ice in the Eurasian Arctic.

With higher temporal resolution, studies on Kolguev Island continue earlier research efforts on coastal dynamics, while thaw slumps on Novaya Sibir' still require a quantitative assessment of their erosion dynamics. Coastal dynamics are analyzed using a whole set of multi-temporal satellite images of high and very-high spatial resolution (GeoEye, WorldView, Alos Prism, SPOT, Formosat, and Kompsat). For orthorectification purposes, the 12 m TanDEM-X DEM has been used. However, since the TanDEM-X DEM is based on averaged bistatic SAR surveys acquired

during the period 2010–2012. This DEM can be used only for orthorectification of images newer than 2012 to determine the exact position of the coastal bluffs and thermocirque edges. We therefore reconstructed the relief along erosive coastline segments by modifying the initial TanDEM-X DEM through extrapolation of coastal bluffs edge elevation values and restoration of the coastal plain relief at 200–300 m towards the sea for orthorectification of images prior to 2012. All raw images were terrain-corrected and georeferenced using a comprehensive block adjustment, resulting in a very high absolute and relative accuracy of all images.

On western part of Kolguev Island coastal retreat rates during the 2002–2012 period varied from 1.7 to 2.4 m/year. Thermo-cirque growth averaged rates were 2.6 m/year, maximum 14.5–15.1 m/year. We are about to extend our observations to more recent high resolution acquisitions.

We are currently processing new data on the Novaya Sibir' Island, where tabular ground ice exposures occur in the northern part of the island in the Mira Bay. This study is carried out in the same way as on the Kolguev Island and will allow to detect commonalities and differences in two contrasting environmental settings with “warm” and very cold permafrost.

Acknowledgements

Supported by RFBR grants №18-05-60080, 18-05-60221 and DFG grant №WE 4390/7-1.

Dynamics of permafrost coasts of Baydaratskaya Bay (Kara Sea) based on multi-temporal remote sensing data

A. Novikova¹, N. Belova¹, A. Baranskaya¹, A. Maslakov¹, D. Aleksyutina¹, N. Shabanova¹, E. Zelenin², & S. Ogorodov¹

¹*Faculty of Geography, Lomonosov Moscow State University, Moscow, Russia;*

²*Geological Institute, Russian Academy of Sciences*

Arctic coasts composed of perennially frozen deposits are extremely sensitive to climate and human impact. They retreat with the average rates of 1–2 meters per year depending on climatic and permafrost conditions [Forbes, 2011]. Recent decades, there is a tendency to increase of coastal retreat rates, especially it is noticeable in the area of resource development. We study coastal dynamics of two key areas (Ural and Yamal coasts) of Baydaratskaya Bay of the Kara Sea, Western sector of Russian Arctic, where the gas pipeline has been constructed. Based on multi-temporal ultra-high resolution aerial and satellite imagery we consider the coastal dynamics during several time lapses, in natural condition and under the human impact, and discuss their temporal variability. Besides planimetric (m/yr), we calculated volumetric (m²/m/yr) retreat of erosional coasts using ArcticDEM. In addition, we estimated influence of geomorphological, lithological and permafrost composition of coasts on spatial variations of their dynamics.

The coasts of the Ural key site retreat with the higher mean rates (1.2 m/yr and 8.7 m²/m/yr for 1964–2016) in compare with the Yamal key site (0.3 m/yr and 3.7 m²/m/yr for 1968–2016) due to their complex lithology, higher ice content and lower coastal bluffs. Retreat of Ural coast is faster and of Yamal coast is slower than the average linear rate for the entire Arctic (0.5 m/yr) [Lantuit et al., 2012]. In planimetric rates 2–4m laida and low (6–8 m height) terraces retreat faster than high (more than 10 m height) terraces, on the contrary in volumetric scale retreat of high terraces is much more considerable. Concerns to lithology, sandy coasts are eroded more intensively than loamy and peaty. A clear contribution of outcrops of massive ice beds and wedge ice to coastal dynamics has not been detected. Since 1960s the coastal retreat shows a growth of rates on the both

coasts, that we associate with the climate warming in the Arctic. Beyond that, during the period of 1960s–2005 the growth was slight, while during 2005–2016 it was rapid, that may be explained by the enhanced wave and thermal action or by the beginning of the resource development in last decade. Originally accumulative sectors of coasts remained relatively stable during the period of 1960s–2005, but a considerable part of them begun to retreat after 2005, that we relate with the changing weather conditions and/or the emerged human impact.

Acknowledgements

The study was supported by Russian Science Foundation project №16-17-00034. We thank ©Digital Globe Foundation for the provided satellite imagery.

References

- D.L. Forbes [2016]: *State of the Arctic coast 2010: scientific review and outlook*. Land-Ocean Interactions in the Coastal Zone, Arctic Monitoring and Assessment Programme, International Permafrost Association, 178 p. <http://arcticcoasts.org>.
- H. Lantuit, P.P. Overduin, N. Couture, S. Wetterich, F. Aré, D. Atkinson, J. Brown, G. Cherkashov, D. Drozdov, D.L. Forbes, A. Graves-Gaylord, M. Grigoriev, H.-W. Hubberten, J. Jordan, T. Jorgenson, R.S. Ødegård, S. Ogorodov, W.H. Pollard, V. Rachold, S. Sedenko, S. Solomon, F. Steenhuisen, I. Streletskaia & A. Vasiliev [2011]: The Arctic Coastal Dynamics database: a new classification scheme and statistics on Arctic permafrost coastlines. *Estuaries and Coasts*, 35, 383–400. doi:10.1007/s12237-010-9362-6.



SESSION

Floating Ice: Sea, River, and Lake Ice

Influence of lake ice formation and break-up on ASCAT backscatter

H. Bergstedt⁴, A. Bartsch^{2,3}, B. M. Jones⁴ & C. Duguay⁵

¹*Interfaculty Department of Geoinformatics – Z_GIS, University Salzburg, Schillerstraße 30, 5020 Salzburg, Austria;*

²*Austrian Polar Research Institute, 1010 Vienna, Austria;*

³*b.geos, 2100 Korneuburg, Austria;*

⁴*Water and Environmental Research Center, Institute of Northern Engineering, University of Alaska Fairbanks, Fairbanks, AK, USA;*

⁵*Department of Geography and Environmental Management, University of Waterloo, Waterloo, Canada*

Lakes of different sizes and extent are a dominant feature in Arctic landscapes. Remote sensing applications in arctic environments, therefore, frequently have to solve problems related to lake masking, mixed pixels and sub-pixel lake features. These issues are particularly relevant for applications relying on data obtained with spaceborne scatterometers, such as soil moisture or freeze/thaw mapping. In areas with many small lakes, the coarse spatial resolution of data sets derived from scatterometer instruments (often 25–50 km) leads to a large number of mixed pixels due to the presence of sub-pixel size lakes.

Previous studies focusing on transitional periods (spring and autumn) have revealed strong differences between scatterometer and synthetic aperture radar (SAR) backscatter derived surface status (frozen versus unfrozen, Bergstedt & Bartsch [2017]), especially in lake rich areas, suggesting the possible influence of lake ice during the freeze-up and break-up periods on the coarse resolution scatterometer data. Transitional periods are crucial for accurate freeze/thaw detection by microwave remote sensing sensors. In our analysis, we therefore focus on the transitional periods where lake ice possibly influences the detection accuracy of freeze/thaw transitions.

In this study, we quantify the contribution of sub-pixel lake areas on the backscatter signal of the Advanced Scatterometer (ASCAT) instrument (C-band)

aboard the Metop satellites. To separate lake and land areas, we created a lake mask based on Sentinel-2 optical data and the Normalized Difference Water Index (NDWI). SAR data from the Sentinel-1 satellite (C-band), which provide backscatter values at a higher spatial resolution than ASCAT (approx. 40 m vs. 25 km, gridded to 12.5 km), was used to quantify the difference between backscatter values of lake and land areas. We then compared average values of both lakes and land areas to the combined backscatter as given by the ASCAT instrument. To increase the representativeness of our results, we chose 18 ASCAT grid cells across the North American (Alaska and Canada) and Scandinavian Arctic as our study sites. The study sites were chosen to represent different lake types (extent and depths) as well as lake fractions.

Preliminary results show differences between spring and autumn, underlining the importance of treating these time periods separately in the following analysis steps. In further steps, we plan to analyze the implications of our findings for the application of different freeze/thaw detection algorithms.

References

Bergstedt, H. & A. Bartsch [2017]: Surface State across Scales; Temporal and Spatial Patterns in Land Surface Freeze/Thaw Dynamics. *Geosciences*, 7(3): 65. doi:[10.3390/geosciences7030065](https://doi.org/10.3390/geosciences7030065).

Eighteen-year MODIS detection of ice breakup on Alaskan rivers wider than 150 m

W. Dolan, T. Pavelsky, S. Zhang, & X. Yang

The University of North Carolina, Chapel Hill, USA

Annual spring river ice breakup in Alaska has major implications for northern ecosystems and infrastructure. Additionally, river ice breakup is impacted by air temperature and is therefore important to study as the Arctic climate changes. Quantification of river ice breakup in the Arctic has been spatially limited due to the lack of ground-based observations. Previous studies have used imagery from the Moderate Resolution Imaging Spectroradiometer (MODIS) to study ice breakup on individual Arctic rivers wider than 500 m. However, rivers narrower than 500 m are much more common than wide rivers and are therefore important to study. Here we present an ice breakup detection algorithm which uses MODIS imagery to detect breakup on all Alaskan river reaches wider than 150 m from 2000 through 2017 (Fig. 1). The algorithm uses reach-specific NIR-band thresholds to account

for the inclusion of vegetation in observations of rivers that are sub-pixel in width. Initial validation of results for ten randomly selected river reaches against low-cloud Landsat images have an overall accuracy of 96.1 % and a kappa statistic of 0.92. Interannual variability is clearly visible in breakup date results (Fig. 1). Out of the 1203 studied reaches, 83.0 % had no statistically significant trend (Mann Kendall test for trend, $\alpha = 0.1$). 16.3 % of reaches had a statistically significant earlier breakup trend, and 0.5 % of reaches had a statistically significant later breakup trend. Findings from this study provide the first historical record of how river ice has changed on all Alaskan rivers wider than 150 m over the last eighteen years. The methods presented here can be expanded to quantify breakup on pan-Arctic rivers.

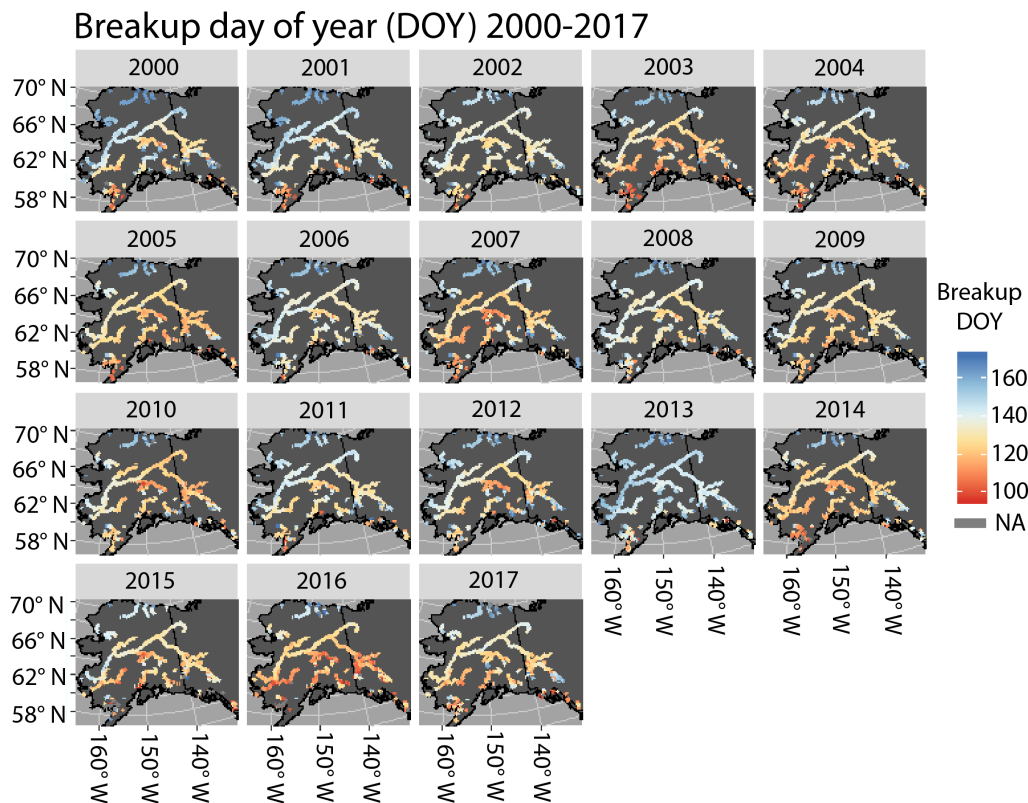


Figure 1: River ice breakup date results for Alaskan rivers wider than 150 m. Top and bottom 1 % of breakup dates are set to NA for display purposes.

Remote sensing; a key tool for understanding change in carbon storage on polar seabeds

C. Held¹, A. Fleming², D. K. A. Barnes², C. J. Sands², B. Moreno³, R. Downey⁴, M. Paulsen⁵, C. Moreau⁶, & N. Bax⁷

¹Alfred Wegner Institute, Bremerhaven, Germany;

²British Antarctic Survey, NERC, Cambridge, UK;

³Universidad Científica del Sur, Lima, Peru;

³Universidad de Concepcion, Chile;

⁴Australian National University, Canberra, Australia;

⁵Bergen University, Bergen, Norway;

⁶Universite de Bruxelles, Bruxelles, Belgium;

⁷University of Tasmania, Hobart, Australia

What little we know of high latitude southern continental shelves suggests that they provide globally important carbon capture and storage. As well as oceanographic CO₂ absorption, biological fixation and trophic cascading are important. Long term carbon stores and genuine sequestration happens at the seabed but is little understood or quantified. Most foodweb carbon is pelagic, recycled through microbial loops but significant masses are accumulated and immobilized within calcareous skeletons of benthos. Carbon storage by benthos has potential of 10⁶ tonnes per year in West Antarctic shelves alone, but we have found them to be highly variable in time and space. Remote sensing is elucidating three of the key causes of this variability,

1. marine ice change,
2. Phytoplankton bloom duration lengthening and
3. sea temperature changes.

This matters because they are all increasing carbon capture and storage in polar waters making it amongst the largest negative (mitigating) feedbacks on climate change.

European, South American and other regional scientists are collaborating on the Antarctic Circumnavigation Expedition (ACE), ICEBERGs and other projects to try to quantify benthic blue carbon storage. A bespoke deep water camera and camera-equipped trawls collected imagery, and benthos samples are allowing us to estimate changes in intra and inter-shelf

variability in benthos density and biomass. Growth models constructed from age structure of sampled species with growth check lines (e.g. bryozoans, bivalves, brachiopods) aid estimation of annual carbon accumulation. Preliminary data and analyses suggest that continental shelves of 40–60°S are globally significant, in carbon storage, and could aid error reduction in climate change. Remote sensing has allowed us to unlock the drivers in that variability – primarily sea ice losses over polar continental shelf but also ice shelf disintegration and glacier retreat.

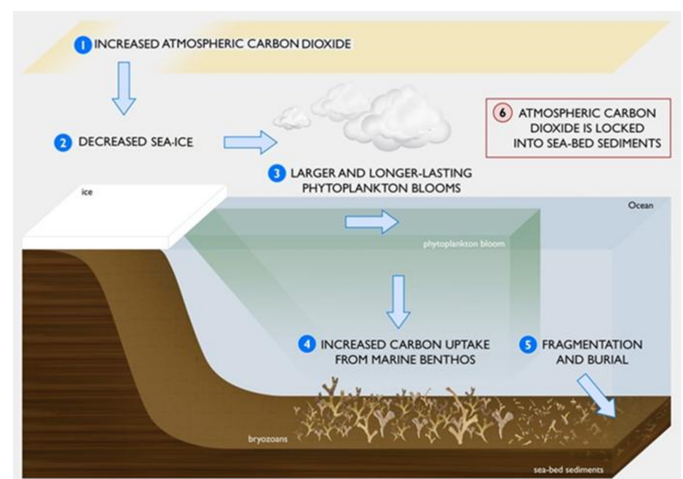


Figure 1: Carbon pathway in a changing climate. Sea ice losses around southern polar waters lead to longer algal blooms. This gives benthic animals longer meal times and increases their growth.



Remote Sensing of Arctic Sea Ice Thickness with Radar Altimeters

Stefan Hendricks¹, Robert Ricker¹, Stephan Paul^{1,2}, & Christian Haas¹

¹*Alfred-Wegener-Institut Helmholtz Zentrum für Polar und Meeresforschung;*

²*Ludwig-Maximilians-Universität München*

Sea ice thickness is one key indicator to understand the causes and consequences of Arctic Change. Climate data records (CDR's) of Arctic sea ice thickness (SIT) with sufficient length are therefore highly anticipated to complement other sub-variables of the essential climate variable (ECV) sea ice, such as concentration, area and extent. While the CryoSat-2 mission was pivotal for establishing routine sea-ice thickness retrieval from satellite altimetry, its current 8-year long data record is too short to separate climate trends from inter-annual thickness variability in the Arctic. Significant efforts have therefore been made to extend the SIT CDR by using CryoSat's radar altimeter predecessor Envisat (2002-2012) in the ESA Climate Change Initiative. Improvements in data quality from the pulse-limited radar altimeter RA-2 on Envisat to the SAR altimeter SIRAL onboard CryoSat-2 however poses a significant challenge for maintaining stability over 15 year long SIT CDR. One issue linked to the radar altimeter type is preferential sampling for mixed surface types which are more often encountered in the larger Envisat foot-

print. A separate challenge is the required stability of auxiliary parameters such as snow depth on sea ice and ice density that are required for the conversion of the freeboard measurement of the altimeter into sea ice thickness.

We discuss scientific results and error characterization for both generations of radar altimeter systems as well as strategies to mitigate intermission biases. From 2018 on, the operational availability of sea ice thickness observations is one objective of the Copernicus Climate Change Service (C3S). We will highlight plans to extend the SIT CDR into the past using the ERS-1/2 missions or beyond the lifetime of CryoSat-2 with the Sentinel-3 constellation and to use data fusion with other Earth Observation data to improve sea ice thickness information in thin ice regions. We will also outline requirements for future evolutions in satellite radar altimetry, such as the potential Polar Ice and Snow Topography mission, to both maintain the SIT CDR and evolve SIT retrieval using satellite radar altimetry.

Microwave emission of sea ice – variability of permittivity and transmissivity at interfaces

M. Huntemann^{1,2} & G. Spreen¹

¹University of Bremen;

²Alfred Wegener Institute for Polar and Marine Research

Passive microwave sensors onboard satellites have been observing the polar regions since the 1970s. Many different algorithms for the retrieval of various sea ice properties such as ice concentration, snow depth, ice type, and ice thickness have been developed and evolved over time. Most of the retrievals used today are empirical, i.e., are trained by other observational or model based data. The primary observed quantity is the emission of comprising contributions from the surface (snow, ice, water) and atmosphere. The main reasons for the absence of physical retrievals are the lack of: firstly, physical constraints, and secondly, understanding of microwave interaction with snow/sea ice.

Layer based microwave emission models for snow such as MEMLS (Microwave Emission model of Layered Snowpacks) and SMRT (Snow Microwave

Radiative Transfer) require knowledge about many input parameters for each layer, like grain size, permittivity, and temperature to determine the emitted radiation at horizontal and vertical polarization. In addition, these radiative transfer (RT) models employ certain approximation to simplify the otherwise complex calculations.

The permittivities of the snow/ice/water mainly determines the emitted radiation. While the permittivity of snow in the microwave regime is well measured and can be theoretically described, for sea ice the permittivity has a much larger variability spanning over an order of magnitude [Huntemann, 2015]. Salinity, temperature, and geometry variations of the brine inclusion in the ice are the main causes of uncertainty (Fig. 1).

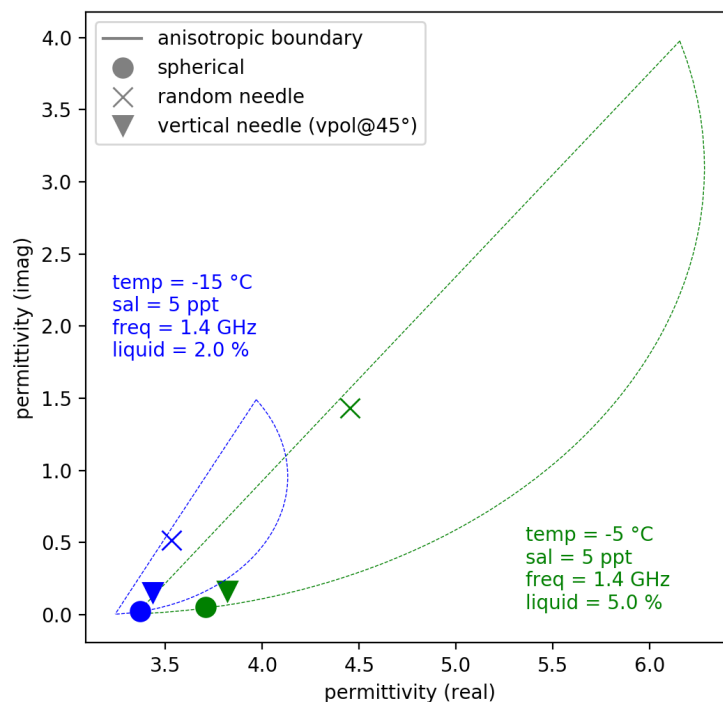


Figure 1: Permittivity of sea ice. Real part on x-axis, imaginary part on y-axis. Permittivities for different geometries of the brine inclusions in the ice (symbols) are shown for different temperatures (colors). Theoretical boundaries of the permittivities for an arbitrary inclusion shape are shown as dashed lines.

We address this variability of permittivity for low microwave frequencies (< 10 GHz) using a Monte Carlo exploration of the permittivity space, based on dielectric mixture models [Sihvola, 2000] for sea ice as a brine/ice/air composite. This allows us also to quantify the uncertainty of sea ice permittivity.

One approximation of current microwave emission model is the assumption of strict layer boundaries to calculate the transmissivity through layer interfaces simply using the Fresnel equations ignoring potential soft interfaces (i.e., gradual permittivity changes) and corresponding coherence effects.

By using a fully coherent RT model, we investigate the interface transmissivity as a function of thickness of transitional layers and frequency. Comparing coherent and incoherent RT through interfaces reveals a major discrepancy between the two methods and suggest a careful handling of layer discretizations when employing RT models.

To resolve issues with unobservable coherent oscillations, spatial variability of typical satellite footprint scales and permittivity variations of sea ice are taken into account. With this method, we are able to assess the contribution from the individual layer depths to the total emitted radiation at lower microwave frequencies.

References

- Huntemann, M. [2015]: Thickness retrieval and emissivity modeling of thin sea ice at L-band for SMOS satellite observations. PhD thesis, University of Bremen. <http://elib.suub.uni-bremen.de/edocs/00105056-1.pdf>.
- Sihvola [2010]: Mixing Rules with Complex Dielectric Coefficients. *Subsurface Sensing Technologies and Applications*, 1(4): 393–415. doi:10.1023/A:1026511515005.



Towards a reliable method for measuring arctic sea ice thickness from satellite radar altimetry during summer months

Jack Landy¹, Alexander Komarov², & Christian Haas³

¹*Bristol Glaciology Centre, University of Bristol, Bristol, UK;*

²*Data Assimilation and Satellite Meteorology Research Section, Environment and Climate Change Canada, Ottawa, Ontario, Canada;*

³*Sea Ice Physics Group, Alfred Wegener Institute, Bremerhaven, Germany*

Pan-Arctic observations of sea ice thickness have been obtained in recent years by satellite altimeters such as Cryosat-2, but traditionally these data are only available during winter months. The conventional technique for separating sea ice from water (i.e. leads within the ice pack) relies on classifying altimeter waveforms through the shape of echoes, but breaks down when meltwater ponds forming at the ice surface appear the same as leads. Our current under-

standing of basin-scale sea ice melting patterns during summer are limited to poorly-constrained ice-ocean model simulations, at a time when the ice cover is most dynamic, not to mention biological productivity and ice-ocean geochemical fluxes are most active.

Here we present first steps to develop a new method for reliably measuring the thickness of Arctic sea ice during summer using Cryosat-2 (Fig. 1).

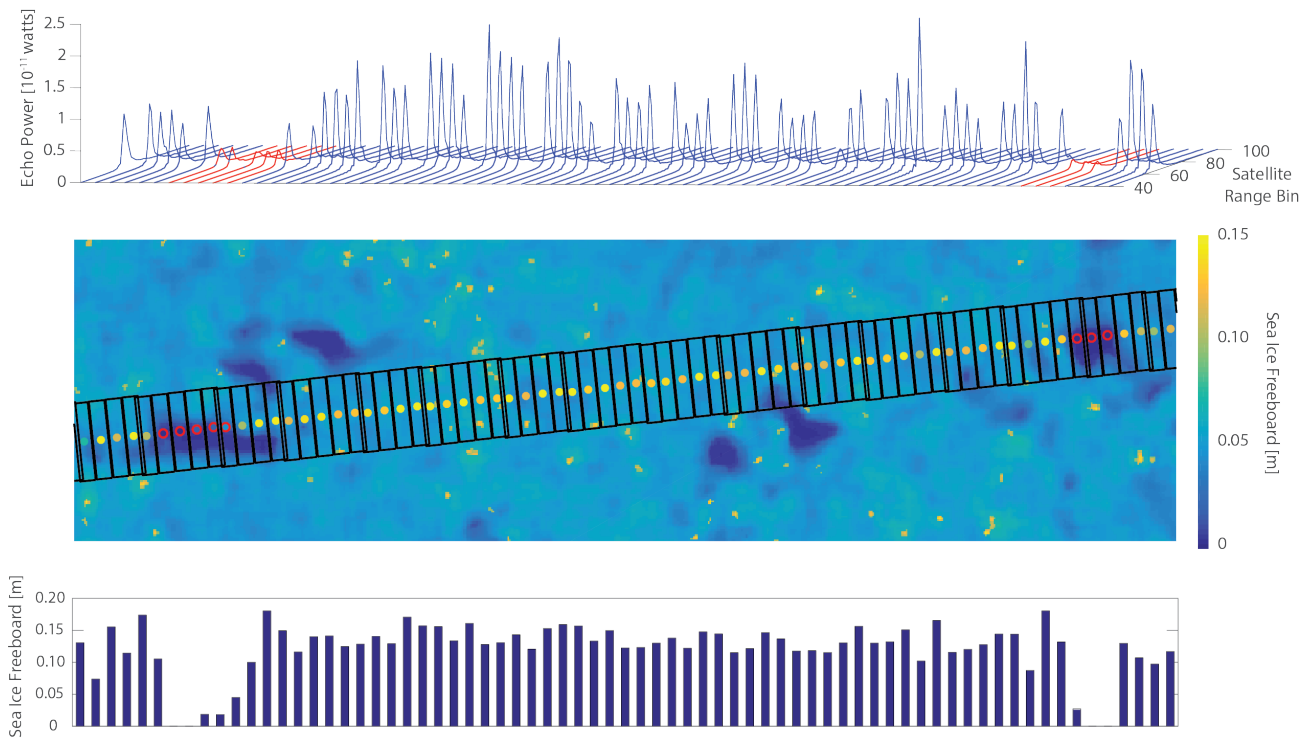


Figure 1: **a.** Series of Cryosat-2 SAR echoes, in raw linear uncalibrated power [watts], acquired over sea ice in the Chukchi Sea on 15th July 2017. Echoes with σ^0 (i.e. calibrated backscattered power) below a defined threshold are classified as leads and highlighted in red; **b.** Cryosat-2 footprints (black boxes) along the track of the satellite, with data points at footprint centres illustrating the sea ice freeboard, overlaid on a coincident Sentinel-1b HH-polarized SAR image. Both the Cryosat-2 σ^0 and surface elevation are clearly lower over leads (dark areas) in the Sentinel-1b image. **c.** Summer sea ice freeboard derived from the Cryosat-2 echoes in a and b using the new classification scheme.

A novel classification algorithm has been created for separating returns from melt ponds and leads, based on parameters of the calibrated backscatter coefficient of the radar. The algorithm is trained and tested against a set of 50+ RADARSAT-2 images acquired coincidentally to Cryosat-2 passes, which have been reliably classified into ice and ocean areas using a recently developed technique. Given the similarity between specular radar returns from melt ponds and leads, additional steps have to be taken to assess and discard altimeter echoes with strong off-nadir reflections. We use a simple threshold first-maximum retracker algorithm (TFMRA) to derive the local time-

dependent sea level anomaly from lead returns and obtain sea ice freeboard from the offset to ice floe surfaces. Ice freeboard is converted to thickness through the hydrostatic equation, accounting for uncertainty introduced by unknown surface melt pond volume.

Preliminary measurements of ice freeboard and thickness are compared to coincident airborne LiDAR observations from Operation IceBridge and Helicopter EM-bird observations, respectively. We will discuss the major uncertainties associated with sea ice ranging during summer and issues that still remain before pan-Arctic maps of summer sea ice thickness can be derived from satellite radar altimetry.

Satellite-derived changes of ice-free period in the Barents and Kara Seas coastal zones

N. Shabanova¹ & P. Shabanov²

¹*Faculty of Geography, Lomonosov Moscow State University, Moscow, Russia;*

²*Shirshov Institute of Oceanology, Russian Academy of Sciences*

It is dependable grounded that polar ice cap has being shrunk in recent 20-30 years significantly. This manifests among other things in ice-free period duration extension at the Arctic coasts. Ice-free period duration, in turn, is crucial for marine and coastal environment and development, including coastal dynamics as far as it determines coastal bluff exposition to waves and, hence, the intensity of mechanical destruction of coast by waves. If speaking about the Arctic coasts development, ice-free period is crucial for navigation period duration and as far as it is getting longer some management decisions may follow.

In the same time IFD assessment is really challenging in the Arctic due to scarce observation net and governmental limitations to data access in Russian Federation. In this situation satellite data appears as the real opportunity to study sea ice characteristics for variety of purposes.

In this work the OSI SAF sea ice concentration data product of Norwegian and Danish meteorological Institutes [EUMETSAT, 2015] is applied for ice-free period duration assessment in Barents and Kara Seas coasts (Baydaratskaya Bay, Pechora Sea, Dvinskaya Bay). It has daily temporal and 12.5 km spatial resolution and the coverage of 1979 – 2016 period. It is the only product among others with the relatively high resolution and long period covered. The difficulty of satellite data usage in coastal zones is great data contamination by the land surface signal. Due to that contamination sea ice concentration data in 2–3-pixel zone along the coast never reaches 0 or 100 % and it really makes IFD detection complicated and uncertain. Still, here we show that OSI SAF-derived IFD has mean accuracy of about 7-12 days (about 10–15 % of mean IFD) which is quite high, but enough to describe interannual variability

and long-term tendencies, as far as long-term trend is characterized by about 20-50 days (30–100 % if compared to the mean value of the 1980s, and 300–600 % for the Franz-Josef land) per 35 years. The IFP start and end dates were detected by the original analyses of sea ice concentration annual evolution curve in the nearest to the observation station OSI SAF net cell. 15 sites in the Barents and Kara Seas (including Marresalya and Varandey, where observation data are available). The method is based on the derivative analyses. Validation was made using the variety of alternating sources, namely: observation and reanalyses (CFSR) data, MODIS images, AARI ice charts and free-access reports of local hydrometeorological services about the navigation situation.

It was shown that some islands of the F-Josef land, which previously in some years were never free of ice, now are characterized by IFD of 30–50 days, what means that the coasts there are now affected by waves for a quite long time during the summer. That my manifest in coastal retreat acceleration and it can hardly be proved, as far as there were no coastal observations previously. It is revealed also that IFD evolution had variations during the 1979-2016 period, which went in-phase with other coastal erosion hydrometeorological factors like air temperature and wave-dangerous wind frequency and might result in stick-slip retreat of coasts.

References

EUMETSAT [2015]: Ocean and Sea Ice Satellite Application Facility. *Global sea ice concentration reprocessing dataset 1978–2015, (v1.2)*. Norwegian and Danish Meteorological Institutes. Available at: <http://osisaf.met.no> [accessed Oct 20, 2016].



Operational Synthetic Aperture Radar based sea ice classification

Suman Singha

Remote Sensing Technology Institute (IMF), German Aerospace Center (DLR)

Over decades, synthetic aperture radar (SAR) has become an invaluable tool for operational and scientific monitoring of ice infested maritime regions. In contrast to optical imaging, SAR is not affected by cloud coverage or lack of daylight. While air-borne and ship-borne SAR cannot always be used during adverse weather conditions, space-borne SAR image acquisition is not impeded by weather incidents and can cover almost any region on the globe with short revisit times. Satellites such as ALOS-1 and ALOS-2 in L-band, RADARSAT-1 and 2, ENVISAT and Sentinel-1 in C-band and TerraSAR-X (TS-X) in X-band have proven the usefulness of SAR sensors for investigating sea ice in Arctic and Antarctic regions. The size of SAR images extends up to a few hundred kilometers in width and length and provides much higher resolution information compared to other conventional sensors (e.g. passive microwave) and are ideal for the long term-monitoring conducted by meteorological services around the world. The operational sea ice classification processing chain is able to process all commercially available SAR images in different frequency band [Singha et al., 2018, Singha & Ressel, 2017]. Our algorithmic approach for an automated sea

ice classification consists of two steps. In the first step, we perform a polarimetric feature extraction procedure. The resulting feature vectors are then ingested into a trained neural network classifier to arrive at a pixel-wise supervised classification. During the symposium we will show examples of above mentioned products which are not only helpful for campaign planning but also might provide useful information to scientists across different scientific domains.

References

- S. Singha, A.M. Johansson, N. Hughes, and S. M. Hvidegaard [2018]: Multi Frequency Fully Polarimetric Sea ice classification and validation using Airborne Laser Scanner. *IEEE Transaction on Geoscience and Remote Sensing*, in press.
- S. Singha and R. Ressel [2016]: Arctic Sea Ice Characterization using RISAT-1 Compact-Pol SAR Imagery and Feature Evaluation: A Case Study Over North-East Greenland. *IEEE Journal of Selected Topics in Applied Earth Observations and Remote Sensing*, Volume 10, Issue 8, Pages 3504–3514. doi:[10.1109/JSTARS.2017.2691258](https://doi.org/10.1109/JSTARS.2017.2691258).



SESSION

Glaciers and Ice Sheets

Detecting and monitoring ice-shelf basal mass balance in Dronning Maud Land, East Antarctica

Sophie Berger¹, Veit Helm¹, Niklas Neckel¹, Nils Dörr¹, Reinhard Drews², Frank Pattyn³, & Olaf Eisen¹

¹Alfred Wegener Institut;

²Earth System Sciences, Tübingen University;

³Laboratoire de glaciologie, Université libre de Bruxelles

Ice shelves control the dynamic mass loss of ice sheets through buttressing. Their integrity also depends on their total mass balance, with the spatial variability of their basal mass balance (BMB), i.e. the difference between basal refreezing and melting, being an important component. Here, we present an improved technique – based on satellite observations – to capture the small-scale variability in the BMB of ice shelves.

We use mass conservation in a Lagrangian framework based on high-resolution horizontal surface velocities, atmospheric-model surface mass balance and hydrostatic ice-thickness fields (derived from TanDEM-X surface elevation). Spatial derivatives are implemented using the total-variation differentiation, which preserves abrupt changes in flow velocities and their spatial gradients. Such changes may reflect a dy-

namic response to localized basal melting and should be included in the mass budget.

After successfully developing the technique with TanDEM-X elevations from 2013-2014 for the Roi Baudouin Ice Shelf, Dronning Maud Land, East Antarctica (Fig. 1), we upscaled our results spatially to all ice shelves in Dronning Maud Land that are located between Fimbul and Roi Baudouin ice shelves. The BMB field we produce shows a large-scale pattern in close agreement with previous studies in coarser resolution. However, our results also indicate that we are in addition able to detect small-scale features in the BMB with unprecedented detail (at a gridding of <50 m). Beyond the static field of BMB we also investigate temporal changes in the BMB by combining our BMB based on TanDEM-X elevations with coarser BMB based on Cryosat-2 data.

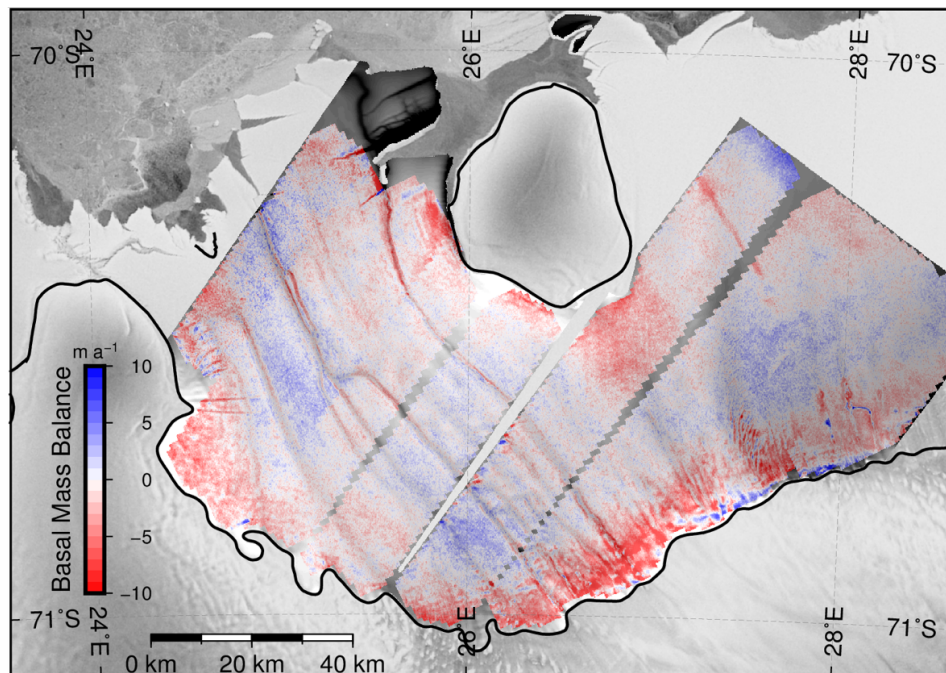


Figure 1: Lagrangian basal mass balance of the Roi Baudouin Ice Shelf, East Antarctica

Sub-glacial bedrock topography of Austfonna, Svalbard derived from potential field modeling

M.-A. Dumais^{1,2} & M. Brønner^{1,2}

¹*Geological Survey of Norway;*

²*Norwegian University of Science and Technology*

Ice caps in the polar regions are often referred to as an important visual expression of the Earth's climate change. A comprehensive monitoring of the polar ice coverage and thickness changes is significant to understand the magnitude of this environmental impact. While satellite observation methods are sufficient to estimate ice sheet surface and elevation change, they fail to provide direct ice thickness measurements or bedrock physical properties which can be relevant to understand the glacier dynamics.

Air- and ground borne ice penetrating radar measurements supply ice thickness estimation but the process is temperature-dependent, which introduces uncertainties. To remedy to this, we propose to include airborne gravity measurements. Due to a significant density contrast between ice and bedrock, sub-glacial topography and ice thickness can be effectively derived from gravity modeling when combined with accurate and reliable altimetry data.

Specifically, Austfonna, on Svalbard archipelago, the largest ice cap in Norway, has been investigated by aero-gravity and -magnetic data to retrieve the sub-glacial topography. Furthermore, interpretation of these so-called potential field data improves our knowledge of the geophysical properties of the sub-surface. This valuable information to quantify the subsurface is especially useful where geological exposures are sparse and on remote and difficult terrains such as Nordaustlandet where Austfonna and several other glaciers lay.

Geophysical parameters and the bedrock topography are quantified with a forward modelling along flown gravity lines. Topographic measurements constrain the model and the synthetic signal output is compared to the free-air and magnetic anomaly. While

the ice thickness model relies primarily on the gravity data, the magnetic signature provides an extra insight of the basement distribution. This contributes to refine the range of density expected under the ice and allow the improvement of the sub-ice model. From this study, a prominent magmatic intrusion is modeled crossing Austfonna from North to South. The model also leads to the sub-surface being characterized with different basement affinities.

With the geophysical parameters of the bedrock defined, the ice thickness and the bedrock topography is extracted. For accuracy and resolution assessment, the resulting bedrock topography is compared to independent bed elevation map previously produced by radio echo sounding (RES) and ground penetrating radar (GPR) data. Discrepancies are pronounced where the RES and GPR data are scarce. Hence, areas with limited coverage are addressed with gravity interpretation, increasing the accuracy of the overall bedrock topography. The bedrock topography (including cavities and obstacles), geothermal sources and the presence of sediments are contributing factors to the glacier basal sliding velocities. Moreover, surge-type glaciers are observed on Austfonna. Numerous statistical studies link surge mechanism to the softness of the bedrock and tectonically active zones. The preliminary results indicate a possible correlation between basal sliding velocity distribution modelled and the bedrock lithology of Austfonna.

Therefore, in addition to improve the understanding of the geology, the magnetic and gravity interpretation also yielded to an enhanced bedrock topography and offered a better control of the physical properties of the bedrock underneath Austfonna in relation to the basal sliding and thermal regime.

Decadal changes of glacial extents and snowline altitude of the Batura Glacier, Karakoram: Classification and spectral unmixing of remote sensing data

A. Mueting, B. Bookhagen, & T. Smith

Institute for Earth and Environmental Sciences, Universität Potsdam, Potsdam, Germany

Located in the Karakoram mountains in northern Pakistan, the Batura glacier is one of the longest and largest glaciers in the middle to low latitudes. Glaciers in the Karakoram have been characterized by stable or even positive mass balances, as well as advancing glacier termini in recent years, illustrating that the response of glaciers to global climate changes is not uniform.

We conducted semi-automated area measurements for the Batura glacier over a time span of 21 years using multi-spectral satellite imagery. Additionally, two different spectral unmixing methods (linear spectral unmixing (LSU) and multiple endmember spectral analysis (MES-MA)) were applied to distinguish snow, ice, and debris coverage. The snow endmember identifies the snowline altitude and extent of the glacier's accumulation zone.

Preliminary results indicate a 6.4 % loss in glacial area between 1996 and 2017, with a decline rate of $1.44 \pm 0.18 \text{ km}^2/\text{yr}$ based on $n = 9$ Landsat TM and OLI images. Whereas the glacier did not show great changes in surface area between 1996 and 2008, decline rates rapidly increased throughout the following years, with a significant drop between 2013 and 2014, and a slight recovery in 2017. Snow and ice covered

areas reduced by 11.4 % with a decline rate of $1.46 \pm 0.21 \text{ km}^2/\text{yr}$. Further analysis on additional satellite images will be used to verify these results.

In contrast to the areal decline, the glacier terminus advanced by about 300 m within the same period. However, terminal fluctuations do not always follow climatic variations and often represent internal glacial variability. The loss in surface area reflects the worldwide trend of shrinking ice caps, even though the rate at which the Batura glacier retreated is quite moderate.

Spectral unmixing revealed an apparent lowering of the snowline by 543 m (LSU) or 567 m (MESMA), while the size of the accumulation zone remained stable. As visible snow limits are highly variable, these results must be considered with care. Nevertheless, both unmixing methods were found to be very useful for determining endmember fractions within a glacier.

Our study documents the disequilibrium dynamics of the Batura glacial system: moderately declining glacial areas and lowering of snowlines which are possibly linked to increased winter precipitation at high elevations and avalanching.

Multi-temporal analysis of the Greenland Ice Sheet based on TanDEM-X DEM data between 2010 and 2017

Christian Wohlfart, Sahra Abdullahi, Birgit Wessel, Martin Huber, Tobias Leichtle, & [Achim Roth](#)

German Aerospace Center (DLR), Earth Observation Center (EOC), Münchner Str. 20, 82234 Wessling, Oberpfaffenhofen, Germany

The Greenland ice sheet represents the world's largest ice mass outside Antarctica covering an area of approximately 1.7 million km². During the last decades, observations reveal dramatic changes, which can be attributed to anthropogenic induced global warming with considerable implications for environment and human society. The melting of the entire Greenland ice sheet would raise global mean sea level by 7.36 m. In view of this, it is crucial to understand spatial and temporal glacial dynamics for determining the contributions to sea level rise and predicting responses to climate change. Interferometric SAR based Digital Elevation Models (DEMs) are powerful techniques to collect information on glaciers and ice sheets worldwide, particularly in polar regions located in high latitudes. To date, multi-date DEMs at high spatial resolution is lacking for entire Greenland. Existing DEM products are either outdated or show low spatial resolution, often mono-temporal. The German TanDEM-X satellite mission offers great potential for monitoring of the Earth's polar regions at unprecedented spatial resolution due to the global availability of consistent and precise interferometric data. However, so far TanDEM-X data have been

mainly used on local scales. The first goal of this study is to provide a novel change detection analysis for the entire Greenland ice sheet at 12 m spatial resolution using TanDEM-X interferometric acquisitions between 2010 and 2017. One major issue with X-band SAR data is related to penetration of the signal into the snow and ice surface, which influences significantly the height accuracies of the delineated DEM. Therefore, we defined a second goal, which aims to investigate the X-band penetration over different snow and ice characteristics to correct possible elevation bias. As a reference, we used IceBridge ATM L2 Elevation data from spring 2012 to analyze the penetration depth over different snow zones, which are determined by specific physical parameters (grain size, snow density, stratigraphy, surface roughness, and water content), which influence the SAR backscatter. Our results reveal penetration depths up to ten meters and a high correlation between penetration depth and backscatter intensity as well as interferometric coherence and height of ambiguities. This information can help to improve vertical accuracy of TanDEM-X data over the Greenland ice sheet to obtain more reliable elevation change from different time spans.



SESSION

New Sensors and Operational Services

A webcam network, open data and free toolbox for monitoring phenology and snow cover

Ali Nadir Arslan¹, Cemal Melih Tanis¹, & Mikko Peltoniemi²

¹*Finnish Meteorological Institute, Erik Palménin aukio 1, P.O.Box 503, FI-00101 Helsinki, Finland;*

²*Natural Resources Institute Finland, Viikinkaari 4, FI-00790 Helsinki, Finland*

In this paper, we present newly established webcam monitoring system in Finland for monitoring phenology and snow cover. Main motivation of this work is to facilitate Earth Observation (EO) systems by providing time-series of field observation for calibration and validation, as well as to improve the assessment of ecosystem services. Images have been used in phenological analyses of birches along a latitudinal gradient across Finland, snow cover and compared to greenhouse gas fluxes on Scots pine and wetland ecosystems. Finnish Meteorological Institute image PROcessing Toolbox (FMIPROT) is developed to analyse the images for the extraction of environmental data. The Images from the camera network, producing a continuous image series in Finland, are used in the analysis of Fractional Snow Cover (FSC) using FMIPROT. We discuss on estimation of FSC using digital imagery and utilizing the digital imagery to complement FSC retrieval algorithms from remote sensing data and/or to validate Earth-observed FSC. The webcam network is established within EU Life+ MONIMET project during 2013-2017. Cameras were mounted at 14 sites, each site having 1-3 cameras. The detail information on cameras, installations and site can be found in our recent paper [Peltoniemi et al., 2018]. In the paper, we documented image data repository consisting of half-hourly images collected between 2014 and 2016, and presented example colour index time series derived from image time series from two contrasting sites. To distribute image time series, we established a community (Phenological time lapse images and data from MONIMET EU Life+ project (LIFE12 ENV/FI/000409) in Zenodo service (<https://www.zenodo.org/>) that is meant for permanent archiving and distribution of research materials. Finnish Meteorological Image PROcessing Tool (FMIPROT) is developed for analysing digital images from multiple camera networks for various applications such as vegetation phenology and monitoring of snow cover. The toolbox has a user-friendly graphical user interface (GUI) which only minimal computer knowledge

and skills are required to use it. Current features are automatic installations, automatic image downloading and handling, GUI, GUI based selection a region of interest (ROI), automatic analysis chain, GUI based plotting, ROI based indices such as green fraction index (GF), red fraction index (RF), blue fraction index (BF), green-red vegetation index (GRVI), green excess (GEI) index as well as brightness and luminance. Importantly, the user is allowed to implement own developed algorithms to extract information from digital image series for any purpose. FMIPROT is freely available from <http://fmiprot.fmi.fi>. We have applied a technique for retrieving temporally very frequent information on the local site-specific FSC, using a network of digital cameras. Based on our results, we conclude that snow cover could be analyzed with consumer grade cameras [Arslan et al., 2017]. The results obtained from automated image analysis of snow cover are compared with reference data estimated by visual inspection of same images. Comparison of estimated FSC and the reference FSC was conducted using the original continuous values, and also by category, in order to present the success rate of the algorithm applied in classifying the images.

References

- Peltoniemi, M., Aurela, M., Böttcher, K., Kolari, P., Loehr, J., Karhu, J., Linkosalmi, M., Tanis, C. M., Tuovinen, J.-P., and Arslan, A. N. [2018]: Webcam network and image database for studies of phenological changes of vegetation and snow cover in Finland, image time series from 2014 to 2016. *Earth Syst. Sci. Data*, 10, 173–184. doi:[10.5194/essd-10-173-2018](https://doi.org/10.5194/essd-10-173-2018), 2018.
- A.N. Arslan, C.M. Tanis, S. Metsämäki, M. Aurela, K. Böttcher, M. Linkosalmi, and M. Peltoniemi [2017]: Automated Webcam Monitoring of Fractional Snow Cover in Northern Boreal Conditions. *Geosciences*, 7(3): 55. doi:[10.3390/geosciences7030055](https://doi.org/10.3390/geosciences7030055).

Circumpolar to global remote sensing of permafrost – contributions of ESA DUE GlobPermafrost to a permafrost information system

A. Bartsch¹, G. Grosse², A. Kääb³, S. Westermann³, T. Strozzi⁴, A. Wiesmann⁴, C. Duguay⁵, F. M. Seifert⁶, J. Obu³, I. Nitze², B. Heim², A. Haas², S. Laboor², S. Muster², & B. Widhalm¹

¹Zentralanstalt für Meteorologie und Geodynamik, Vienna, Austria;

²Alfred Wegener Institute Helmholtz Center for Polar and Marine Research, Potsdam, Germany;

³Department of Geosciences, University of Oslo, Oslo, Norway;

⁴Gamma Remote Sensing, Gümligen, Switzerland;

⁵DH2O Geomatics, Canada;

⁶ESA - ESRIN, Italy

Coarse resolution soil moisture datasets are available globally. Their utilization in permafrost areas is however limited due to heterogeneity within the footprint. Validation across the Arctic does also not exist due to only very few monitoring sites which measure soil moisture. There is in addition the discrepancy between typical measurement depth and satellite data representativeness.

C-band scatterometer information is of specific interest in heterogeneous environments due to the availability of higher spatial resolution Synthetic Aperture Radar (SAR) data at this wavelength. The C-band scatterometer ASCAT (on board of several Metop platforms) provides operational data in near real time since 2007. The microwave backscatter variations are expected to correspond to soil moisture variations. Surface roughness and volume scattering, which also contribute to the backscatter signal, are parameterized or assumed to be constant under certain conditions. This provides the basis for a global near surface soil moisture product available through EUMETSAT.

We designed a monitoring set-up for measuring moisture very close to the surface in the Lena River

Delta, Siberia to specifically investigate Metop ASCAT derived surface soil moisture. Four sites have been covered representing two different ASCAT footprints and settings. Samoylov Island is dominated by a polygonal wet tundra landscape. The Yedoma landscape unit Kurungnakh is located only a few kilometres south from Samoylov Island. The measurement stations were installed in August 2013 on Kurungnakh and Samoylov and data were collected in August 2014. Three stations were placed on Kurungnakh and one on Samoylov. The Volumetric Water Content (VWC) and temperature sensors have been in the moss organic layer in order to account for the limited penetration depth of the signal. VWC measured at the different sites within the Lena Delta correlate well with each other. This indicates representativeness of single station records for ASCAT validation regarding temporal patterns. ASCAT backscatter variations are in general very small, in line with low variability of in situ VWC. Short term changes after complete thaw of the upper organic layer seem to be however mostly influenced by temperature.

FireBIRD- High Dynamic Range Thermal Infrared Satellite Systems for hot and cold temperature environments

C. Fischer, T. Bucher, Thomas Säuberlich, & W. Halle,

DLR – German Aerospace Center, Institute of Optical Sensor Systems, Berlin, Germany

FireBIRD is a satellite constellation of the German Aerospace Center (DLR) consisting of two small satellites, TET-1 (Technology Experiment Carrier) and BIROS (Berlin InfraRed Optical System), which were initially designed for high temperature anomaly detection and characterization of wildfires [Wooster et al. \[2003\]](#). The main payload of both satellites consists of VIS (RGB) and Infrared (IR) camera systems with one band in the mid-wave (MWIR) and one band in the longwave-infrared (LWIR) spectral range. Both satellites are flying sun-synchronously in a low-earth orbit at approximately 500 km altitude. With a ground sampling distance (GSD) of ≈ 170 m the spatial resolution of the TIR channels is rather high compared to MODIS or Sentinel-3. Additionally, the high agility and $\pm 30^\circ$ across-track pointing capability of the satellites allow image acquisition on several consecutive days and guarantee a repetition rate of 5 days. The BIROS IR sensor system has been optimized enabling the system also to acquire images for areas with comparable low surface temperatures as well. Background land-surface temperature can be measured accurately. [Mettig et al. \[2017\]](#) has shown the ability of FireBIRD for sea surface temperature (SST) monitoring. Recent activities, also with the Alfred-Wegener Institute (AWI) in Potsdam, include the multi-temporal acquisition of data over different test sites, located in Russian and Alaskan polar regions, including the Lena and Pechora delta and Lake Toolik to evaluate the ability of the system to measure temperatures and geomorphologic changes in permafrost regions. The relatively high spatial resolution combined with a potentially high repetition rate offer a chance to fill the gap of multi-temporal high spatial resolution input data for monitoring of permafrost processes and climate modelling.

Acquired imagery is processed and archived by DLR and is publicly available.



Figure 1: MWIR and LWIR BIROS images of Greenland (11.04.2017).

References

- Wooster, M., Zhukov, B. & D. Oertel, D. [2003]: Fire radiative energy release for quantitative study of biomass burning: Derivation from BIRD experimental satellite and comparison to MODIS fire products. *Remote Sensing of Environment*, 86: 83–107. doi:[10.1016/S0034-4257\(03\)00070-1](https://doi.org/10.1016/S0034-4257(03)00070-1).
- Mettig, N., Reulke, R., Fischer, J., Preusker, R. & E. Lorenz [2017]: Sensitivitätsstudie zur Bestimmung der Meeresoberflächentemperatur aus Messungen des Satelliten TET-1. In: *Publikationen der DGPF*, 26. 37. Wissenschaftlich-Technische Jahrestagung der DGPF, Würzburg.

A customized airborne optical remote sensing system for polar environments

T. Bucher¹, J. Brauchle¹, & T. Steinhage²,

¹*DLR – German Aerospace Center, Institute of Optical Sensor Systems, Berlin, Germany;*

²*Alfred Wegener Institute Helmholtz Centre for Polar and Marine Research, Bremerhaven, Germany*

The DLR Institute of Optical Sensor Systems has developed a Modular Aerial Camera System specifically designed for extreme environmental conditions (MACS-POLAR). It is integrated on the AWI Polar-5 research aircraft for permafrost campaigns in Alaska and Canada in summer 2018.

MACS is a modular family of project-customized aerial camera systems adapted to specific scientific and operational requirements. Based on the MACS-Himalaya, a system designed for the extreme radiometry and geometry of high mountain ranges, the design of the MACS-POLAR has maintained its robustness (low temperature, low pressure). It comprises a High Dynamic Range (HDR)-Mode for extreme contrast (ice, snow, dark rocks) and a high frame rate for fast velocities and low flight paths, still maintaining sufficient image overlap for 3D-reconstruction.

The optical design consists of two overlapping tilted RGB camera heads and a nadir looking near-infrared (IR) camera (ground sampling distance RGB: 9 cm; IR: 15 cm @ 1000 m above ground). The sensor head can be separated from the processing unit to enable installation in small compartments (Fig. 1).

In the system small and lightweight industrial grade camera heads are used. Direct georeferencing, real-time processing of image mosaics and multitemporal

monitoring without the need of ground control points is possible due to the use of its GNSS (Global Navigation Satellite System) and INS (Inertial Navigation System) units. The operation of the system is highly automated, a remote real-time mission control and access to the images during data acquisition is given to the operator if needed.

Products such as dense point clouds, Digital Surface Models and true orthomosaics will be used for scientific analysis of permafrost regions. Near real-time mosaics can be used during the campaign for quality control and planning of ground campaigns.

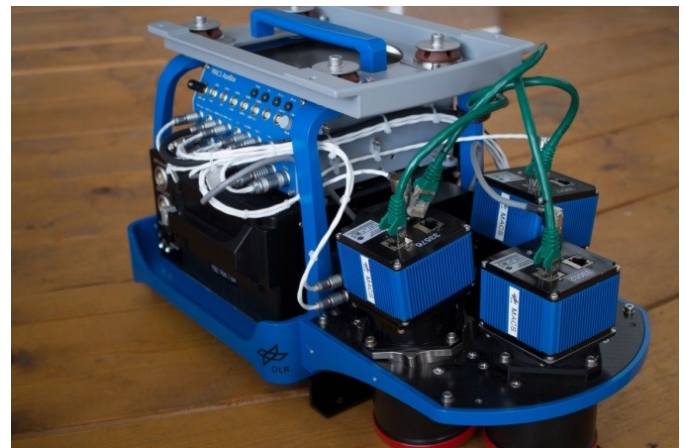


Figure 1: MACS-POLAR camera head (front part), processing unit can be separated.



PerSys – WebGIS-based permafrost data visualisation system for ESA GlobPermafrost

Antonie Haas¹, Andreas Walter¹, Birgit Heim¹, Guido Grosse^{1,2}, Sina Muster¹, Sebastian Laboor¹, Antonia Immerz¹, Christian Schäfer-Neth¹, Annett Bartsch³, & Frank Martin Seifert⁴

¹*Alfred Wegener Institute Helmholtz Centre for Polar and Marine Research, Germany;*

²*Institute of Earth and Environmental Sciences, University of Potsdam, Germany;*

³*Zentralanstalt für Meteorologie und Geodynamik ZAMG, Austria;*

⁴*European Space Agency ESRIN, Italy*

ESA DUE GlobPermafrost provides a remote sensing data service (<http://globpermafrost.info>) for permafrost research and applications. This service comprises of the generation of remote sensing products for various regions and spatial scales, and specific infrastructures for visualisation, dissemination and access to datasets. PerSys is the ESA GlobPermafrost geospatial information service for publishing and visualisation of information and data products to the public. Data products are described and searchable in the PerSys Data Catalogue, a core component of the Arctic Permafrost Geospatial Centre (APGC), established within the framework of ERC PETA-CARB at AWI. The data visualisation employs the AWI WebGIS-infrastructure maps@awi (<http://maps.awi.de>), a highly scalable data visualisation unit within the AWI data-workflow framework O2A, from Observation to Archive.

WebGIS technology in maps@awi supports the project-specific visualisation of raster and vector data products of diverse spatial resolutions and remote sensing sources. This is a prerequisite for the visualisation of the wide range of GlobPermafrost remote sensing products like: Landsat multispectral index trends (Tasseled Cap Brightness, Greenness, Wetness; Normalized Vegetation Index NDVI), Arctic land cover (e.g., shrub height, vegetation composition), lake ice

grounding, InSAR-based land surface deformation, rock glacier velocities and a spatially distributed permafrost model output with permafrost probability and ground temperature per pixel. All WebGIS projects are adapted to the products specific spatial scale. For example, the WebGIS “Arctic” visualises the Circum-Arctic products. Higher spatial resolution products for rock glacier movements are visualised on regional scales in the WebGIS projects “Alps”, “Andes”, and “Central Asia”.

GIS services were created and designed using ArcGIS for Desktop (10.4) and finally published as a Web Map Service (WMS), an internationally standardized format (Open Geospatial Consortium (OGC)), using ArcGIS for Server (10.4). The project-specific data WMS as well as a resolution-specific background map WMS are embedded into a GIS viewer application based on Leaflet, an open-source JavaScript library. The GIS viewer application was adapted to interlink all WebGIS projects, and especially to enable their direct accessibility via the GlobPermafrost Overview WebGIS project. The PerSys WebGIS is accessible via the GlobPermafrost project webpage and linked to the respective product groups as well as on maps@awi (<http://maps.awi.de>). All GlobPermafrost data products will be DOI-registered and archived in PANGAEA.

Remote sensing the ocean-induced magnetic field in polar regions

Christopher Irrgang¹, Jan Saynisch¹, Johannes Petereit^{1,2}, & Maik Thomas^{1,2}

¹*Helmholtz Centre Potsdam GFZ German Research Centre for Geosciences;*

²*Institute of Meteorology, Freie Universität Berlin*

Ocean currents generate characteristic magnetic fields by interactions between the electrically conducting seawater and the geomagnetic field generated in the Earth's core (see Fig. 1). These oceanic magnetic signals are emitted outside of the ocean and can be recorded with different remote sensing techniques, e.g., ESA's low-Earth-orbiting Swarm satellites, or terrestrial magnetometers. We present an overview of the manifold opportunities that arise from observing oceanic magnetic signals.

Space-borne observations of the magnetic field induced by the general ocean circulation could provide new constraints on oceanic water and heat transports. These, in turn, can be used to correct and to improve numerical simulations of the general ocean circulation. We have investigated this novel opportunity in an observing system simulation experiment (OSSE) by assimilating synthetic satellite observations of the ocean-induced magnetic field into an ocean general circulation model [Irrgang et al., 2017]. A further perspective is given by magnetic signals that are generated by the well-known periodic ocean tides. These are predominantly sensitive towards spatio-temporal changes in ocean heat and salinity. Thus, long time series of oceanic magnetic signals allow to indirectly monitor climate change processes in the ocean, e.g., fresh water fluxes into the ocean due ice sheet melting [Saynisch et al., 2017].

In addition to space-borne observation systems, we propose to deploy high-precision magnetometers on top of ice shelves. Oceanic ice is (thermo)dynamically coupled to the underlying sea-water. However, the oceanographic conditions under the ice are not well known and melting processes are not yet fully understood. Respective observations under the ice are very expensive and risky. Our technique is less expensive, less restrictive, and less risky compared to traditional terrestrial approaches. Through the ice, the magnetometers can detect magnetic fields induced by tidal waves. The signals are sensitive towards depth, trans-

port, and conductance of the sea-water below. Deviations in temporal behavior of the magnetic signals could be inverted for horizontal conductance gradients under the ice, which may give information about local melt rates and runoff. If the water depth is known, the signals can be converted to large-scale oceanic conductance. Sustained observations in the same location will reveal climate-change-induced conductance trends and can provide validation data for current and future satellite missions.

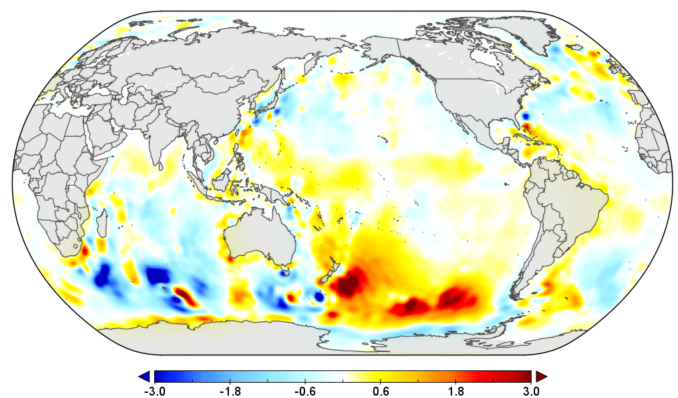


Figure 1: Ocean circulation induced magnetic field [nT].

References

- Christopher Irrgang, Jan Saynisch, and Maik Thomas [2017]: Utilizing oceanic electromagnetic induction to constrain an ocean general circulation model: A data assimilation twin experiment. *J. Adv. Model. Earth Syst.*, 9(3): 1703–1720. doi:[10.1002/2017MS000951](https://doi.org/10.1002/2017MS000951).
- Jan Saynisch, Johannes Petereit, Christopher Irrgang, and Maik Thomas [2017]: Impact of global warming on electromagnetic oceanic tidal signals – a CMIP5 climate model based sensitivity study. *Geophys. Res. Lett.*, 44. doi:[10.1002/2017GL073683](https://doi.org/10.1002/2017GL073683).

The Data Catalogue of the Permafrost Information System PerSys – An Open Access geospatial data dissemination and visualization portal for products from ESA DUE GlobPermafrost

Sebastian Laboor¹, Guido Grosse^{1,2}, Sina Muster¹, Birgit Heim¹, Antonie Haas¹, Christian Schäfer-Neth¹, Ingmar Nitze¹, Annett Bartsch³, & Kirsten Elger⁴

¹Alfred Wegener Institute Helmholtz Centre for Polar and Marine Research, Germany;

²Institute of Earth and Environmental Sciences, University of Potsdam, Germany;

³Zentralanstalt für Meteorologie und Geodynamik ZAMG, Vienna, Austria;

⁴Helmholtz Centre Potsdam – GFZ German Research Centre for Geosciences, Potsdam, Germany

Abstract

The objective of the GlobPermafrost Project (2016–2019) initiated by the European Space Agency (ESA) is to better understand the global impact of changes in permafrost by providing earth observation data for the science community. For this purpose, various remote sensing products on the subject of permafrost are developed, discussed and optimized with the users of these products. The Permafrost Information System (PerSys) was developed for the user-friendly provision and visualization of these data products and is part of the Arctic Permafrost Geospatial Center (APGC). PerSys allows users to conveniently search for permafrost related datasets, obtain metadata and previews, receive information on data prototypes and download the final published data products.

Introduction

Remote sensing has become an essential tool for quantitatively detecting and monitoring changes in permafrost landscapes over large regions and with repeated observations. The European Space Agency (ESA) has supported permafrost-focused remote sensing activities in two recent projects, ESA DUE Permafrost (2009–2012) and ESA DUE GlobPermafrost (2016–2019; <http://globpermafrost.info>). The Permafrost project validated and implemented earth observation data to support research communities and international organizations in their work on better understanding permafrost characteristics and dynamics. Now, the GlobPermafrost project expands on this successful approach by including both polar hemispheres as well as mountain permafrost regions. Here, we present the PerSys Data Catalogue (Fig. 1).

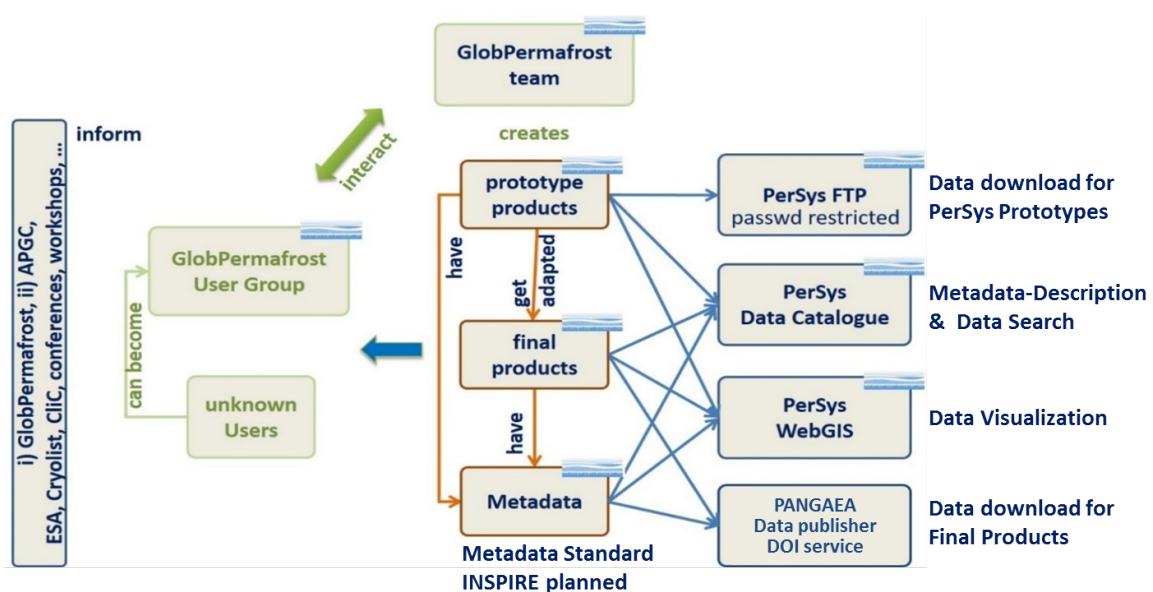


Figure 1: PerSys conception



The PerSys Data Catalogue

To bring the resulting data products of GlobPermafrost closer to the permafrost user communities, PerSys has been conceptualized as an open access geospatial data dissemination and visualization portal for remote sensing derived datasets produced within the GlobPermafrost project. The prototype and final remote sensing products and their metadata are documented in the PerSys Data Catalogue and visualized in the PerSys WebGIS. PerSys provides access to all mature-state and final-state GlobPermafrost products and their metadata.

The catalogue is available within APGC since early 2017 (<http://apgc.awi.de>). The APGC framework features a range of permafrost-specific geospatial data projects, including PerSys, and allows searching for project-specific geospatial data by tags, keywords, data type and format, license type, or by location.

In addition, the Open Access data library PANGAEA serves as permanent archive for the GlobPermafrost final products, providing permanent Digital Object Identifiers (DOIs) for each archived dataset. Products currently featured in the catalogue include circum-arctic land surface temperature from 2007–2013, Landsat-based trend analysis of land surface indices (NDVI, NDWI etc.), high- and medium-resolution waterbody inventories, and many more.

The final GlobPermafrost remote sensing products published in PANGAEA will remain catalogued, searchable and accessible via the PerSys Catalogue.

Acknowledgments

This work was supported by the European Space Agency project DUE GlobPermafrost (Contract Number 4000116196/15/I-NB) as well as ERC PETA-CARB # 338335.

From basic research to application – technology transfer from AWI

E. J. Sauter¹, L. Rabenstein², B. Heim³, & E. Precht¹

¹*Alfred Wegener Institute, Helmholtz Center for Polar and Marine Research, Technology Transfer Office, Bremerhaven, Germany;*

²*Drift & Noise Polar Services GmbH, Bremen, Germany;*

³*Alfred Wegener Institute, Helmholtz Center for Polar and Marine Research, Research Group Polar Terrestrial Environmental Systems, Potsdam, Germany*

For a responsible development of the Arctic, new remote sensing technologies and services are of great importance. Many of such innovations are based on scientific research. However, it is not trivial that they find their way into application. In order to ease this kind of transfer across the interface between academia and industry, the Alfred Wegener Institute has established a technology transfer office (TTO). The TTO takes up inventions and business ideas emerging from scientific research and supports innovators and entrepreneurs to progress them into the respective markets. The other way round, the TTO serves as the contact point for stakeholders from industry, governmental and non-governmental bodies to forward specific problems into the scientific community.

Here we present two examples to illustrate the AWI technology transfer approach:

1) Planned for 2022, the German hyperspectral earth observation satellite EnMAP (Environmental Mapping and Analysis Programme) will measure the reflected radiance from the earth's surface over a wide hyperspectral wavelength range (from visible to short wave infrared). In order to provide correct hyperspectral satellite products such as land cover (natural surfaces, urban), surface waters, surface mineralogy, hydrology (snow, moisture) etc. in a correct manner, it is necessary to normalize for the incidence and the reflection of light depending on the zenith and azimuth viewing geometries. This is performed by providing the bidirectional reflectance distribution function BRDF for different materials. Determination of BRDFs for terrestrial surfaces is very challenging especially for high latitudes due to the low solar altitude. For Arctic vegetation mapping, a spe-

cific satellite field goniometer was developed at AWI to perform such ground truthing [Buchhorn et al., 2013]. The goniometer allows for mobile ground-based measurements in order to determine the BRDF for different vegetation types. It consists of an azimuth angle adjustment module mounted on a tripod with a zenith arc with sensor sled equipped with two portable spectro-radiometers, a GPS receiver, an NC-Eye camera system and a white reference panel (Fig. 1a). The goniometer was prototyped, patented and licensed to a precision mechanics manufacturer. The commercial system in this case addresses the scientific community and specialized service providers.

2) Starting with geophysical ice thickness measurements on sea-ice and using air-borne electromagnetic measuring systems [Krumpfen et al., 2011] a group of AWI scientists developed specific sea-ice related services for scientific, governmental and private sector customers operating in Arctic sea-ice. Subsequently the AWI spin-off Drift & Noise Polar Services was established in 2014. The new business was developed towards near real-time remote sensing ice information products and sea-ice consultancy for safer and faster navigation through ice-covered waters. Ice charts and weather information are generated from SAR and optical imagery (e.g. Sentinel 1 and 2). Since reliable broadband data transfer channels do not exist, particularly for high latitudes, the start-up also develops appropriate data compaction and transfer protocols combined with hand-held mobile systems (Fig. 1b) for nautical officers which allow for near real-time access to latest ice data onboard ship. Thus shipping companies are able to save time and fuel by adapting their route while increasing safety.

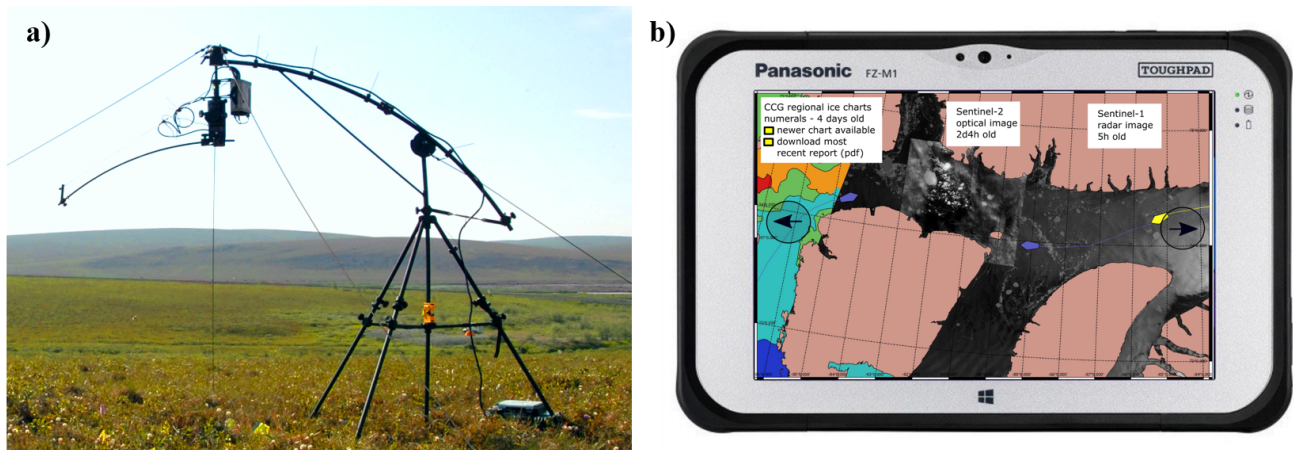


Figure 1: (a) Portable field spectro-goniometer for EnMAP ground truthing. (b) Hand-held sea-ice information system “Ice Pad” using merged optical and SAR imagery.

References

M. Buchhorn, R. Petereit & B. Heim [2013]: A Manual Transportable Instrument Platform for Ground-Based Spectro-Directional Observations (ManTIS) and the Resultant Hyperspectral Field Goniometer System. *Sensors*, 13 (12), 16105–16128. doi:[10.3390/s131216105](https://doi.org/10.3390/s131216105).

T. Krumpen, L. Rabenstein, & J. Hoesemann [2011]: Quantifying Sea Ice Formation Rates in the Laptev Sea by Means of ENVISAT SAR Scenes and Airborne Ice Thickness Measurements. *International Union of Geodesy and Geophysics (IUGG) General Assembly*, Melbourne, Australia, 29 June 2011 – 7 July 2011 [hdl:10013/epic.38551](https://hdl.handle.net/10013/epic.38551).



The EUMETSAT Network of Satellite Application Facilities (SAF Network): Operational data and software products for polar regions

L. Schüller

EUMETSAT

Satellite Application Facilities (SAFs) are dedicated centres of excellence for processing satellite data and they form an integral component of EUMETSAT's distributed applications ground segment. Located at National Meteorological Services in Member States, they use the expertise of the EUMETSAT community to process application-specific data from geostationary and polar orbiting satellites for the generation of data products and tools for the meteorological and climate data user communities and beyond.

The SAF Network was created in the late 1990s when EUMETSAT recognised the technological and scientific development during the last decades together with new capabilities arising from the advanced European operational meteorological satellite programmes (Meteosat Second Generation MSG and the EUMETSAT Polar System EPS). These new capabilities offered new possibilities for supporting application areas and disciplines with satellite based data and services appeared and with the sophisticated instrumentation of MSG and EPS (Metop) a wide range of applications and services became feasible. This

led to concept of a distributed Application Ground Segment, including the Central Facility in Darmstadt, Germany, and a network of elements, known as Satellite Application Facilities (SAF), as specialised development and processing centres. Each SAF is led by the National Meteorological Service of a EUMETSAT Member State, working with a consortium of cooperating entities.

The current development activities of the SAFs are focussed on providing new products of increased coverage and quality as well as on the preparation for the next generation of EUMETSAT's satellites, namely the Meteosat Third Generation (MTG) and the EPS Second Generation.

The presentation will focus on development and operational activities relevant for the polar regions, covering the remote sensing of snow, sea ice, vegetation, water management and many more. It will address as well the access to the data, the interaction with users and the requirements for evolving and new applications.



The role of satellite-based information to inform change in arctic ecosystems at the Canadian High Arctic Research Station, Nunavut

J. Wagner & D. McLennan

Polar Knowledge Canada (POLAR), Cambridge Bay, Nunavut, Canada

Polar Knowledge Canada's Canadian High Arctic Research Station (CHARS) in Cambridge Bay, Nunavut, has a mission to develop the CHARS Experimental and Reference Area (CHARS ERA) as a Flagship Arctic monitoring and research site conducting and supporting world class environmental science by POLAR science staff, and by visiting Canadian and international scientists. The CHARS Monitoring Plan describes a broad, whole-of-ecosystem approach that includes long-term experiment-based monitoring of terrestrial, freshwater and coastal-marine ecosystems, and their interactions, all within a social-ecological context in the CHARS ERA. This presentation describes how the use of remote sensing data is being used to inform the terrestrial component of the Plan, which will follow the approaches laid out in the CAFF CBMP Terrestrial Monitoring Plan. Baseline inventories and studies, and piloted monitoring programs have been initiated since 2014 and will be accelerating now that the first CHARS science staff is located full time at the station in Cambridge Bay. Engagement of Kitikmeot communities and residents is another important component of proposed work in the CHARS ERA, and evolving plans for that engagement will be presented. The approach is to also engage regional governments, industry, academia, and NGOs in the development and delivery of the monitoring program. In evolving partnerships with the Canadian Space Agency (CSA), academics, and the National Aeronautical and Space Administration (NASA) optical, SAR and other data sources will be utilized through a range of modeling approaches to scale up ground experiments to the regional scale of the CHARS ERA. To provide an ecological template for designing and extrapolating ground observations, we are developing

the Canadian Arctic-Subarctic Biogeoclimatic Ecosystem Classification (CASBEC) system to describe and classify local and regional terrestrial ecosystems. Given a local ecosystem classification, we are combining variables developed from digital surface models with optical imagery at a range of scales to develop very accurate models of high resolution local ecosystem maps (Worldview), and medium scale (Landsat 8) regional ecosystem maps. Ecosystem maps will be used to extrapolate the results of long term monitoring experiments, e.g., C flux, C storage, caribou habitat quality, active layer depths, to the CHARS ERA. We are also planning to utilize CSA SAR data to track change in snow season, and in lake and sea ice within the CHARS ERA. Academic partners are using ground calibration-validation data on snow characteristics in the CHARS ERA to inform regional changes in snow depth and structure (especially rain on snow events as they impact caribou foraging) using passive and active microwave data. Through our partnership with NASA we have acquired AVIRIS data for our focal watershed near Cambridge Bay and are working to test the usefulness of AVIRIS data as a predictor of terrestrial ecosystem structure and leaf chemical characteristics. In partnership with the British Antarctic Survey we collected detailed LiDAR data over the focal watershed to support the development of a high resolution digital surface model and to inform predictions of snow water equivalent. This presentation will present the summarize the work than has been completed to date by CHARS staff and co-investigators, will outline the monitoring and research framework that is described in the CHARS Monitoring Plan, and will describe remote sensing related work to be conducted over the 2018 and 2019 field seasons.



SESSION

Observing Permafrost State and Changes

Thaw subsidence of a yedoma landscape in northern Siberia, measured *in situ* and estimated from TerraSAR-X interferometry

Sofia Antonova^{1,2}, Henriette Sudhaus³, Tazio Strozzi⁴, Simon Zwieback⁵, Andreas Käab⁶, Birgit Heim¹, Moritz Langer^{1,7}, Niko Bornemann¹, & Julia Boike^{1,7}

¹*Alfred Wegener Institute Helmholtz Center for Polar and Marine Research, Potsdam, Germany;*

²*Institute of Geography, Heidelberg University, Heidelberg, Germany;*

³*Institute of Geosciences, Kiel University, Kiel, Germany;*

⁴*Gamma Remote Sensing, Gümligen, Switzerland;*

⁵*Department of Geography, University of Guelph, Guelph, Canada;*

⁶*Department of Geosciences, University of Oslo, Oslo, Norway;*

⁷*Department of Geography, Humboldt University of Berlin, Berlin, Germany*

In permafrost areas, seasonal freeze-thaw cycles of active layer result in upward and downward movements of the ground. Additionally, relatively uniform thawing of the ice-rich layer at the permafrost table, contributing to net long-term surface lowering, was reported for some Arctic locations. We use a simple method to quantify surface lowering (subsidence) and uplift in a yedoma area of the Lena River Delta, Siberian Arctic, using reference rods installed deeply in permafrost. The seasonal subsidence was 1.7 ± 1.5 cm in the cold summer of 2013 and 4.8 ± 2 cm in the warm summer of 2014. Furthermore, we measured a pronounced multi-year net subsidence of 9.3 ± 5.7 cm from spring 2013 to the end of summer 2017. Additionally, we observed a high spatial variability of subsidence of up to 6 cm across a sub-meter horizontal scale. This variability limits the usage of a pointwise measurement for a validation of spatially extensive remote sensing products. In summer 2013, we accompanied our field measurements with Differential Synthetic Aperture Radar Interferometry (DInSAR)

on repeat-pass TerraSAR-X (TSX) data over the same study area. Interferometry was strongly affected by a fast phase coherence loss, atmospheric artifacts, and possibly the choice of reference point. A cumulative ground displacement map, built from a continuous interferogram stack, did not reveal a meaningful signal on the upland but showed a distinct subsidence of up to 2 cm in most of the thermokarst basins. There, the spatial pattern of displacement corresponded well with relative surface wetness identified with the near infra-red band of a high-resolution optical image. Our study suggests that

- i although X-band SAR has serious limitations for ground movement monitoring in permafrost landscapes, it can provide valuable information for specific environments like thermokarst basins, and
- ii due to the high sub-pixel spatial variability of ground movements, a validation scheme needs to be developed and implemented for future DInSAR studies in permafrost environments.

Predicting potential permafrost distribution based on land surface variables and remote sensing data in Southern Carpathians (Romania)

F. Sîrbu, F. Ardelean, & A. Onaca

West University of Timișoara

In the recent years the investigations of permafrost occurrence in the Southern Carpathians have experienced an apparent renewal. Intact rock glaciers and other openwork periglacial structures hosting permafrost were documented in different mountain ranges above 2000 m. Despite of this, no analyses of the permafrost distribution at a regional scale have yet been performed. In this study we analysed the possibility of permafrost occurrence in the whole Southern Carpathian range and found suitable conditions in three different massifs: Retezat, Parâng and Făgăraș.

We introduce a modelling methodology based on the Random Forest (RF) classification algorithm [Breiman, 2001]. RF is a machine learning algorithm that learns all the characteristics of the independent variables for the training area (for both the areas with permafrost and without permafrost) and searches for similar characteristics of the independent variables in the rest of the study area. It has several advantages among which the most important are: the input data can be both numerical and categorical; there is no need for the input data to have a specific distribution; it is not sensible to outliers in the input data; it can use a great number of independent variables. These characteristics allows the RF model to be run on a big set of predictor variables that can be extracted from both a digital elevation model (DEM) and satellite images.

The input data for the model is based on areas with known presence or absence of permafrost, based on

previous studies. Because the extent of permafrost is limited to small patches the input data is split about $\frac{2}{3}$ for areas without permafrost and $\frac{1}{3}$ for area with permafrost, rather than an equal proportion. As predictor variables we used 21 topographical variables derived from a 30m spatial resolution DEM and two land cover variables derived from a Landsat8 satellite image. The model produces three outputs: the permafrost extent, the uncertainty associated with the permafrost extent output and the importance of the independent variables. The accuracy of the model was tested using an error matrix and using the Area under the receiver operating curve (AUC).

The resulted map of permafrost extent shows a high probability of permafrost existence in areas located in deep glacial cirques, mostly where rock glaciers are present, at altitudes between 1950 and 2300. Most of the ridges are found to have a low probability of permafrost existence although they are at higher altitudes, thus confirming the previous studies that, until now, did not reported any signs of permafrost presence on ridges and rock walls. The results indicate that, in the Southern Carpathians, permafrost conditions are favoured mostly by shading and terrain surface roughness than by altitude.

References

Breiman, L. [2014]: Random Forests. *Machine Learning*, 45(1):5–32. doi:[10.1023/A:1010933404324](https://doi.org/10.1023/A:1010933404324).

The impact of exceptional warming conditions in 2016 on central Yamal – observations *in situ* and from space

A. Bartsch^{1,2,3}, T. Strozzi⁴, M. Leibman^{5,6}, B. Widhalm¹, A. Khomutov^{5,6}, D. Mullanurov⁵, A. Gubarkov⁷

¹Zentralanstalt für Meteorologie und Geodynamik, Vienna, Austria;

²Austrian Polar Research Institute, Vienna, Austria;

³b.geos, Korneuburg, Austria;

⁴Gamma Remote Sensing, Gümliigen, Switzerland;

⁵Earth Cryosphere Institute, Tyumen Scientific Center SB RAS, Tyumen, Russia;

⁶University of Tyumen, Tyumen, Russia;

⁷Tyumen Industrial University, Tyumen, Russia

The ESA DUE GlobPermafrost project develops, validates and implements Earth Observation (EO) products to support research communities and international organisations in their work on better understanding permafrost characteristics and dynamics. Globally available datasets are exploited for permafrost modelling. Regional studies cover different aspects of permafrost by integrating *in situ* measurements of subsurface properties and surface properties, Earth Observation, and modelling to provide a improved understanding of permafrost today. The project extends local process and permafrost monitoring to broader spatial domains, supports permafrost distribution modelling, and helps to implement permafrost landscape and feature mapping in a GIS framework. Both lowland (latitudinal) and mountain (altitudinal) permafrost issues are addressed.

This presentation will provide an overview on the chosen observation strategy, methods, datasets, validation results and the status of the Permafrost Information System which includes a catalogue and a

WebGIS. Currently available prototypes of GlobPermafrost datasets include:

- Modelled mean annual ground temperature for the Arctic based on satellite-derived land surface temperature and snow water equivalent
- Tundra land surface characterization including shrub height, land cover and parameters related to surface roughness from Sentinel-1 and Sentinel-2
- Temporal trends in multispectral indices from Landsat Time series over four continental-scale transects of the northern permafrost domain
- Analyses of subsidence, ground fast lake ice, land surface features and rock glacier monitoring at selected mountain and lowland permafrost sites based on Synthetic Aperture Radar data

More information: www.globpermafrost.info

Large-scale monitoring of rapid permafrost thaw with satellite radar Interferometry

Philipp Bernhard¹, Simon Zwieback², & Irena Hajnsek¹

¹*Institute for Environmental Engineering, ETH Zürich, Stefano-Franscini-Platz 3, 8093 Zürich, Switzerland;*

²*Institute of Geography, University of Guelph, 50 Stone Road East Guelph, ON, Canada*

Vast areas of the Arctic host ice-rich permafrost, which is becoming increasingly vulnerable to rapid thaw in a warming climate. Permafrost degradation has major impacts on the local hydrology and ecosystems, and can also reinforce climate change by mobilizing organic carbon leading to the emission of large amounts of the greenhouse gases CO₂ and CH₄ [Schuur et al., 2015]. However, on the pan-Arctic scale the prevalence and rates of rapid thaw remain poorly constrained, and so is their contribution to climate change. Here we outline an observational strategy to quantify hillslope thermokarst and its contribution to the carbon-climate feedback on the pan-Arctic scale. At its core are radar interferometric data acquired by

the German TanDEM-X satellite, from which accurate measurements of elevation changes can be derived. The data we will be using are obtained during the TanDEM-X operational phase between 2011 to 2017. This provides us with at least three observations over this timespan to generate digital elevation models (DEMs). Due to the spatial resolution of about 12m and the height sensitivity of 0.5–1 m we will focus on forms of abrupt permafrost thaw that are noticeable at these scales, in particular retrogressive thaw slumps (RTS). RTS evolve by retreat of the headwall which lead to the mobilization of soil resulting in height changes in the landscape that are detectable by DEM differencing (Fig. 1).

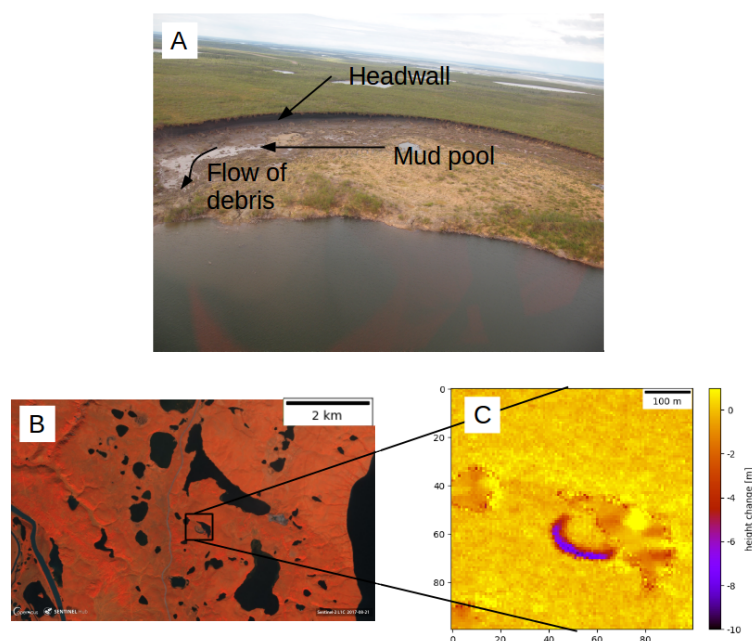


Figure 1: Observations of a thaw slump in the Mackenzie River Delta region, Canada. A: Aerial photo of a thaw slump (picture by Simon Zwieback) B: Sentinel-2 L1C image of part of the area in the Mackenzie River Delta (Date: 21.08.2017), C: Result after DEM generation process for single-pass TanDEM-X observation in the Science Phase (01.06.2015). The height change shows the difference to a previous TanDEM-X DEM from 2013. The strong height changes of up to -8m indicate that the thaw slump shown in A was increasing in size between the two observations

Annual rates of headwall retreat can reach rates of several tens of meters per summer [Jorgenson & Grosse, 2016].

We use the Gamma Remote Sensing Software for processing and generating DEMs from the TanDEM-X data. To be able to cover large areas this process should be optimized and automated as much as possible. The height accuracy of a bistatic SAR observation is determined by the phase noise which can be estimated using the effective baseline between the two satellites as well as the measured coherence magnitude depending on the incidence angle and surface characteristics. This leaves us with DEMs with changing height accuracy not only between observations, but also on a pixel level and require a detailed statistical analysis. We apply DEM differencing to obtain height change maps between the observations and use a rule-based classifier to detect changes due to active RTSs taking into account the different accuracies and identify changes that are not due to RTSs and are induced e.g. by old firn patches, vegetation or water bodies. After the correct classification we will be able to investigate our dataset with regard to spatial variability as well as volumetric changes which are a first

estimate for the amount of carbon that is mobilized.

Here we will present first results of our detection and classification method of active RTSs for areas in the Mackenzie River Delta, Canada as well as on the Yamal Peninsula, Russia. Furthermore, we will discuss possibilities and limitations of the proposed RTS detection method with special emphasis on the TanDEM-X data availability regarding the temporal coverage and the height accuracy for the application of RTS detection on a pan-Arctic scale.

References

- Schuur E.A.G., McGuire A., Schädel C., Grosse G., Harden J.W., Hayes D.J., Hugelius G., Koven C.D., Kuhry P., Lawrence D.M., Natali S.M., Olefeldt D., Romanovsky V.E., Schaefer K., Turetsky M.R., Treat C.C., & Vonk J.E. [2015]: Climate change and the permafrost carbon feedback. *Nature*, 520 (7546): 171–179. doi:[10.1038/nature14338](https://doi.org/10.1038/nature14338).
- Jorgenson, M.T. & Grosse, G. [2016]: Remote Sensing of Landscape Change in Permafrost Regions. *Permafrost and Periglacial Processes*, 27: 324–338. doi:[10.1002/ppp.1914](https://doi.org/10.1002/ppp.1914).

Global-scale mapping of periglacial landforms on Earth and Mars using deep convolutional networks

L. Fanara^{1,2}, E. Hauber¹, R. Hänsch³, K. Gwinner¹, J. Oberst^{1,2}, A. Morgenstern⁴ & G. Grosse⁴

¹German Aerospace Center (DLR) Planetary Research Institute; ²Technical University Berlin Institute of Geodesy and Geoinformation Science; ³Technical University Berlin Institute of Mechanical Engineering and Microelectronics; ⁴Alfred Wegener Institute Helmholtz Centre for Polar and Marine Research, Potsdam

We will develop a machine learning system based on high-resolution airborne and satellite images of Earth and Mars for classifying periglacial landscape features, detecting their temporal changes, and assessing their global distribution as well as their potential as indicator for climate conditions and changes. Earth periglacial landscape phenomena such as ice wedge polygons, thermo-erosional gullies, blockfields, and rock glaciers, are closely linked to permafrost dynamics including permafrost aggradation and degradation, repeated freeze-thaw cycles, and the presence of water and ice in the subsurface. Ice wedge polygons, which are widespread in Arctic lowlands, constitute an important indicator for ground ice content. Ground ice makes permafrost vulnerable to thaw and subsidence, thus leading to massive changes in topography, hydrology, and biogeochemical processes [Liljedahl et al., 2016]. On Mars, large volumes of excess ice exist in the shallow subsurface of mid-latitude regions [Dundas et al., 2018], where various young landforms resemble glacial and periglacial ones on Earth. A major debate focusses on whether Martian surface dynamics resulted in landforms indicating active freeze-thaw processes, such as ice-wedge polygons, in the geologically recent past. If true, this would be conflicting with the current Martian environment, which ostensibly prevents the generation of liquid water, and would therefore have implications for the recent hydrologic past of Mars. While local studies have demonstrated that these features as well as their changes can be observed with remote sensing, quantification of periglacial features on regional- to global-scale has not been done for either of the planets so far. Big data approaches relying on high-resolution imagery, highly automated image processing, machine learning classification, and feature detection now allows scaling of these mapping efforts to very large regions. For Earth we have access to historical and modern high-resolution aerial photo and satellite image datasets (<1 m resolution) from periglacial regions in Alaska, Siberia, and Canada

with a total area of several 100 000 km² of Arctic tundra. For Mars we can use tens of thousands of images of the northern mid-latitudes with resolutions of up to 0.25 m. In this new project we are developing a machine learning system in order to identify the most appropriate image features characteristic for each landform. Amongst the available machine learning methods, deep convolutional networks achieve the best performance, given that the amount of training data suffices. Ice wedge polygons are morphologically very similar on both planets, which may provide the possibility to combine training datasets from both planets. To maximize the amount of training data, these databases will be expanded through data augmentation by transforming the available images as well as by including synthetic data. Our project explores the potential for a deep convolutional network and of data augmentation with synthetic data to detect periglacial phenomena by exploiting big datasets available for large regions of Earth and Mars. The resulting near global-scale mapping of ice wedge polygons, gullies and blockfields will provide insights regarding the distribution of ground ice, freeze-thaw process dynamics, and the permafrost vulnerabilities to changing climates on Earth, as well as about the recent role of liquid water on Mars. The former are linked to life and biogeochemical processes on Earth, while the latter to the evolution of climate and potential habitability of Mars.

References

- A.K. Liljedahl et al. [2016]: Pan-Arctic ice-wedge degradation in warming permafrost and its influence on tundra hydrology. *Nature Geoscience*, 9, 312. doi:[10.1038/ngeo2674](https://doi.org/10.1038/ngeo2674).
- C.M. Dundas et al. [2018]: Exposed subsurface ice sheets in the Martian mid-latitudes. *Science*, 359, 199–201. doi:[10.1126/science.aao1619](https://doi.org/10.1126/science.aao1619).

Multi-model assessment of climate change impacts on Arctic infrastructure

A. Gädeke¹, K. Thonicke¹, J. Boike², E. J. Burke³, J. Chang⁴, P. Ciais⁴, M. Langer², S. Ostberg¹, S. Schaphoff¹, H. Müller-Schmied⁵, S. Seneviratne⁶ & W. Thiery^{6,7}

¹Potsdam Institute for Climate Impact Research, Earth System Analysis, Potsdam, Germany;

²Alfred Wegener Institute for Polar and Marine Research, Potsdam, Germany;

³Met Office Hadley Centre, FitzRoy Road, Exeter, EX1 3PB, UK;

⁴Laboratoire des Sciences du Climat et de l'Environnement, LSCE/IPSL, Université Paris-Saclay, France;

⁵Institute of Physical Geography, Goethe-University Frankfurt, Frankfurt, Germany;

⁶Institute for Atmospheric and Climate Science, ETH Zurich, Zurich, Switzerland;

⁷Department of Hydrology and Hydraulic Engineering, Vrije Universiteit Brussel, Brussels, Belgium

The Arctic has experienced increases in the development of natural resource, transportation networks and human infrastructure during the second half of the twentieth century. Concurrently, the high latitude climate has warmed at an amplified rate which has resulted in permafrost warming and increases in active layer thickness as well as in changes to the Arctic freshwater resources [Instanes et al., 2016]. Natural resource development, transportation networks and human infrastructure rely on permafrost stability and accessibility to freshwater resources. There currently exists large uncertainty as to how the spatial and temporal patterns of permafrost and freshwater system change at the regional to pan-Arctic scale with anticipated climate warming.

Here we identify hazards zones for Arctic infrastructure under climate change by comparing historical and future simulations of three Land-Surface Models (LSM) of ISIMIP2b (LPJmL, CLM4.5 and ORCHIDEE). The LSM simulations were performed based on a common protocol and input data [Frieler et al., 2017]. Specifically, we assess the number of thawing and freezing degree-days, and permafrost stability (permafrost temperature, active layer thickness). Changes in freshwater resources are evaluated in terms of end-of-winter SWE, mean annual stream flow, snowmelt and late summer runoff (via annual 7-day high and low flow, respectively, and timing) and soil moisture. Our analysis spans over the pan-Arctic permafrost region (North of 50°) and four focus regions (Prudhoe Bay (Alaska USA), Inuvik-Tuktoyaktuk Highway (Northwest Territories, Canada), Yamal Peninsula and Norilsk (Russia)) where modeled outputs are evaluated against regional/local studies and measurements.

Our simulation results show continuing permafrost warming and increasing active layer thickness

both resulting in decreasing ground bearing capacity. Permafrost-related changes are largest in the discontinuous, southern permafrost zone. Although the simulated permafrost temperatures and active layer thicknesses differ in magnitude between the LSMs, the overall trend is consistent across them. Freshwater resources are likely to increase in response to increasing annual precipitation in the future. Their seasonal distribution, timing and rate of snowmelt remain, however, highly uncertain. The low-cost winter transportation via ice roads is likely to be reduced in most parts of the pan-Arctic because of the decreasing numbers of freezing degree-days while open-water river travel may increase.

The results of our study suggest a high vulnerability and increasing maintenance costs of existing transportation networks and human infrastructure under climate change. Ultimately, however, the local population will be impacted most strongly and large efforts in adapting their lifestyle will be necessary.

References

- Frieler, K., Lange, S., Piontek, F., Reyer, C.P.O., Schewe, J., Warszawski, L., Zhao, F., Chini, L., Denvil, S., Emanuel, K., Geiger, T., Halladay, K., Hurtt, G. et al. [2017]: Assessing the impacts of 1.5 °C global warming – simulation protocol of the Inter-Sectoral Impact Model Intercomparison Project (ISIMIP2b). *Geosci. Model Dev.*, 10(12), p. 4321–4345. doi:[10.5194/gmd-10-4321-2017](https://doi.org/10.5194/gmd-10-4321-2017).
- Instanes, A., Kokorev, V., Janowicz, R., Bruland, O., Sand, K. and Prowse, T. [2016]: Changes to freshwater systems affecting Arctic infrastructure and natural resources. *Journal of Geophysical Research: Biogeosciences*, 121(3), 567–585. doi:[10.1002/2015JG003125](https://doi.org/10.1002/2015JG003125).

Polarimetric D-InSAR for ground deformation estimation over permafrost environment

Franck Garestier¹, Stephane Guillaso², Elena Zakharova^{3,4}, Alexei Kouraev^{3,4,5} & Roman Desyatkin⁶

¹UMR 6143 CNRS M2C, Caen, France;

²GFZ, Berlin, Germany;

³UMR 5566 CNRS LEGOS, Toulouse, France;

⁴State Oceanographic Institute, St Petersburg, Vasilyevskiy ostrov, Beringa 38, 119397 Russia;

⁵Tomsk State University, Tomsk, Pr. Lenina 36, 634050 Russia;

⁶Melnikov Permafrost Institute, SB RAS, Yakutsk, Merzlotnaya 36, 677010 Russia;

High-latitude permafrost regions store vast amounts of organic carbon. Temperatures increase induces thaw of the frozen grounds, facilitating the microbial decomposition and conversion of soil organic carbon into the greenhouse gases carbon dioxide and methane, that represents a positive feedback effect that may accelerate climate change. The thawing is restricted to some meters below the top layer of soil and a permafrost layer remains frozen below the surface. In such areas, the top layer of soil that thaws during the summer and freezes in winter -known as the active layer- warms up enough to enable plants to grow during the spring and summer. For an accurate assessment of the carbon transfers, the active layer thickness over different soils and surface types needs to be known, as well as the dynamics of soil moisture during the annual freeze/thaw cycle.

In this work, SAR differential interferometry is used for following the surface deformation during the freeze/thaw cycle, as it is an indicator of the active layer thickness and of the hydrological transfers. Time series of X-Band SAR data has been acquired over two sites located around 50 km at east of Yakutsk (Central Siberia) every 11 days during one year to cover a whole freeze/thaw cycle. The selected polarimetric channels were HH and HV ensuring sensitivity to vegetation dynamics and enabling polarimetric optimization of the coherence and ground phase estimation under vegetation. Several ground measurements have been performed over the two sites. Active layer depth, soil moisture gradient, vegetation height and type were collected synchronously with the spaceborne acquisitions. Temperature vertical profiles continuously measured over instrumented sites during height years, from 2000 to 2008 are also available. These profiles were established over 5 typical East-Siberian environments: two alas (thermokarstic depressions) composed by grass

and other herbaceous vegetation and lakes, and three other sites covered respectively by birch, larch and pine forests. A specific InSAR approach has been developed to follow the deformation in time, with a 11 day revisit time, to estimate the non-linear ground movements affecting the periglacial environment. To improve chance to detect deformation occurred within the sensor revisit time using only two acquisitions, the sensor polarimetric capability is employed for polarimetric optimization of the coherence, and for ground movement estimation under vegetation, by exploiting the polarimetric diversity of the interferometric coherence [Garestier et al., 2017a,b]. The deformation patterns are then compared with to the ground measurements for analyzing the thermal and hydrological processes affecting the ground during the whole freeze/thaw cycle.

References

- Franck Garestier, Stéphane Guillaso, Elena Zakharova, Alexei. A. Kouraev, Roman Desyatkin [2017a]: Following deformation over permafrost environment during a whole freeze/thaw cycle using Pol-DInSAR. *V International Field Symposium "West Siberian Peatlands and Carbon Cycle : Past and Present" and International Conference "Carbon Balance of Western Siberian Mires in the Context of Climate Change" (WSPCC-2017)*, Jun 2017, Khanty-Mansiysk, Russia.
- F. Garestier, S Guillaso, E. A. Zakharova, A. V. Kouraev, Roman Desyatkin [2017b]: Following deformation over permafrost environment during a whole freeze/thaw cycle using Pol-D-InSAR. *The 2nd Asian Conference on Permafrost (ACOP2017)*, Jul 2017, Sapporo, Japan.

Remote sensing of drained thermokarst lake basin successions

Guido Grosse^{1,2}, Ingmar Nitze^{1,2}, Benjamin M. Jones³, Juliane Wolter¹, Alexandra Runge^{1,2}, Matthias Fuchs^{1,2}, Frank Günther¹, Alexandra Veremeeva⁴, & Sebastian Westermann⁵

¹Alfred Wegener Institute for Polar and Marine Research, Telegrafenberg A45, 14473 Potsdam, Germany;

²Institute of Earth and Environmental Sciences, University of Potsdam, Germany;

³Water and Environmental Research Center, Institute of Northern Engineering, University of Alaska Fairbanks, Fairbanks, AK, USA;

⁴Institute of Physicochemical and Biological Problems in Soil Science, Russian Academy of Sciences, Pushchino, Russia; ⁵University of Oslo, Norway

Thermokarst lakes are important factors for permafrost landscape dynamics and carbon cycling. Thermokarst lake cover is particularly high in Arctic lowlands with ice-rich permafrost. In many of these vast lowland regions, drained thermokarst lake basins of different age have been identified that overlap each other in space, suggesting intense dynamics of repeated lake formation and loss with complex carbon cycle histories during the Holocene [Grosse et al., 2013]. Observing the permafrost and ecosystem succession patterns following thermokarst lake drainage will help to better determining the landscape and regional scale impacts of lake loss on northern hydrology, permafrost aggradation, vegetation succession, carbon cycling, as well as spectral land surface property changes. Previous remote sensing approaches to study drained thermokarst lake basins used a combination of Landsat, high resolution satellite and aerial, and field data to quantify carbon stocks accumulated in post-drainage peat in drained thermokarst lake basins (DTLBs) for the northern Seward Peninsula in Northwest Alaska [Jones et al., 2012]. We here expand on this method by using different remote sensing products in combination with dating of lake drainage events. These events are identified based on the historical remote sensing record and accelerated mass spectrometry radiocarbon dating. The joint use of remote sensing and geochronological field data allows to assess the specific succession patterns of various DTLB types and their impacts on land surface properties in different Arctic permafrost regions (North Alaska, Northwest Alaska, North Siberia).

The datasets used in this analysis include a range of remote sensing and topographic data, such as aerial photography, historic topographic maps, high resolution satellite images (Corona, Spot, Ikonos, Quickbird, Worldview, GeoEye), and imagery from the full Landsat archive as well as from the Moderate Resol-

ution Imaging Spectrometer (MODIS) sensors. We report temporal trends of spectral properties based on Landsat multispectral indices for individual DTLBs of different ages, but also employ landscape-scale chronosequences allowing the analysis succession trajectories of DTLBs that drained well before the start of the remote sensing record. Here we are particularly focusing on the long-term impacts of lake drainage on changes in normalized difference vegetation index (NDVI), normalized difference moisture index (NDMI), normalized difference water index (NDWI), Tasseled Cap index (brightness, greenness, wetness), land surface temperatures, and albedo. We further conducted field studies including reconnaissance flights targeting historically drained lakes and cored DTLBs to sample for radiocarbon-dating of terrestrial peat layers indicative of the drainage event.

Results of this ongoing study suggest a strong impact exerted by thermokarst lake drainage on land surface reflectance characteristics in thermokarst lowland regions. The information may be useful for parameterizing surface properties in land surface models of thermokarst-affected regions, particularly where increased lake drainage is projected to take place.

References

- M.C. Jones, G. Grosse, B. M. Jones, & K. Walter Anthony [2012]: Peat accumulation in drained thermokarst lake basins in continuous, ice-rich permafrost, northern Seward Peninsula, Alaska. *Journal of Geophysical Research: Biogeosciences*, G00M07. doi:[10.1029/2011JG001766](https://doi.org/10.1029/2011JG001766).
- G. Grosse, B. Jones, & C. Arp [2013]: Thermokarst Lakes, Drainage, and Drained Basins. In: Shroder, F. (ed.), *Treatise on Geomorphology*, Academic Press, p. 325–353. doi:[10.1016/B978-0-12-374739-6.00216-5](https://doi.org/10.1016/B978-0-12-374739-6.00216-5).

Spatial analysis of periglacial processes and landforms on Hurd Peninsula, Livingston Island, Antarctica, using advanced SAR techniques

S. Guillaso¹, T. Schmid², & J. López-Martínez³

¹*Helmholtz Centre Potsdam, GFZ German Research Center for Geoscience, Potsdam, Germany;*

²*CIEMAT, Madrid, Spain;*

³*Dpto. Geología y Geoquímica, Facultad de Ciencias, Universidad Autónoma de Madrid, Spain*

Periglacial processes and landforms together with the presence of permafrost are common within ice-free areas in the northern Antarctic Peninsula region [López-Martínez et al., 2005]. Their distribution affects the hydrology and has consequences for often complex and fragile ecosystems found in these areas. Mainly due to natural causes, such as global warming, but also due to human induced activities, it is important to be able to characterize and monitor changes occurring in the ice-free areas. In the global warming context, most glaciers and snow fields are retreating in the studied region, leading to large ice-free areas. The region where is located the Hurd Peninsula, in Livingston Island, has a mean annual air temperature around -2 °C with higher temperatures (> 0 °C) during the summer period. Under these conditions, freeze-thaw cycles are favored implying dynamic processes in the active layer of the permafrost. During the Antarctic summer of 2016/2017 and 2017/2018, field campaigns were made in order to collect information on periglacial processes and associated landforms within the ice-free areas. This information is related to different types of soil surface covers, that are represented by pattern ground, stone fields, glacial deposits, rock outcrops as well as the influence of human activities carried out in the vicinity of the Spanish and Bulgarian bases. During the campaigns, training areas were selected for applying the random forest classifier as well as validating the classification results. The field work consisted in describing the specific surface cover of 30 × 30 m as well as determining physical properties that are sensitive to the Synthetic Aperture Radar (SAR) system such particle size and ruggedness. The objective of this study is to investigate the potential of using machine learning tools such as the random forest classifier, in order to map the different

landforms present on Hurd Peninsula. A new speckle noise-like filter is presented [D'Hondt et al., 2005], that can be applied to single channel SAR images or to fully polarimetric images. This filter, based on the combination of non-local means with bilateral distance calculation is extended to the estimation of texture parameters which are added to the number of features that are extracted from the polarimetric data. The random forest classifier determines the influence of the individual feature according to different soil surface properties. We applied our approach to fully polarimetric RADARSAT-2 data of Hurd Peninsula acquired in March 2014. Thereafter, we extended our approach to single channel SAR imagery provided by the ESA-Sentinel-1 mission where data have been acquired during the field campaign. Results obtained in this study show an improvement in the classification results, principally due to the new developed texture features. The distribution of surface covers obtained with this approach can be used in time series analysis and therefore for future monitoring of changes in Hurd Peninsula. This would be a novel approach to monitor active geomorphic processes.

References

- López-Martínez, J., Serrano, E., Schmid, T., Mink, S., & Linés, C. [2012]: Periglacial processes and landforms in the South Shetland Islands (northern Antarctic Peninsula region). *Geomorphology*, 155–156: 62–79. doi:[10.1016/j.geomorph.2011.12.018](https://doi.org/10.1016/j.geomorph.2011.12.018).
- D'Hondt, O., López-Martínez, C., Guillaso, S., & Hellwich, O. [2017]: Non-Local Filtering Applied to 3D Reconstruction of Tomographic SAR Data. *IEEE Transaction on Geoscience and Remote Sensing*, 55(12): 1–14. doi:[10.1109/IGARSS.2017.8127495](https://doi.org/10.1109/IGARSS.2017.8127495).

Repeat terrestrial LiDAR for quantification of extensive thaw subsidence within different tundra vegetation groups

Frank Günther¹, Guido Grosse^{1,2}, Georgy T. Maximov³, Alexandra A. Veremeeva⁴, Andreas Fricke⁵, Mahmud H. Haghighi⁶, & Alexander I. Kizyakov⁷

¹*Alfred Wegener Institute Helmholtz Centre for Polar and Marine Research, Potsdam, Germany;*

²*Institute of Earth and Environmental Sciences, University of Potsdam, Germany;*

³*Mel'nikov Permafrost Institute, Russian Academy of Sciences, Siberian Branch, Yakutsk, Russia;*

⁴*Institute of Physicochemical and Biological Problems in Soil Science, Russian Academy of Sciences, Pushchino, Russia;*

⁵*Chair of Computer Graphic Systems, Hasso Plattner Institute, Potsdam, Germany;*

⁶*GFZ German Research Centre for Geosciences, Potsdam, Germany;*

⁷*Department of Cryolithology and Glaciology, Faculty of Geography, Lomonosov Moscow State University, Moscow, Russia*

Permanently frozen ground in the Arctic is being destabilized by continuing permafrost degradation, an indicator of climate change in the northern high latitudes. Increased intensity of ground settlement through ground ice melt caused by rising summer air temperatures result in widespread geomorphological activity. Because these phenomena are hard to detect, they have received not much attention, despite their potentially global significance through the permafrost carbon feedback. The objective of our study is to analyze time series of repeat terrestrial laser scanning (rLiDAR) for quantification of extensive land surface lowering through thaw subsidence, which is the main unknown in terms of recent landscape development in the vast but neglected East Siberian Arctic. Local field measurements (active layer thickness, meteorology, ground temperature, geodetic surveys) during several recent Russian-German Arctic expeditions on Sobo-Sise Island in the eastern Lena Delta and on the Bykovsky Peninsula close to Tiksi help differentiating factors causing relief and land cover changes. Our work aims at finding commonalities and differences of change or no change on yedoma uplands and surrounding slopes, where we expect recent changes to take place first.

First repeat measurements have been made during the Lena Delta expedition in August 2016. We operated the Leica MultiStation MS50, a hybrid instrument combining high-accuracy surveying with fast

laser scanning capabilities, from many different positions inside the survey grids. Resulting point clouds have been interpolated to DEM rasters, portraying the land surface in unprecedented detail. Complementing our surveys, we conducted botanical mapping within the extent of our survey grids. This allows us to relate elevation differences to specific surface conditions and enhances our capabilities to extrapolate our local observations to larger areas through land-cover classifications of multispectral remote sensing data such as RapidEye, WorldView-2, and WorldView-3. Additionally, highly detailed digital elevation models (DEMs) with sub-metre accuracy have been stereophotogrammetrically derived from WorldView-1, WorldView-2 and GeoEye satellite data for all study sites. These DEMs are not only an essential prerequisite for the conversion of oblique imagery into ortho-images with the geometry of a map, allowing temporal image stacking for enhanced multispectral classification of tundra vegetation communities, but also contain valuable terrain height information for the evaluation of subsidence-relief interdependencies. When calculated as rates over time, land surface lowering in the ice-rich permafrost regions of northern Siberia amounts to 3-10 cm per year. This local understanding of processes will help to interpret InSAR-based permafrost degradation quantification efforts over large remote polar regions with high temporal earth observation missions such as the Sentinel-1 satellite constellation.

Measuring elevation change in arctic permafrost landscape using SAR interferometry

Mahmud H. Haghighi^{1,2}, Frank Günther³, Birgit Heim³, & Mahdi Motagh^{1,2}

¹*GFZ German Research Centre for Geosciences, Potsdam, Germany;*

²*Leibniz University Hannover, Hanover, Germany;*

³*Alfred Wegener Institute Helmholtz Centre for Polar and Marine Research, Potsdam, Germany*

Here we aim to measure summer thaw subsidence as well as inter-annual elevation change in tundra permafrost landscape using Synthetic Aperture Radar interferometry (InSAR). We select two study areas, Barrow, the northernmost point of Alaska and Bykovsky Peninsula, southeast of Lena Delta, Siberia. Thick permafrost underlines both areas with large ice volumes in the upper layer. Barrow has a relatively flat topography while Bykovsky has a hilly tundra landscape.

Information on summer and inter-annual subsidence of permafrost is valuable and yet rare information limited to a few spots in these regions. We use SAR satellite images to estimate elevation change of permafrost landscape across large areas and with a high spatial resolution. The SAR data used in this study includes an extensive collection of images acquired by

German TerraSAR-X, Japanese ALOS, and European Sentinel-1 satellites. Using the available SAR data, we perform InSAR analysis to obtain time series of elevation change from beginning to end of the thaw season as well as elevation change between different years.

The elevation change maps from different datasets are in general agreement and reveal cm-scale subsidence from the beginning of summer to the end of the thaw season and slightly lower rates of long-term elevation change. In both study areas, the magnitude of subsidence correlates with vegetation cover and microrelief. In particular, comparison of InSAR results with satellite optical images, confirm the wetter depressions basins show a higher magnitude of subsidence and the drier areas show a lower magnitude of subsidence.



Linking tundra landscapes with its disturbance history. A ThawTrendr pilot study in Nome, Alaska.

W. Hantson¹, S. Serbin², J. Kilbride¹, & D. Hayes¹

¹*University of Maine;*

²*Brookshaven National Lab*

Tundra landscapes are a key ecosystem in the Arctic Boreal Region (ABR) and the risk of permafrost thaw makes them extremely vulnerable to the effects of climate change. With temperatures that rise almost twice as fast as the global average, the tundra permafrost is at risk. When all the soil organic carbon, previously stored in the permafrost, comes available for decomposition more greenhouse gasses are produced adding to global warming.

The landscape sensitivity to climate change depends on disturbance history. Including disturbance history will help explaining the current landscape observed by hyperspectral remote sensing and makes it possible to determine the sensitivity patterns of the tundra, and the underlying permafrost, to climate change.

In Nome (AK) two year of field- and remote sensing data was collected to document the current state of the

tundra. Field and drone based spectral measurement in combination with AVIRIS data from the NASA ABoVE project are used to characterize the vegetation structure and composition. ThawTrendr detects pixel-based differences in the historical trend of the Landsat archive. Non-parametric classifiers are used to classify the different disturbance trends detected, creating the disturbance history for the time of the Landsat archive. Advanced spatio-temporal analysis will be used to detect the intensity of the disturbance(s) in space and time. Examples of disturbance regimes for the Nome area drained thermokarst lakes, wetting/drying of the landscape, and shrub expansion. Disturbance metrics from ThawTrendr will then be linked to the current state of the tundra, showing the vulnerability of the tundra ecosystem to warming and disturbance.

Thawtrendr: Characterizing patterns of disturbance history in permafrost landscapes using Landsat time-series segmentation algorithms

D. J. Hayes¹, W. Hantson¹, R. E. Kennedy², B. M. Jones³, S. Serbin⁴, & G. Grosse^{5,6}

¹University of Maine;

²Oregon State University;

³University of Alaska Fairbanks;

⁴Brookhaven National Laboratory;

⁵Alfred Wegener Institute;

⁶University of Potsdam

Landscapes across the Circumpolar North are undergoing rapid, widespread and unprecedented change in recent decades due to thawing permafrost associated with climate warming. This has globally important consequences for the social-ecological systems supported by these landscapes, including wildlife habitat and subsistence resources, infrastructure and transportation, hydrology and energy balance, and carbon-climate feedbacks. However, we lack a consistent and comprehensive source of information for landscape change across large, remote and inaccessible permafrost regions. Recognizing the vulnerability of these ecosystems to change, scientists and decision-makers have identified a critical need for research that employs remote sensing technologies and methodologies to observe, monitor and understand changes in Arctic and Boreal ecosystems. The availability of long-term, historical records of remote sensing imagery – and the maturation of algorithms and computing resources to extract information from them – offer new capabilities for characterizing thaw-related landscape change at high resolution and continental-scale coverage. Here, we demonstrate a proof-of-concept of the *Thawtrendr* approach that leverages existing Landsat-based, time-series segmentation algorithms tailored to detecting and attributing the key indicators of permafrost landscape dynamics, including changes in vegetation composition, landscape wetting and drying, wildfire, and thermokarst processes.

The core concept of the approach presented here is based on the idea that current landscape conditions with respect to ecosystem composition, structure and function are an outcome of their past disturbance history. This concept has been demonstrated in studies that used disturbance history metrics calculated from

time-series of Landsat vegetation indices to predict biomass in temperate forests. We contend that these algorithms can be extended to permafrost regions, and tailored to detect vegetation disturbance and recovery trajectories over time in arctic tundra and boreal forest ecosystems. Here, we describe the *Thawtrendr* approach that

1. calculates landscape change metrics generated by a time-series segmentation algorithm working on temporally-dense image stacks from the Landsat archive (1984 – present), and
2. spectral data indices from current-year Landsat 8 imagery.

To demonstrate this approach, we conducted targeted studies for existing research areas in Alaska, USA, where known permafrost disturbance agents are driving landscape changes in both tundra and forest ecosystems. The time-series segmentation algorithm was run on the Google Earth Engine to map disturbance history metrics for each of these sites. The disturbance history metrics and the spectral data indices were input to classification algorithms trained on *in situ* and expert interpretation data sets developed at these sites. We show the preliminary results of this approach for its utility in detecting vegetation disturbances and characterizing various thaw-driven landscape change trajectories. Finally, we discuss the potential for this approach to serve as a key tool for scaling the airborne and field-based data being collected from the large-scale ecosystem modeling studies on-going in this region, including NASA's Arctic-Boreal Vulnerability Experiment (ABOVE) and DOE's Next Generation Ecosystem Experiment (NGEE-Arctic).

Thermokarst lake monitoring on the Bykovsky Peninsula using high-resolution remote sensing data

Theresa Henning¹, Frank Günther², Alexander I. Kizyakov³, & Guido Grosse^{2,4}

¹*Technische Universität Dresden, Faculty of Environmental Science, Institute of Geography, Dresden Germany;*

²*Alfred Wegener Institute Helmholtz Centre for Polar and Marine Research, Potsdam, Germany;*

³*Department of Cryolithology and Glaciology, Faculty of Geography, Lomonosov Moscow State University, Moscow, Russia;*

⁴*Institute of Earth and Environmental Sciences, University of Potsdam, Germany*

Thermokarst lakes are a characteristic element of Arctic permafrost regions and subject to dynamic alterations that mirror the vulnerable response of permafrost landscapes towards changing environmental and climatic conditions. Investigating long-term lake dynamics in the Arctic contributes to a better understanding of driving processes of change, to the assessment of local and regional permafrost vulnerability, to the evaluation of effects on landscape characteristics as well as to the estimation of the impact on the permafrost carbon budget [Grosse et al., 2013].

As thermokarst lakes are abundant in Arctic lowlands with ice-rich yedoma permafrost, the Bykovsky Peninsula in northeast Siberia currently exhibits more than 400 lakes larger than 1000 m² on a land surface area of 163 km². The objective of our study is to create a time series of high-resolution orthorectified imagery and to map thermokarst lakes on the Bykovsky Peninsula in four time steps, spanning an observation period of 64 years. Based on historic greyscale aerial photographs from 1951 and 1981/82 and modern panchromatic satellite imagery from 2006 (SPOT-5) and 2015/16 (WorldView-1/2), thermokarst lakes with a surface area larger 1000 m² were mapped at a high level of detail, allowing the monitoring of lake formation, expansion, shrinkage and drainage. Complemented by a TanDEM-X digital elevation model from 2014, tendencies of lake change with respect to elevation were investigated as well as potential mechanism for lake expansion and drainage were examined. WorldView data at 0.5 m resolution consisted

of two panchromatic stereo pairs that were used for digital elevation model extraction at 1 m resolution. Ground control points (GCP) collected in the field and subsequent orthorectification of WorldView imagery provided a highly consistent georeferencing basis for other datasets. Georeferencing and GCP collection of the SPOT-5 satellite image was based on the WorldView image mosaic, whereas the TanDEM-X DEM at 12 m ground resolution and 1 m vertical accuracy was used for its orthorectification. Air photo bundle block adjustment was done according to Günther et al. [2015] and air photos were resampled to 0.9 m and 0.7 m, respectively. After terrain correction of single air photos and mosaicking to map geometry, lake shoreline mapping was done manually in airborne photographs as well as in SPOT-5 image and semi-automatically in panchromatic WorldView data using a threshold based on digital number values. Finally, vector datasets were incorporated into GIS to measure lake area changes.

The results of thermokarst lake changes over the 1951 to 2015 period revealed a net lake shrinkage tendency (Tab. 1). Approximately 17.7 % of the 1951 lake area was lost until 2015 due to coastal erosion or the development of drainage networks. In parallel, coastal erosion driven land loss amounts to 2.5 % of the peninsula. Over the three observation periods (1951–1982, 1982–2006, 2006–2015) both drainage and expansion rates were constantly increasing, suggesting intensified dynamics of thermokarst lakes on the peninsula.

Table 1. Main parameters of land and thermokarst lake changes according multi-temporal data.

	1951	1981/82	2006	2015/2016
Total land area (km ²)	166.7	165.1	163	162.6
Total lake area (km ²)	21.1	18.4	18.1	17.4
Limnicity (%)	12.7	11.2	11.1	10.7
Lake number (> 1000 m ²)	676	646	552	421

We found interconnections between coastal erosion and lake change, as well as lake change dependency on land elevation in a developed alas-yedoma thermokarst relief.

Our findings suggest that thermokarst lakes on the Bykovsky Peninsula are subject to high dynamics. Intensified thermokarst lake changes over the observation period indicate the vulnerability of the study region towards environmental disturbances and altering climatic conditions in an ongoing changing Arctic.

References

- G. Grosse, B. Jones, & C. Arp [2013]: Thermokarst Lakes, Drainage, and Drained Basins. In: Shroder, F. (ed.), *Treatise on Geomorphology*, Academic Press, p. 325–353. doi:[10.1016/B978-0-12-374739-6.00216-5](https://doi.org/10.1016/B978-0-12-374739-6.00216-5).
- F. Günther, P. P. Overduin, I. A. Yakshina, T. Opel, A. V. Baranskaya, & M. N. Grigoriev [2015]: Observing Muostakh disappear: permafrost thaw subsidence and erosion of a ground-ice-rich island in response to arctic summer warming and sea ice reduction. *The Cryosphere*, 9, 151–178. doi:[0.5194/tc-9-151-2015](https://doi.org/10.5194/tc-9-151-2015).

Identifying erosional hot spots around thermokarst lakes using RapidEye imagery

S. Kaiser^{1,2}, T. Schneider von Deimling^{1,2}, S. Jacobi¹, R. Mommertz^{1,3}, & M. Langer^{1,2}

¹Alfred Wegener Institute Helmholtz Centre for Polar and Marine Research, Potsdam, Germany;

²Department of Geography, Humboldt-Universität zu Berlin, Berlin, Germany;

³University of Potsdam, Potsdam, Germany

Research Objective

Thermokarst lakes are one of the most abundant landforms in periglacial landscapes. In continuous permafrost regions, they form as a consequence of soil subsidence that is triggered by the thawing of excess ground ice [Pienitz et al., 2008]. When a resulting depression fills with melt water of degrading ice, it forms a pond that can cause – due to the waterbody's heating property and the formation of a talik beneath the basin – further thawing processes [Pienitz et al., 2008]. As a result of the thermal erosion, the size of the pond increases both vertically and horizontally and can eventually turn into a larger lake further shaping the hydrological network of the surrounding landscape.

While the previous scientific work regards the dynamics of thermokarst lakes over a substantial time span, our study focuses on a detailed quantification and estimation of annual shoreline erosion rates and their spatial and temporal variability. The findings will contribute to the advancement of the land surface scheme CryoGrid3 [Langer et al., 2016].

Methodology

The study area close to Prudhoe Bay, Alaska lies within the zone of continuous permafrost and is characterized by high ground ice contents. The landscape displays vast natural and human-caused thermokarst features. The local infrastructure consists of gravel pads providing access to the oil production sites and pipelines that are exposed to risks emerging from ground subsidence, thaw pond development and thermokarst expansion. By applying a combination of high resolution optical imagery and complementary radar data, this study aims at

- (i) quantifying shoreline erosion rates of thermokarst lakes,

- (ii) identifying spatial patterns of the lake expansion and drainage, and
- (iii) identifying the controlling factors of the lake dynamics (e.g. size, ice type, vegetation etc.).

For the derivation of ground characteristics and the shoreline movement rates we use RapidEye imagery from 2010 to 2017 (5 m spatial resolution). The classification of the thermal regime is based on the Copernicus' Sentinel 1 Synthetic Aperture Radar data to distinguish between bedfast and floating ice lakes.

Results

RapidEye data analysis successfully detects shoreline movements for the years 2010 and 2017. However, it only identifies lakes with supposedly high erosion rates ignoring smaller-scale shoreline changes. An annual quantification is also not possible at this point, underlining the need for data with a higher spatial resolution, e.g. from Unmanned Aerial Vehicles (UAV) and/or Light Detection and Ranging (LIDAR) sensors to achieve a more detailed estimation of erosion rates.

References

- M. Langer, S. Westermann, J. Boike, G. Kirillin, G. Grosse, S. Peng & G. Krinner [2016]: Rapid degradation of permafrost underneath waterbodies in tundra landscapes – Toward a representation of thermokarst in land surface models. *Journal of Geophysical Research: Earth Surface*, 121(12), 2446–2470. doi:[10.1002/2016JF003956](https://doi.org/10.1002/2016JF003956).
- R. Pienitz, P. T. Doran, S. F. Lamoureux [2008]: Origin and geomorphology of lakes in the polar regions. In: W. F. Vincent & J. Laybourn-Parry (eds.), *Polar Lakes and Rivers: Limnology of Arctic and Antarctic Aquatic Ecosystems*, Oxford University Press, p. 25–42. doi:[10.1093/acprof:oso/9780199213887.003.0002](https://doi.org/10.1093/acprof:oso/9780199213887.003.0002).

Representation of mean annual ground temperature by satellite derived surface status

Christine Kroisleitner^{1,2,3}, Annett Bartsch^{1,2,3}, & Helena Bergstedt^{4,2}

¹Zentralanstalt für Meteorologie und Geodynamik, Vienna, Austria;

²Austrian Polar Research Institute, Vienna, Austria;

³b.geos, Korneuburg, Austria;

⁴Department of Geoinformatics – Z_GIS, University Salzburg, 5020 Salzburg, Austria

Land surface state, frozen versus unfrozen conditions, can be captured globally with satellite data obtained by microwave sensors. The number of frozen days can be derived in case of daily availability of measurements. Such a sampling density can be achieved in high latitudes from coarse resolution sensors such as scatterometer and radiometers. It has been hypothesized that the number of frozen days can give an estimate for mean annual ground temperature, although it does not account for crucial factors such as soil and snow properties. The aim of the study was to quantify the accuracy of such an approach and discuss the uncertainties with respect to different sensor types and environmental conditions.

Coarse spatial resolution microwave satellite data (Metop Advanced Scatterometer – ASCAT - and Spe-

cial Sensor Microwave Imager – SSM/I; 12.5 km and 25 km nominal resolution; 2007–2012) which provide the necessary temporal sampling were used. The MAGT from GTN-P (Global Terrestrial Network – Permafrost) borehole records at coldest sensor depth was derived and used for calibration and validation (separated into two distinct time periods).

MAGT could be obtained with an RMSE of 2.2 °C from ASCAT and 2.5 °C from SSM/I surface state records using a linear model. Comparison to Snow Water Equivalent data (GlobSnow) and consideration of melt day information from ASCAT demonstrated the discrepancies of the simple approach. Difference between years and datasets showed that especially central Siberia and southern Yakutia are regions with higher complexity regarding MAGT retrieval.

Relief modification caused by formation of gas-emission craters, remote-sensing and field studies

M. O. Leibman^{1,2}, A. I. Kizyakov³, M. V. Zimin⁴, E. A. Babkina¹, Yu. A. Dvornikov¹, R. R. Khairullin^{5,1}, & A. V. Khomutov^{1,2,6}

¹*Earth Cryosphere Institute, Tyumen Scientific Centre SB RAS, Tyumen, Russia;*

²*University of Tyumen, Tyumen, Russia;*

³*Moscow State University, Faculty of Geography, Moscow, Russia;*

⁴*ScanEx Research and Development Center, Moscow, Russia;*

⁵*St. Petersburg State University, St.-Petersburg, Russia;*

⁶*Industrial University of Tyumen, Tyumen, Russia*

Six gas-emission craters (GECs) were documented in the north of West Siberia. The role GECs formation in the terrain changes is not limited to the crater itself, but also to positive and negative microforms around the GEC (Fig. 1). Positive microforms around GECs are characteristic of all craters and consist of the ejected frozen deposits, later thawed. These deposits either form a single parapet, or isolated piles and ridges 0.2–3.5 m in diameter and 0.1–0.8 m in height. Negative microforms are found only around three of six GECs, and comprise rounded hollows up to 13 m in diameter and up to 1.5 m in depth, surrounded by an edging of extruded deposits. Origin

of these microforms was debatable. We used remote sensing data specifically for interpretation of landform origin, measuring distances and density of material scattering, identifying scattered material through analysis of repeated imagery, and determining the area of the “risk zone” where falling blocks can be expected in case of “eruption”.

Data obtained by analysis of imagery, photographs and field survey provides sufficient evidence in favor of the hypothesis that the hollows around GECs are impact microforms associated with a hit from falling large blocks of frozen deposits.

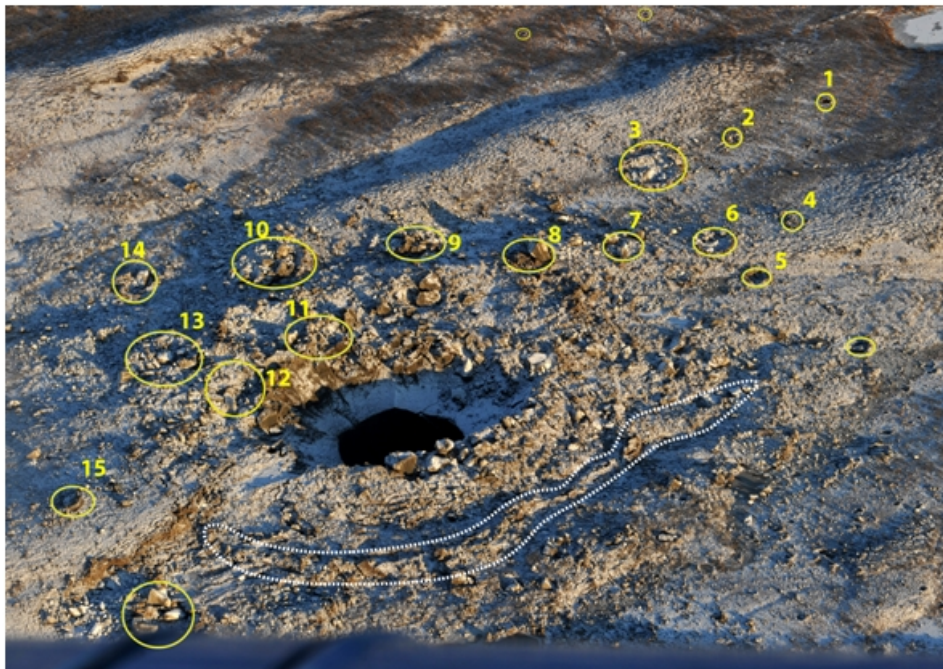


Figure 1: Photograph from the helicopter on 14 November 2012, characterizing the location of blocks of ice and frozen deposits ejected from GEC-2. Numbers indicate impact hollows and blocks of icy deposits reliably correlated with these blocks on imagery.

Remote-sensing based global map of permafrost

J. Obu¹, S. Westermann¹, A. Kääb¹, & A. Bartsch²

¹University of Oslo;

²Zentralanstalt für Meteorologie und Geodynamik

Permafrost cannot be directly detected from space, but many permafrost surface features and properties are observable with a variety of earth observation sensors. ESA's GlobPermafrost project develops, validates and implements different permafrost information products to support the research communities and related international organizations. Within GlobPermafrost project, we aim to produce a global map of permafrost temperatures and extent.

The thermal state of the ground cannot be directly inferred from spaceborne platforms with current remote sensing technologies. We overcome these limitations by combining the information content of several remote sensing products and reanalysis data, namely time series of remotely sensed land surface temperature (LST), snow cover information, land cover classification and wetness classes. These products are employed to force ground thermal model, which deliver ground temperatures and probability of permafrost occurrence within a grid cell.

We used a TTOP model [Smith & Riseborough, 1996] to calculate mean annual ground temperature (MAGT) at 1 km spatial resolution for 2000–2016 time period. The main input are freezing and thawing degree days (FDD and TDD) that are multiplied with semi-empirical adjustment factors. We use MODIS land surface temperatures and down-scaled ERA-Interim reanalysis temperature to calculate FDD and TDD for the model. Nf-factors are calculated from a snow cover that we calculated from ERA Interim precipitation and a T-index model. Rk-factors are defined based on ESA CCI (European Space Agency Climate Change Initiative) landcover

product and tundra wetness classification. We ran 200 ensemble runs with varying nf and rk-factors, which represent subcell variability of snow and soil wetness according to land cover classification. A mean of ensemble runs was used for a MAGT at the top of the permafrost product. Permafrost occurrence probability is a fraction of model runs with $MAGT < 0\text{ }^{\circ}\text{C}$. The permafrost occurrence probability is reclassified to established permafrost zonation.

The permafrost area (MAGT below $0\text{ }^{\circ}\text{C}$) of the Northern Hemisphere covers $13.91 \times 10^6\text{ km}^2$, which is 14.6 % of the Northern Hemisphere exposed land. The permafrost region (continuous, discontinuous, sporadic zones and isolated patches zones) covers $20.76 \times 10^6\text{ km}^2$, which corresponds to 21.8 % of exposed land area. The validation with 920 boreholes resulted in root mean square error of $2.0\text{ }^{\circ}\text{C}$. According to the borehole data, the difference between modelled and measured MAGT is smaller than $0.5\text{ }^{\circ}\text{C}$ in Russia, Alaska and Mongolia. The modelled MAGT is for $1\text{ }^{\circ}\text{C}$ too cold in Canada and China, whereas the modelled MAGT is too high in mountainous regions as Scandinavia, Greenland, Alps and Svalbard. In general, the model performs well in sparsely vegetated regions and less in densely vegetated regions.

References

- Smith, M. W. and Riseborough, D. W. [1996]: Permafrost monitoring and detection of climate change. *Permafrost Periglac. Process.*, 7: 301–309. doi:[10.1002/\(SICI\)1099-1530\(199610\)7:4<301::AID-PPP231>3.0.CO;2-R](https://doi.org/10.1002/(SICI)1099-1530(199610)7:4<301::AID-PPP231>3.0.CO;2-R).



Ground displacement in permafrost terrain from Sentinel-1 time-series SAR interferometry

K. Teshebaeva & Ko J. van Huissteden

Vrije Universiteit, Department of Earth Sciences, Earth and Climate Cluster, Netherlands

Widespread thawing of permafrost in the northern Eurasian continent cause severe problems for infrastructure and global climate. We test the potential of Sentinel-1 SAR imagery to enhance detection of surface changes in the Siberian lowlands of the northern Eurasian continent at Kytalyk research station site. We use InSAR time-series technique to detect seasonal surface movements related to permafrost active layer changes. The InSAR time-series derived seasonal ground displacement patterns align well with lithology and probably reflect the thaw of Yedoma plateaus. We consider also the fact of poor signal or lost coherence in thaw lake basins due to denser vegetation.

We hypothesize that at least three explanation could be relevant for the fact that surface movements

appear on “yedoma” plateaus and appear to be absent in the thaw lake basins. First, the ice volume in the yedoma plateaus may be larger, since ice accumulation in these areas already started during the last glacial, together with sedimentation. The thaw lake basins also may have a large ice volume but this is generally restricted to the surface top layer of 1–2 m thick. The ice-rich yedoma sediments may be subject to much larger volume loss by thaw than the lake basins. Second, on many yedoma surfaces there is abundant evidence of small-scale runoff channels and erosion, by which the surface subsides; the eroded material is deposited as slope material on the side slopes of the plateaus. Third, possibly slow creep of the ice-rich material occurs. To investigate these hypothesis, further monitoring is required.



UAS remote sensing in detection of the rapid decay of palsa mires

M. Verdonen, T. Kumpula, & P. Korpelainen

Department of Geographical and Historical studies, University of Eastern Finland, Yliopistokatu 7, 80101, Joensuu, Finland

Palsas (peat-covered mounds with perennially frozen cores) occur in the narrow circumpolar zone of sporadic permafrost in the northern hemisphere. Previous studies have shown palsa mounds melting and collapsing in many regions. In Fennoscandia, palsas are likely to disappear almost completely by the middle of this century as a result of warming climate and increasing precipitation.

Currently available aerial imagery of spatial resolution up to 0.5 m allow tracking areal changes of palsas in Finnish Lapland from ca. 1950's only to 2012. Active layer and high accuracy GPS measurements have been conducted on two palsa sites in Kilpisjärvi area, about 470 m.a.s.l. (68°54'N, 20°58'E) annually since 2007. In addition to aerial photography time series, we have collected Unmanned Aerial Systems

(UAS) data since 2015/16 by using various drones and sensors. Agisoft PhotoScan and ArcMap 10.5 were used to process and to analyze the data.

The ultra-high (ca. 3 cm) spatial resolution of UAS orthomosaics, Digital Elevation Models (DEM) and point cloud data allow more accurate detection of boundaries between palsa mounds and surrounding mire, which is often hindered by shrubs and other vegetation. Therefore, the new data improves our knowledge about palsas' extent, and gives us detailed information about their topographical heterogeneity. While the analysis of aerial imagery time series 1950's–2012 confirm the general trend of palsas being degrading in Finnish Lapland, the UAS data is invaluable in order to detect interannual changes, especially in the mires not covered by the field measurements.

Analyzing tundra vegetation characteristics for terrestrial LiDAR surveys of permafrost thaw subsidence

A. Veremeeva¹, F. Günther², A. Kizyakov³, & G. Grosse^{2,4}

¹*Institute of Physicochemical and Biological Problems in Soil Science, Russian Academy of Sciences, Pushchino, Russia;*

²*Alfred Wegener Institute Helmholtz Centre for Polar and Marine Research, Potsdam, Germany;*

³*Department of Cryolithology and Glaciology, Faculty of Geography, Lomonosov Moscow State University, Moscow, Russia;*

⁴*University of Potsdam, Institute of Earth and Environmental Sciences, Potsdam, Germany*

Surface subsidence is a widespread phenomenon in Arctic lowlands characterized by permafrost deposits. Together with active layer thickness dynamics surface subsidence is an important indicator of permafrost degradation in climate warming conditions. Due to small changes of surface heights of several centimeters or less per year, high-resolution and high-accuracy data are necessary to detect thaw subsidence dynamics in tundra lowlands. An appropriate method to receive such data is repeat terrestrial laser scanning (LiDAR). However, for LiDAR data analysis, uncertainties connected with vegetation dynamics should be taken into account. For example the cotton grass tussocks (*Eriophorum vaginatum*) with large areal coverage of up to 70–80 % on Yedoma uplands may exhibit significant interannual variability in leaf length and tussock density. Depending on wetness, possible influences might result from moss-lichen cover and its thickness

dynamics. The vegetation type and its succession also interacts with the microrelief and is a major endogenous parameter for active layer development, resulting in an areal differentiation of surface heights changes. In this study we present some results of the vegetation characteristics and dynamics in context of its impact on the terrestrial LiDAR investigations for thaw subsidence assessment in an ice-rich permafrost region.

During expeditions to the Lena Delta and the Bykovsky Peninsula in Northern Yakutia in 2015–2016, repeat terrestrial laser scanning was conducted on Yedoma uplands consisting of very ice-rich Ice Complex deposits. On the Bykovsky Peninsula, detailed vegetation descriptions of the main vegetation types were done including all species projective cover, cotton grass tussocks height and area sizes, moss-lichen thickness and ALT measurements (Fig. 1).

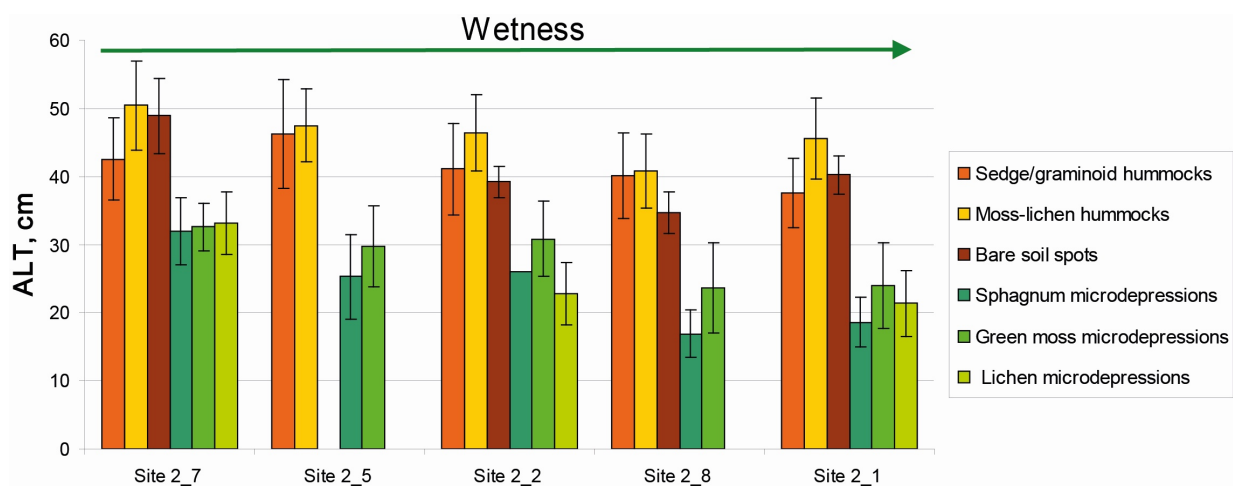


Figure 1: ALT measurements within main vegetation types for different species.

To understand the relationship between the distance, incidence angle, penetration depth and vegetation, a laser scanning experiment was done using a soil and vegetation excavation on a flat desk that was scanned at varying distinct distances.

Subsidence was about 3.5 cm on average and is mostly observed on drained inclined sites with dwarf-shrub graminoid, cotton-grass, moss-lichen tundra, representing initial baydzherakhs (thermocarst mounds). Surface heave is observed mainly within bogged depressions with sedge, moss tundra. The average ALT was 39 ± 4.1 cm and 32 ± 5.6 cm in 2015 and 2016, respectively. However, the ALT significantly varies locally and depends on the vegetation type and species (Fig. 1).

Cotton grass leaves average length decreased from 14.4 in 2015 to 12.9 as well as tussock area size

(0.32 m^2 in 2015, and 0.13 m^2 in 2016). This data can be used for the interpretation of LiDAR data for sites with cotton grass prevalence.

Less deep ALT and cotton grass size in 2016 indicate that climate conditions were less favorable for seasonal subsidence development in 2016. The sum of positive daily air temperatures was almost in the same order of magnitude in 2016 as in 2015 for the period until end of August (636 degree days in 2015 and 628 degree days in 2016). However, interannual surface subsidence was progressing, indicating a decreased resistivity of Yedoma uplands in terms of thaw subsidence under current, generally warmer conditions.

Our results shows the importance of considering vegetation and their dynamics for the interpretation of repeat terrestrial LiDAR data for thaw subsidence estimation.

Sensitivity of soil freezing process to snow cover changes and permafrost active layer dynamics in Arctic Alaska

Yonghong Yi¹, John S. Kimball², Richard H. Chen³, Mahta Moghaddam³, & Charles Miller¹

¹Jet Propulsion Laboratory, California Institute of Technology, 4800 Oak Grove Drive, Pasadena CA, USA;

²Numerical Terradynamic Simulation Group, The University of Montana, Missoula MT, USA;

³Department of Electrical Engineering, University of Southern California, CA, USA

Contribution of cold season soil respiration to the boreal-arctic carbon cycle and its potential feedbacks to climate change remain poorly quantified, which can be largely attributed to a poor understanding of changes in the soil thermal regime and zero-curtain period during seasonal soil freezing. Here, we investigated underlying processes controlling the soil freezing process in Arctic Alaska using an integrated approach combining *in-situ* observations, local-scale (≈ 50 m) airborne longwave (P-band) radar retrievals and a remote sensing based permafrost model. The observed mean zero-curtain periods at 25 cm, 35 cm, and 45 cm soil depths were 61.2 ± 11.2 , 69.2 ± 12.6

and 73.0 ± 15.1 days respectively, based on *in-situ* soil temperature observations at sites across a 2° latitudinal zone and using a cutoff temperature of -0.35°C (Fig. 1).

The model simulated zero-curtain period was generally consistent with the *in-situ* observations, with a mean R value of 0.6 ± 0.2 and RMSE value of 19.6 ± 6.1 days at depth of 35 cm. The zero-curtain period derived from both *in-situ* data and model simulations is positively correlated ($R > 0.55$, $p < 0.01$) with MODIS (MODerate resolution Imaging Spectroradiometer) snow cover extent (SCE) during the early snow season (September–October).

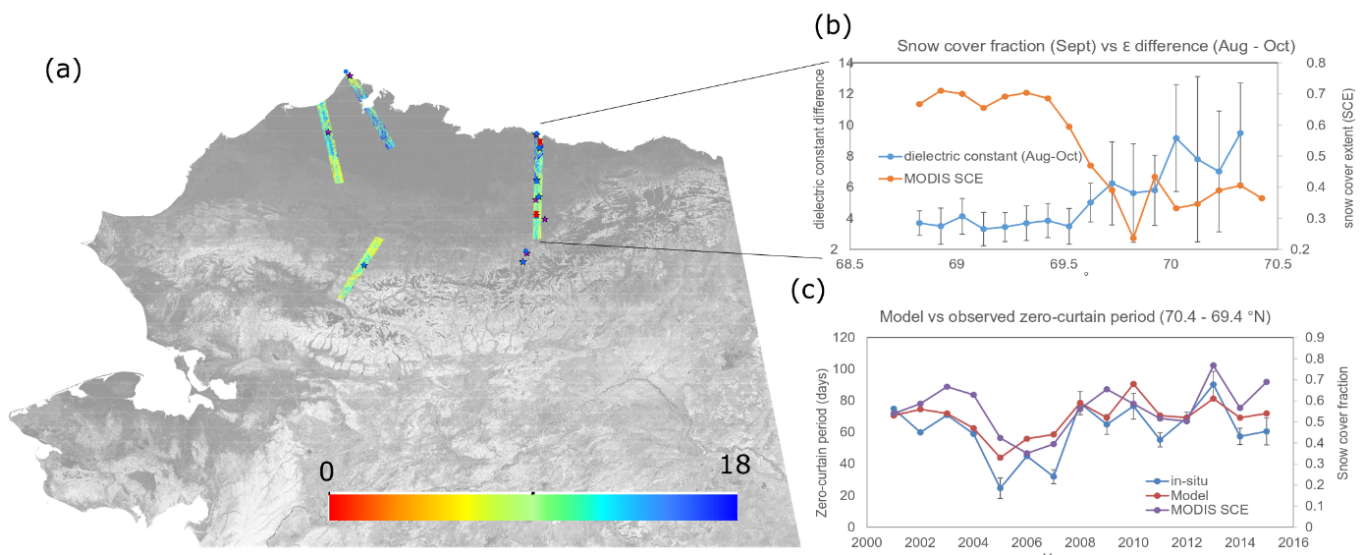


Figure 1: a) Study area in Arctic Alaska with multiple AirMOSS radar flights available. The radar retrieved surface soil dielectric constant in August, 2015, was shown here and the background image is a permafrost probability map with darker color indicating higher permafrost probability. *In-situ* measurements including soil temperature from GTN-P (Global Terrestrial Network for Permafrost) sites (blue stars), active layer thickness from CALM (Circumpolar Active Layer Monitoring) sites (magenta stars), soil temperature and dielectric constant measurements from two SoilSCAPE sites (red dots); b) Latitudinal variations of MODIS SCE versus difference of radar retrieved surface soil dielectric constant between August and early October, and c) comparisons of model simulated and observed zero-curtain period at soil depth of 35 cm versus MODIS SCE, along one of the AirMOSS flights.

This was also supported by Airborne Microwave Observatory of Subcanopy and Subsurface (AirMOSS) radar dielectric constant (ϵ) retrievals. The ϵ difference of surface soils between August and early October retrievals is negatively correlated with snow cover fraction in September derived from MODIS SCE data ($R = -0.77$, $p < 0.01$, Fig. 1b); areas with lower SCE ($>69.7^\circ\text{N}$) show a larger ϵ difference (mean = 7.32 ± 7.58), indicating earlier frozen condition. At regional scale, the model simulated soil freezing onset and zero-curtain period within the surface soil layer (<45 cm depth) do not show a significant trend due to large interannual variability in early season snow conditions over the satellite record (2001–2016). However, deeper soils generally show a later soil freezing onset, with a mean lagging rate of 0.79 ± 0.52 days/cm at 35 cm depth. Therefore, a deepening active layer associated with climate warming will likely lead to a longer unfrozen period in deeper soils and potentially greater soil carbon loss

during the cold season. Potential mapping of surface organic layer, freeze/thaw and soil moisture profiles using low frequency radar may improve regional assessment and modeling of soil active layer dynamics, enabling more accurate predictions of boreal and arctic environmental changes.

References

- Yi, Y., Kimball, J. S., Chen, R. H., Moghaddam, M., Reichle, R. H., Mishra, U., Zona, D., and Oechel, W. C. [2018]: Characterizing permafrost active layer dynamics and sensitivity to landscape spatial heterogeneity in Alaska. *The Cryosphere*, 12, 145–161; doi:[10.5194/tc-12-145-2018](https://doi.org/10.5194/tc-12-145-2018).
- R. H. Chen, A. Tabatabaenejad, and M. Moghaddam: Retrieval of Permafrost Active Layer Properties Using Time-Series P-Band Radar Observations. *IEEE Trans. Geosci. Remote Sens.*, in review.

Investigating the decadal changes of frozen ground at Resolute Bay in the Canadian High Arctic through surface elevation changes measured by GPS Interferometric Reflectometry

J. Zhang¹ L. Liu¹, & Y. Hu²

¹Earth System Science Programme, Faculty of Science, The Chinese University of Hong Kong, Hong Kong, China;

²School of Geodesy and Geomatics, Wuhan University, Wuhan, China

Over permafrost, the ground surface undergoes seasonal subsidence and uplift due to annual thawing or freezing, while decadal changes are associated with permafrost degradation or aggradation. Building on the successful use of the GPS Interferometric Reflectometry (GPS-IR) technique to study frozen ground [Liu & Larson, 2018], we apply this technique to a station (ID: RESO, coordinates: 74.69° N, 265.11° E) located at Resolute Bay in the Canadian High Arctic. We aim to quantify decadal changes of ground surface elevation and investigate the response of the active layer and the uppermost permafrost to the recent warming. We construct a 12-years-long (2003–2014) time series of ground surface elevation, showing a secular subsidence trend of 0.68 ± 0.02 cm/year (Fig. 1). We also find strong summer heave in a few years (2003, 2006, and 2007), possibly due to downward migration

of soil moisture and subsequent refreeze at the base of the active layer. Moreover, the end-of-thaw-season elevations showed large interannual variability, and were highly correlated with thaw indices represented by the square-root of degree days of thawing (\sqrt{DDT}). Lower surface vertical positions at the end of thaw seasons were associated with larger \sqrt{DDT} , and vice versa. After the warmest summer of our study period in 2011, the end-of-thaw-season elevations and \sqrt{DDT} were weakly correlated. This Markovian behavior is possibly due to that the response of the active layer and the uppermost permafrost was reset after 2011 [Hinkel & Nelson, 2003]. Our study shows that, at Resolute Bay, the ground surface vertical movement in thaw seasons was highly related with changes in air and ground temperatures and indicates permafrost degradation from 2003 to 2014.

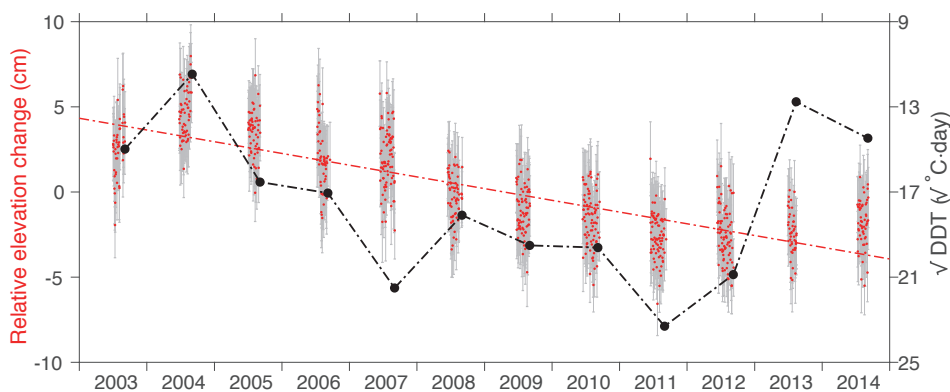


Figure 1: Time series of relative ground surface elevation changes (red dots with error bars) and annual \sqrt{DDT} (black solid dots) from 2003 to 2014. The red dashed line shows the secular subsidence trend of ground surface. Note that the vertical axis of \sqrt{DDT} is flipped to better illustrate their correlation with the elevation changes.

References

L. Liu & M.K. Larson [2018]: Decadal changes of surface elevation over permafrost area estimated using reflected GPS signals. *The Cryosphere*, 12, 477–489, doi:10.5194/tc-12-477-2018.

K.M. Hinkel & F.E. Nelson [2003]: Spatial and temporal patterns of active layer thickness at Circumpolar Active Layer Monitoring (CALM) sites in northern Alaska, 1995–2000. *Journal of Geophysical Research*, 108, p. 8168, doi:10.1029/2001JD000927.



SESSION

Oceanography of Polar Seas

Validation of ocean colour products for the Arctic Ocean

A. Bracher¹, Y. Liu¹, R. Goncalves-Araujo¹, I. Peeken², & T. Dinter¹

¹*Phytooptics Group at the Alfred-Wegener-Institute Helmholtz Centre for Polar & Marine Research, Bremerhaven, Germany;*

²*Polare Biologische Ozeanographie at the Alfred-Wegener-Institute Helmholtz Centre for Polar & Marine Research, Bremerhaven, Germany*

We have conducted various field campaigns from 2011 to 2017 in the Arctic Ocean to measure remote sensing reflectance (RRS), chlorophyll-a (Chl) and absorption by detrital matter (adg) and specifically by colored dissolved organic matter (CDOM). The data have been used to assess the quality of satellite retrievals, particularly applied to MODIS-Aqua and Sentinel-3 OLCI satellite data. Results (published in [Gonçalves et al. \[2018\]](#)) showed that in the central and Eastern Arctic Ocean that global and regionally tuned empirical algorithms provide poor chl estimates. The semi-analytical algorithm of Garver-Siegel-Maritorena (GSM; Maritorena et al. 2002) implemented in the

Generalized Inherent Optical Property model (GIOP, Werdell et al. 2013) and on the other hand, provide robust estimates of Chl-a and adg. Applying GSM with modifications proposed for the western Arctic Ocean produced reliable information on adg, and specifically for CDOM. We also assessed the quality of Chl algorithms applied to MODIS and OLCI particularly for the Fram Strait by comparison to validation by High Pressure Liquid Chromatography (HPLC) determined and derived from measurements of hyperspectral absorption and transmissiometry with an underway spectrophotometer ([Liu et al. \[2018\]](#), see Figure 1).

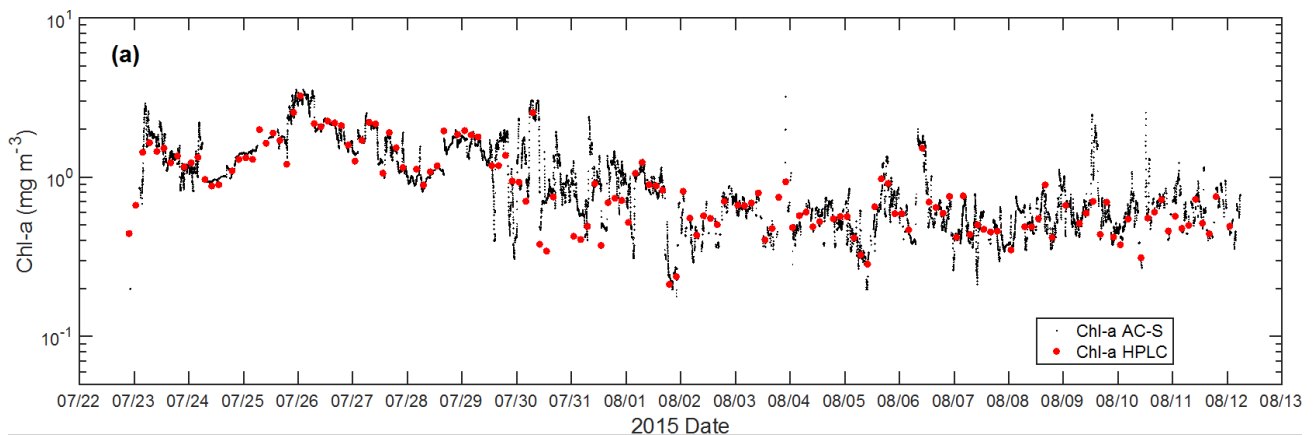


Figure 1: Example for Fram Strait Polarstern cruise PS99 (Jun-Jul 2017) Chl validation data sets (black: from underway spectroscopy, red: water samples analysed with HPLC after filtration)

Results showed that Chl measured using HPLC (HPLC) was well related ($R^2 = 0.90$) to the collocated particulate absorption line height and derived Chla data set of the underway spectrophotometry based Chl-a data sets. The later proved to be a much more sufficient data source by generating over 10 to 20 times more match-ups than those obtained from discrete water samples. Overall, the band ratio (OCI, OC4) Chl-a operational products from MODIS-A and OLCI as well as OLCI C2RCC products showed acceptable results, however results of OLCI Chl from im-

proved atmospheric correction (Polymer and C2RCC algorithms) showed much better agreement to the in-situ validation data sets. In addition we also assessed the RRS satellite data in the Fram Strait from OLCI with the in-situ RRS determined from underwater optical light fields. Results showed reasonable results for OLCI 2nd reprocessing data (Jan 2018) for most wavelengths but a clear high bias for the blue wavebands leading to an underestimation of Chl at low concentrations.



References

- Gonçalves R., Rabe B., Peeken I. & Bracher A. [2018]: High colored dissolved organic matter (CDOM) absorption by waters of the central-eastern Arctic Ocean: implications for biogeochemistry and ocean color algorithms. *PLoS ONE*, 13(1): e0190838. doi:[10.1371/journal.pone.0190838](https://doi.org/10.1371/journal.pone.0190838).
- Liu. Y., Roettgers R., Ramírez-Pérez M., Dinter T., Steinmetz F., Noethig E.-M., Hellmann S., Wiegmann S., & Bracher A. [2016]: Underway spectrophotometry in the Fram Strait (European Arctic Ocean): a highly resolved chlorophyll a data source for complementing satellite ocean color. *Optics Express*: in press.

Analyzing arctic seasonal phytoplankton dynamics with MERIS satellite fluorescence

J. R. El Kassar, B. Juhls, R. Preusker, & J. Fischer

Institute of Space Sciences, Freie Universität Berlin

We studied spatial and temporal variations in MERIS satellite fluorescence (F_{sat}) and fluorescence efficiency (Φ_{sat}) over the Arctic Ocean (60–90N) in order to understand the relationship between chlorophyll-a (Chl-a) and F_{sat} and its influence factors. Analysing 10 years of MERIS data we focused on the months May to September due to satellite data availability being limited by ice extent, viewing geometry and lack of sunlight during the rest of the year. Due to the heterogeneity of the Arctic we also separated the domain into subdomains (e.g. the Greenland-Norwegian Sea, Barents Sea, etc.).

F_{sat} and Φ_{sat} show strong seasonal variability with overall lower values in summer (June to August), whereas the seasonal cycle differed highly from region to region. On the one hand temporal variations align with seasonal changes in stratification and nutrient availability, on the other hand spatial variations correspond with ocean currents in the Arctic such as the North Atlantic Current (NAC) and Trans Polar Drift (TPD). This feature can be seen in figure 1 showing the Φ_{sat} climatology for summer.

To test certain hypotheses on the influence factors on Φ_{sat} we compared the MERIS data with climatologies of nutrients, salinity and mixed layer depth. Depending on month and area the major factors affecting Φ_{sat} varied. Results show, that in some cases nutrient stress is linked to a reduction of fluorescence efficiency leading to a lower F_{sat} signal. Another major contribution, however, is the stratification and creation of subsurface Chl-a maxima by a shallowing of the mixed layer depth. Under these conditions the MERIS still detects some Chl-a but the F_{sat} signal is strongly decreased due to the high absorption by water at the fluorescence wavelength 683 nm [Fischer & Kronfeld, 1990].

The seasonal and regional changes we observed in Φ_{sat} correspond with the current understanding of phytoplankton dynamics in the Arctic such as cycles

of stratification [Chiswell et al., 2014] and advection of nutrient rich (e.g. Arctic) or depleted (e.g. Atlantic) water.

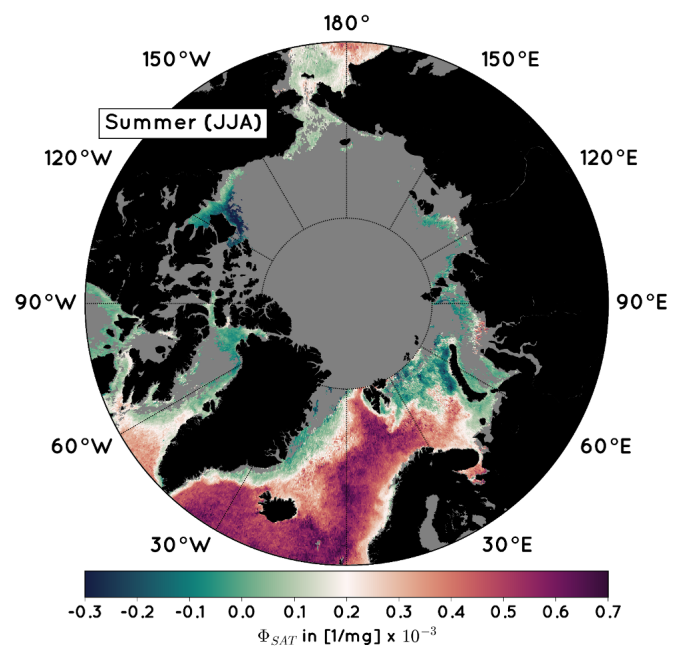


Figure 1: summer climatology of Φ_{sat} from MERIS. High Φ_{sat} in red, low Φ_{sat} in green, negative F_{sat} values were not discarded since they showed a coherent behaviour with Chl-a. Grey areas show invalid pixels at any given time in the climatology (May-Sep. 2002-2012).

References

- J. Fischer & U. Kronfeld [1990]: Sun-stimulated chlorophyll fluorescence 1: Influence of oceanic properties. *International Journal of Plankton Research*, Vol 11:12, 2125–2147. doi:1080/01431169008955166.
- S. Chiswell, P. Calil, & P. Boyd [1990]: Spring blooms and annual cycles of phytoplankton: A unified perspective. *International Journal of Plankton Research*, Vol 37:3, 500–508. doi:10.1093/plankt/fbv021.

Measuring bio-optical properties in coastal waters of the Laptev Sea and Lena River for the improvement of Ocean Color algorithms

B. Juhls¹, P. P. Overduin², & J. Fischer¹

¹*Freie Universität Berlin, Institute of Space Sciences, Germany;*

²*Alfred-Wegener-Institute Helmholtz Center for Polar and Marine Research, Potsdam, Germany*

Thermal degradation of permafrost and intensified coastal erosion result in remobilization of organic carbon in the Arctic coastal areas, changing transport pathways and the magnitude of land-to-sea fluxes. Near-coastal waters in the Laptev Sea show extremely high absorption by colored dissolved organic matter (aCDOM), most of which derives from the huge discharge of the Lena River. Satellite retrievals of aCDOM and a strong relationship between aCDOM and dissolved organic carbon (DOC) in river-influenced waters offer the potential to identify DOC transport pathways and changes of fluxes.

To retrieve aCDOM in Arctic coastal waters, Ocean Color processors and bio-optical models require bio-optical properties parametrized for a specific region. However, we lack *in situ* information. For example, the contribution of CDOM to the total absorption coefficient and the exponential slopes of aCDOM and non-algal particle absorption (aNAP) are unknown and often set constant in bio-optical models.

To parameterize these properties, inherent optical properties (IOPs), apparent optical properties (AOPs) and the concentrations of constituents were simultaneously measured *in situ* in coastal waters of the Laptev Sea and in the Lena River.

These unique multi-year observations show extreme spatial and temporal variations within the transition zone from river to ocean. Turbulent and chaotic regional processes, such as the spring ice break-up and mixing processes of river-, melt- and sea-water, result in rapid changes of optical properties. We implement the observed variability of parameters to semi-analytical algorithms. With this, we aim to improve the satellite retrieval of aCDOM in optically complex Arctic coastal waters.

Better quality of retrieved products as well as a growing number of satellite-borne optical imaging sensors will help to better understand surface water processes in Arctic shelf waters.

Assessing nearshore sediment and sea surface temperature dynamics using Landsat satellite imagery at Herschel Island, western Canadian Arctic

K. P. Klein¹, H. Lantuit^{1,2}, B. Heim¹, F. Fell³, D. J. Jong⁴, & J. E. Vonk⁴

¹*Alfred Wegener Institute Helmholtz Centre for Polar and Marine Research, Potsdam, Germany;*

²*Institute of Earth and Environmental Sciences, University of Potsdam, Potsdam, Germany;*

³*Informus GmbH;*

⁴*Utrecht University, Department of Earth Sciences, Utrecht and University of Groningen, Arctic Center, Groningen, The Netherlands*

The Arctic is subject to substantial changes due to the greenhouse gas induced climate change. While impacts on lateral transport pathways such as rivers have been extensively studied yet, there is little knowledge about ecological and geological reactions of nearshore environments, even though those are of high importance for native communities. In this study, we use the extensive Landsat archive with comparable data from 1982 on to investigate sediment dispersal and sea surface temperatures under changing seasonal wind conditions in the nearshore zone of Herschel Island in the western Canadian Arctic. Even in the absence of an extensive *in-situ* dataset, we reveal clear differences between the two prevailing wind conditions (E and

NW). During E wind conditions, the Mackenzie River Plume gets distributed over large parts of the Canadian Beaufort Shelf and is the main influencing factor for nearshore sediment dispersal and sea surface temperature dynamics. Contrary, the nearshore dynamics during NW wind conditions are not affected by the Mackenzie River plume, revealing the local nature of the nearshore environment. First field measurements from summer 2017 indicate that recently published SPM and turbidity models are not able to reflect this local nature and strongly underestimate reality. In future, we plan to collect an extensive validation dataset in Arctic nearshore environments to calculate accurate bio-optical models.



Highly resolved data set on different phytoplankton pigments and functional types retrieved from underway spectrophotometry in the Fram Strait

Y. Liu^{1,2}, E. Boss⁴, A. Chase⁴, Y. Pan⁵, H. Xi¹, E. Nöthig¹, S. Wiegmann¹, & A. Bracher^{1,3}

¹*Alfred Wegener Institute Helmholtz Centre for Polar and Marine Research, Bussesstr. 24, 27570 Bremerhaven, Germany;*

²*Faculty of Biology and Chemistry, University of Bremen, Leobener Str. NW 2, 28359 Bremen, Germany;*

³*Institute of Environmental Physics, University of Bremen, Otto-Hahn-Allee 1, 28359 Bremen, Germany;*

⁴*University of Maine, 5706 Aubert Hall, Orono, ME, 04469, USA;*

⁵*State Key Laboratory of Estuarine and Coastal Research, East China Normal University, Shanghai, 200062, China*

Four approaches to estimate phytoplankton pigment concentration from particulate absorption spectra, namely Gaussian decomposition, singular value decomposition, neural network and empirical orthogonal function analysis, are evaluated and intercompared and finally evaluated. The neural network model is found to best estimate 14 phytoplankton pigments concentrations (r ranges from 0.45 to 0.96, log₁₀ based RMSE ranges from 0.005 to 0.248). The estim-

ated pigments concentrations are further exploited based on CHEMTAX analysis to derive phytoplankton functional types (PFTs). By the application of this method to the particulate absorption spectra collected by underway spectrophotometry during three summer cruises in 2015–2017 to the Fram Strait (European Arctic Ocean), continuous surface PFTs are estimated along the cruise course.

Phytoplankton diversity in the Southern Ocean retrieved from hyperspectral satellite observations

Julia Oelker¹, Svetlana N. Losa², Mariana A. Soppa², Tilman Dinter², Vladimir V. Rozanov¹, Andreas Richter¹, John P. Burrows¹, & Astrid Bracher^{1,2},

¹*Institute of Environmental Physics, University Bremen, Bremen, Germany;*

²*Alfred Wegener Institute Helmholtz Centre for Polar and Marine Research, Bremerhaven, Germany*

Biological productivity in the Southern Ocean plays a key role in the global carbon cycle. In a changing environment, monitoring the phytoplankton diversity in this biogeochemically important region is of great interest to predict associated changes in carbon export and biogeochemical fluxes. Long-time and large-scale observations of the phytoplankton diversity in the Southern Ocean are desirable. The PhytoDOAS method provides a mean for such investigations by exploiting the spectral signatures of absorption spectra of different phytoplankton functional types (PFT) imprinted in top-of-atmosphere radiances measured by hyperspectral satellite sensors such as the Scanning Imaging Absorption Spectrometer for Atmospheric Chartography (SCIAMACHY) [Bracher et al., 2009]. Since available hyperspectral sensors have generally a worse spatial resolution than traditional multispectral ocean color sensors, PFT information from multispectral and hyperspectral satellite observations have been combined synergistically [Losa et al., 2017]. In this synergistic approach, the advantages of both sensor types are exploited by combining the high spatial resolution of multispectral sensors with the less-empirical, spectral-based PFT retrieval methods on hyperspectral sensors. Since SCIAMACHY stopped measuring in 2012, newer hyperspectral sensors with

improved spatial resolution are available for extending the PFT time series from 2012 onwards. Here, we are presenting coccolithophores and diatom concentrations in the Southern Ocean retrieved from the Ozone Monitoring Instrument (OMI) in comparison to the SCIAMACHY PFT product. To increase sampling limited by high cloud coverage and massive OMI sensor degradation from 2008 on, we further extended the synergistic approach used in Losa et al. [2017] and applied it to OMI PFT.

References

- Losa, S. N., Soppa, M. A., Dinter, T., Wolanin A., Brewin R. J. W., Bricaud A., Oelker, J., Peeken I., Gentili B., Rozanov V. V., Bracher, A. [2017]: Synergistic exploitation of hyper- and multispectral Sentinel measurements to determine Phytoplankton Functional Types (SynSenPFT). *Frontiers in Marine Science*, 4, 203. doi:[10.3389/fmars.2017.00203](https://doi.org/10.3389/fmars.2017.00203).
- Bracher, A., Vountas, M., Dinter, T., Burrows, J.P., Röttgers, R., Peeken, I. [2009]: Quantitative observation of cyanobacteria and diatoms from space using PhytoDOAS on SCIAMACHY data. *Biogeosciences*, 6, 751–764, doi:[10.5194/bg-6-751-2009](https://doi.org/10.5194/bg-6-751-2009).

First steps towards assessing the radiation budget in the shelf areas of the Laptev Sea by remote sensing and radiative transfer modelling

V. Pefanis¹, M. A. Soppa¹, S. Hellmann², J. Hölemann¹, M. A. Janout¹, F. Martynov³, B. Heim⁴, V. Rozanov⁵, S. Loza¹, T. Dinter¹, & A. Bracher^{1,5}

¹Alfred Wegener Institute, Helmholtz Centre for Polar and Marine Research, Bremerhaven, Germany;

²Swiss Federal Institute of Technology, Zurich, Switzerland;

³Arctic and Antarctic Research Institute, St. Petersburg, Russia;

⁴Alfred Wegener Institute, Helmholtz Centre for Polar and Marine Research, Potsdam, Germany;

⁵Institute for Environmental Physics, University of Bremen, Bremen, Germany

The Arctic Ocean receives considerable input of terrigenous carbon supplied by the Arctic rivers. In the context of climate change and thawing permafrost in Eastern Siberia, freshwater discharge and subsequently the riverine input may increase in the future, affecting the radiation budget in the region. Here, we examine the effect of the water optically active constituents on the radiation budget of the Laptev Sea surface waters. We use a coupled atmosphere-ocean radiative transfer model (RTM), MERIS data and in situ measurements of CDOM absorption (aCDOM), total suspended matter (TSM) and chlorophyll concentration (Chla) to simulate the radiative heating. As a first step, we evaluate RTM simulation capabilities by implementing MERIS imaging geometry and collocating every *in-situ* station to MERIS data to simulate the top of the atmosphere radiance. Additionally, we demonstrate the significant influence of CDOM and TSM on the energy budget of the Laptev

Sea surface waters. Results show that high CDOM absorption may lead to 11.4 % more absorbed energy in the surface layer (upper 2m) compared to low CDOM waters, which corresponds to an increased heating rate of about 1.3 °C/day. Regarding TSM, high concentration leads to an increase of 10.6 % in the absorbed energy and 1.2 °C/day in the heating rate compared to low concentrations, while the impact of phytoplankton is almost negligible. As more energy is trapped in the surface, cooling occurs in the sub-surface layer (>2 m). We further examine the influence of the absorbed solar energy on the melting of sea ice and the induced surface fluxes to the atmosphere. In addition, using satellite remote sensing retrievals of aCDOM, TSM, Chla and sea surface temperature data as input to the RTM simulations, we present the spatial distribution of potential radiative heating of Laptev Sea surface waters.

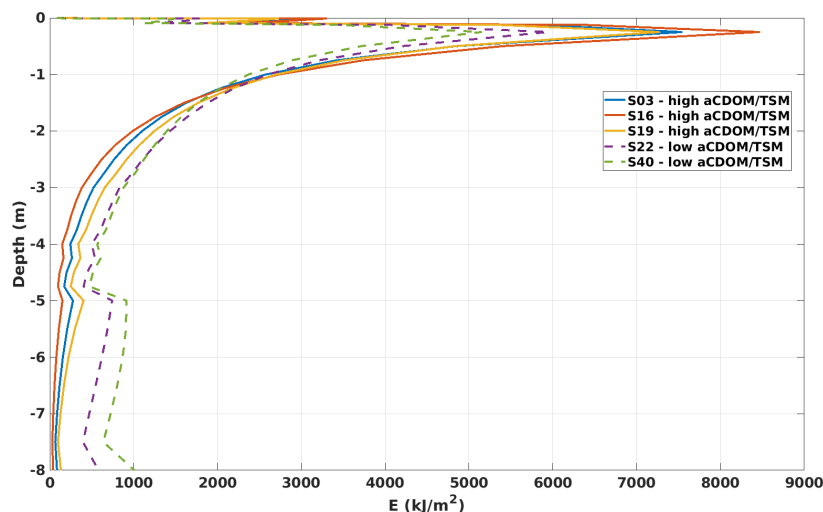


Figure 1: Daily energy absorbed in the surface layer (2 m) for selected *in-situ* stations. CDOM absorption ranges from 0.2 m^{-1} (S40) to 1.67 m^{-1} (S03) and TSM concentration from 0.4 g m^{-3} (S40) to 7.2 g m^{-3} (S16).

Spatio-temporal patterns of the carbon-to-chlorophyll ratio of natural phytoplankton communities in the Southern Ocean

C. M. Robinson¹, N. Schuback², T. J. Ryan-Keogh³, W. Moutier⁴, S. J. Thomalla³, & D. Antoine¹

¹*Remote Sensing and Satellite Research Group, Curtin University, Kent Street, Bentley 6102, WA, Australia;*

²*Swiss Polar Institute, Ecole Polytechnique Federale De Lausanne ENT-R SPI-GE, GR C2 505, Station 2, 1015 Lausanne, Switzerland;*

³*Southern Ocean Carbon and Climate Observatory, Natural Resources and Environment, CSIR, Rosebank, Cape Town 7700, South Africa;*

⁴*Koninklijk Meteorologisch Instituut, Institut Royal Meteorologique, Ringlaan 3 Avenue Circulaire, 1180 Brussel, Bruxelles, Belgium*

The Southern Ocean is a major sink of anthropogenic carbon dioxide (CO₂) whereby biological and physical pumps drawdown and convert CO₂ to organic carbon, for transfer through the food web, remineralization or sequestration to the ocean floor. Phytoplankton primary production drives the fixation of carbon to an organic form via the process of photosynthesis. Primary production and phytoplankton growth in the Southern Ocean are both mediated by an extensive list of bottom-up processes including micronutrients and macronutrients, light and mixed layer depth, sea ice, CO₂ concentration, grazing & senescence. However, rates of primary production and rates of growth often become uncoupled due to their differential responses to changed environment conditions. A link between phytoplankton primary production and growth is the carbon-to-chlorophyll (C:Chl) ratio which, as a single parameter can provide an assessment of the physiological acclimation state of phytoplankton.

Phytoplankton carbon and chlorophyll are the two most commonly measured proxies of phytoplankton biomass and both can be estimated optically and remotely using measurements of absorption, backscat-

tering, fluorescence or reflectance. Studying the ratio of carbon to chlorophyll can reveal the environmental controls on phytoplankton growth, photosynthesis and primary production especially with respect to nutrient stress and light stress. The use of satellites to optically monitor phytoplankton is challenging in polar regions due to persistent cloud cover, low solar elevations and a sampling depth limited to the first optical depth as experienced globally. We first explore spatio-temporal patterns in the phytoplankton C:Chl ratio using bio-Argo autonomous float observations which can support satellite observations to provide higher spatial and temporal resolution and capture processes occurring at depth at dynamic hydrographic frontal boundaries found between 40–60 °S. This study will report the C:Chl ratios and factors influencing the C:Chl ratio across the Southern Ocean between 40–60 °S and 0–180 °E. Of particular focus will be the photoacclimation response of phytoplankton in response to the available irradiance within the mixed layer. Patterns observed in the bio-Argo dataset will be compared to patterns derived from the long-term MODIS-Aqua & VIIRS satellite records.

Reassessing satellite algorithms for phytoplankton in the Southern Ocean

C. M. Robinson¹, N. Schuback², T. J. Ryan-Keogh³, W. Moutier⁴, S. J. Thomalla³, & D. Antoine¹

¹*Remote Sensing and Satellite Research Group, Curtin University, Kent Street, Bentley 6102, WA, Australia;*

²*Swiss Polar Institute, Ecole Polytechnique Federale De Lausanne ENT-R SPI-GE, GR C2 505, Station 2, 1015 Lausanne, Switzerland;*

³*Southern Ocean Carbon and Climate Observatory, Natural Resources and Environment, CSIR, Rosebank, Cape Town 7700, South Africa;*

⁴*Koninklijk Meteorologisch Instituut, Institut Royal Meteorologique, Ringlaan 3 Avenue Circulaire, 1180 Brussel, Bruxelles, Belgium*

The Southern Ocean is an ideal area for the application of remote sensing due to its vast remoteness and difficult conditions for *in-situ* sampling. However, it is for these same reasons that the *in-situ* validation of satellite products in the Southern Ocean region has been less frequent and more spatially constrained as compared to other ocean basins. Generally, satellite algorithms estimating optical properties and phytoplankton related parameters such as chlorophyll- α and particulate organic carbon have performed poorly in the Southern Ocean. Recent validation efforts employed the use of autonomous bio-Argo floats with chlorophyll fluorescence sensors embedded in the sensor package and suggested that the poor performance of existing algorithms is due to the limited spatial and temporal representation of existing *in-situ* validation datasets and satellite matchups rather than issues with the global algorithms themselves. In fact, the global chlorophyll- α and particulate organic carbon algorithms performed very well, however there is still some debate as to how representative chlorophyll fluorescence is of phytoplankton pigment biomass which is more robustly measured using high performance liquid chromatography (HPLC) analysis of water samples. The Antarctic Circumpolar Expedition (ACE) during the Austral summer of 2016–2017 was the first scientific circumnavigation of Antarctica since historical expeditions of the 19th century. The expedition presented an unprecedented opportunity to collect the largest spatially representative dataset of optical properties and phytoplankton characterist-

ics (See Fig. 1). Sampling on board the ship included high resolution sampling of in-water optics from the underway flow-through seawater system, and discrete sampling of phytoplankton characteristics every 4 hours. Depth specific phytoplankton characteristics and optical properties were supplied from rosette casts and deployment of an inherent optical property instrument package. Discrete sampling at the bow provided some measurements of above-water radiometry along the voyage track. Comparisons were made between surface total chlorophyll- α concentrations determined by HPLC and satellite chlorophyll- α products chlor- α (OCI-OC3 transition) and OC3, and also surface particulate organic carbon concentrations (POC) determined using a Carbon-Hydrogen-Nitrogen analyser and the satellite POC product. Generally, the chlorophyll- α and POC algorithms for both the Moderate Resolution Imaging Spectroradiometer (MODIS) Aqua and Visible Infrared Imaging Radiometer Suite (VIIRS) sensors underestimated total chlorophyll- α and particulate organic carbon. The slopes of the linear regression between the *in-situ* sample measurement and level 3 satellite products varied from 0.16–0.57 for chlorophyll- α and 0.27–0.51 for POC. There was no clear dependency on pixel size, pixel window size or the length of the temporal composite. Using particulate absorption, total absorption, back-scattering and radiometry data we try to explain the underestimation of chlorophyll- α and POC by satellite products for the ACE voyage dataset.

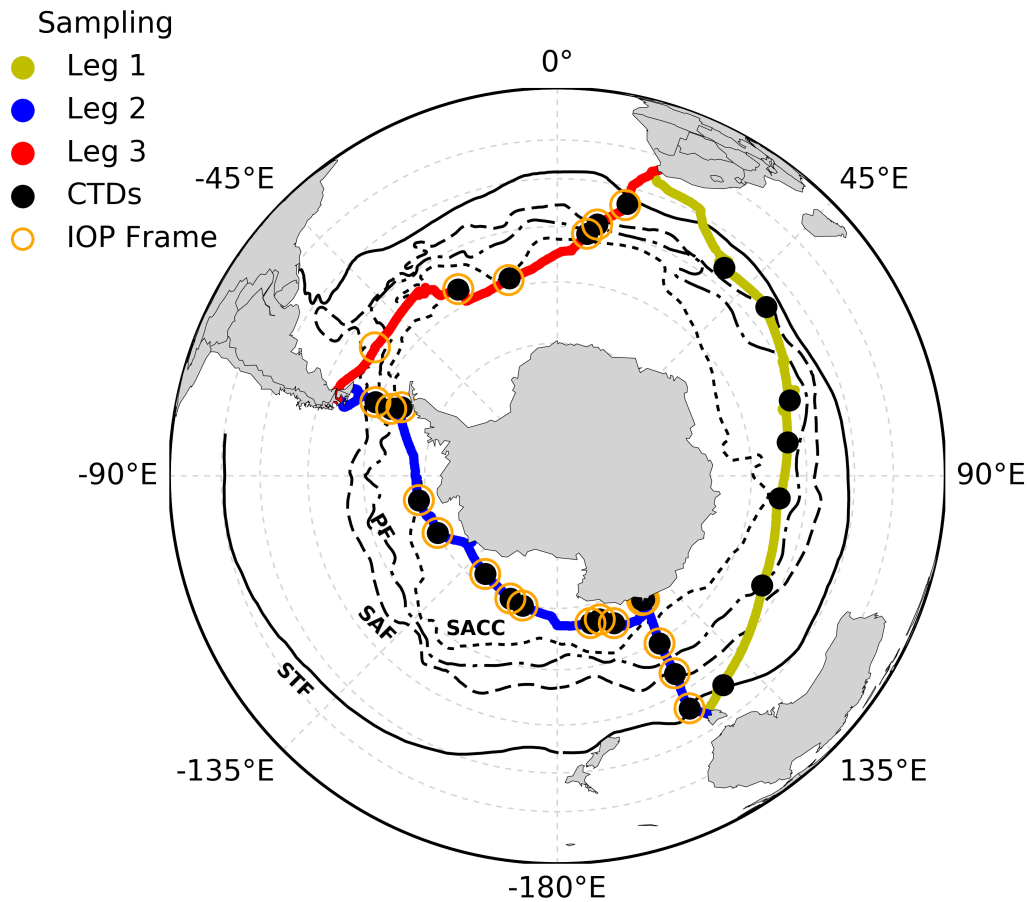


Figure 1: Antarctic Circumpolar Expedition voyage and sampling track, including leg 1 (20/12/16-19/01/16), leg 2 (22/01/17-22/02/17) and leg 3 (25/02/17-19/03/17). Black circles indicate the positions of rosette casts with conductivity-temperature-depth sensors (CTDs) attached and open orange circles indicate the position of the inherent optical property (IOP) sensor frame deployments. Major frontal boundaries as determined by Orsi et al. (1995) are marked including the sub-tropical front (STF), sub-Antarctic front (SAF), polar front (PF) and Southern Antarctic Circumpolar Current (SACC), note though that these boundaries are dynamic.

References

- A.H. Orsi, T. Whitworth III, and W.D. Nowlin Jr [2005]: On the meridional extent and fronts of the Antarctic Circumpolar Current. *Deep Sea Research I*, 42, p. 641–673. doi:[10.1016/0967-0637\(95\)00021-W](https://doi.org/10.1016/0967-0637(95)00021-W).



SESSION

Polar Lake Dynamics

Terrestrial CDOM in lakes of Yamal Peninsula: Connection to lake and lake catchment properties – a remote sensing study

Yury Dvornikov^{1,2}, Marina Leibman^{1,3}, Birgit Heim², Annett Bartsch^{4,5,6}, Ulrike Herzschuh^{2,7}, Tatiana Skorospekhova⁸, Irina Fedorova^{9,10}, Artem Khomutov^{1,3}, Barbara Widhalm⁵, Anatoly Gubarkov¹¹, & Sebastian Rößler¹²

¹Earth Cryosphere Institute Tyumen Scientific Centre SB RAS, 625026 Tyumen, Russia;

²Alfred Wegener Institute Helmholtz Centre for Polar and Marine Research, 14473 Potsdam, Germany;

³University of Tyumen, International Institute of Cryology and Cryosophy, 625003 Tyumen, Russia;

⁴b.geos, 2100 Korneuburg, Austria;

⁵Zentralanstalt für Meteorologie und Geodynamik, 1190 Vienna, Austria;

⁶Austrian Polar Research Institute, 1090 Vienna, Austria;

⁷Institute of Earth and Environmental Sciences, University of Potsdam, 14469 Potsdam, Germany;

⁸Arctic and Antarctic Research Institute, 199397 Saint-Petersburg, Russia;

⁹Institute of Earth Science, Saint-Petersburg State University, 199178 Saint-Petersburg, Russia;

¹⁰Kazan Federal University, 420008 Kazan, Russia;

¹¹Tyumen Industrial University, 625000 Tyumen, Russia;

¹²FIELAX, 27568 Bremerhaven, Germany

In this study, we analyze interactions in lake and lake catchment systems of a continuous permafrost area. We assessed colored dissolved organic matter (CDOM) absorption at 440 nm ($a(440)_{CDOM}$) and absorption slope ($S_{300-500}$) in lakes using field sampling and optical remote sensing data for an area of 350 km² in Central Yamal, Siberia. Applying a CDOM algorithm (ratio of green and red band reflectance) for two high spatial resolution multispectral GeoEye-1 and Worldview-2 satellite images, we were able to extrapolate the $a(\lambda)_{CDOM}$ data from 18 lakes sampled in the field to 356 lakes in the study area (model $R^2 = 0.79$). Values of $a(440)_{CDOM}$ in 356 lakes varied from 0.48 to 8.35 m⁻¹ with a median of 1.43 m⁻¹. This $a(\lambda)_{CDOM}$ dataset was used to relate lake CDOM to 17 lake and lake catchment parameters derived from optical and radar remote sensing data and from digital elevation model analysis in order to establish the parameters controlling CDOM in lakes on the Yamal Peninsula. Regression tree model and boosted regression tree analysis showed that the activity of cryogenic processes (thermocirques) in the lake shores and lake water level were the two most important controls, explaining 48.4 % and 28.4 % of lake CDOM, respectively ($R^2 = 0.61$). Activation of thermocirques led to a large input of terrestrial organic matter and sediments from catchments and thawed permafrost to lakes ($n = 15$, mean $a(440)_{CDOM} = 5.3$ m⁻¹). Large lakes on the floodplain with a connection to Mordy-

Yakha River received more CDOM ($n = 7$, mean $a(440)_{CDOM} = 3.8$ m⁻¹) compared to lakes located on higher terraces.

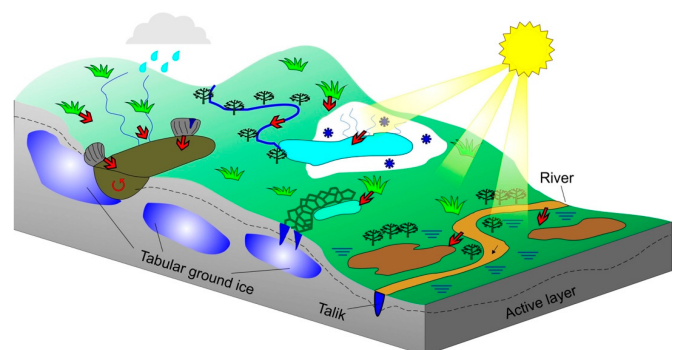


Figure 1: Theoretical scheme of the organic matter transport in Central Yamal lakes. Lakes are shown in different colors: thermocirque-impacted and floodplain lakes are more colored (brownish color) representing higher CDOM concentration. Red arrows represent the ways of organic matter transport to lakes from surrounding catchments.

References

- Y.A. Dvornikov, M.O. Leibman, B. Heim, A.V. Khomutov, S. Roessler, A.A. Gubarkov [2017]: Thermodenudation on Yamal peninsula as a source of the dissolved organic matter increase in thaw lakes. *Kriosf. Zemli*, 21: 33–42. doi:10.21782/EC2541-9994-2017-1(28-37).

Detection of recent permafrost region disturbances across the Arctic and Subarctic with Landsat time-series and machine-learning classification

I. Nitze¹, G. Grosse^{1,2}, B. M. Jones³, V. E. Romanovsky⁴, & J. Boike^{1,5}

¹*Alfred Wegener Institute Helmholtz Centre for Polar and Marine Research;*

²*Institute of Earth and Environmental Sciences, University of Potsdam Germany;*

³*Water and Environmental Research Center, Institute of Northern Engineering, University of Alaska Fairbanks, Fairbanks, USA;*

⁴*Geophysical Institute, University of Alaska Fairbanks, USA;*

⁵*Geography Department, Humboldt-University Berlin, Berlin, Germany*

Local observations indicate that climate change and shifting disturbance regimes are causing near-surface permafrost degradation in Arctic and Boreal regions. Here, we quantify the abundance and distribution of key permafrost region disturbances (PRDs: lakes and lake dynamics, wildfires, and retrogressive thaw slumps) using dense time series analysis of 30-m resolution Landsat satellite imagery from 1999 to 2014 in conjunction with machine-learning classification, object-based image analysis and auxiliary data sources. Our dataset spans four latitudinal, continental-scale transects in North America (Alaska, Eastern Canada) and Eurasia (Western Siberia, Eastern Siberia), covering $\approx 10\%$ of the northern permafrost region.

For the more than 640,000 lakes covering 5.04 % of the study area a net decreasing lake area (-1.45 %) was detected. We observed major lake area decrease in north-western Siberia and parts of western Alaska, while continental eastern Siberia (Central Yakutia) was affected by a significant increase in lake area. The Alaskan and Siberian Transects showed complex spatial dynamics with several influencing factors, such as permafrost extent, geomorphology or climate. The formerly glaciated Eastern Canadian Transect with predominantly bedrock geology exhibited a gradual transition from stable lakes in the south towards in-

creasingly shrinking lakes in the north. Fires were the most extensive PRD across boreal regions (6.62 %), with major abundance in dry continental regions, such as interior Alaska (8.89 %), Eastern Siberia (8.15 %) and boreal Eastern Canada (5.06 %). Western Siberia, with high abundance of wetlands, was less affected by wildfires (2.43 %). Within our study regions, tundra fires were limited to northern and western Alaska (1.07 %).

Active retrogressive thaw slumps, while dramatic on local scales, were spatially restricted to around 5 km² within the analyzed region. Due to their small size likely below the detection limit, many RTS may have not been identified safely. However, their clustered occurrence, mainly along former glacial margins (ice-sheets and mountain glaciers) and very ice-rich permafrost in Siberia and Alaska, can help to target their identification with higher spatial resolution data.

Our analysis demonstrates the global-scale vulnerability of permafrost terrain and carbon pools to disturbances and potentially rapid future thaw across very large regions. Our findings highlight that these PRDs need to be included in next generation land surface models to correctly capture the permafrost carbon feedback.

Towards understanding the contribution of permafrost waterbodies to methane emissions on a regional scale using aircraft measurements and remote sensing data

K. Kohnert¹, B. Juhls^{1,2}, S. Muster³, S. Antonova^{3,4}, A. Serafimovich¹, S. Metzger^{5,6}, J. Hartmann⁷, & T. Sachs^{1,8}

¹GFZ German Research Centre for Geosciences, Telegrafenberg, 14473 Potsdam, Germany;

²Now at: Institute for Space Sciences, Department of Earth Sciences, Freie Universität Berlin, Carl-Heinrich-Becker-Weg 6-10, 12165 Berlin, Germany;

³Alfred Wegener Institute, Helmholtz Centre for Polar and Marine Research, 14473 Potsdam, Germany;

⁴GIScience, Department of Geography, Heidelberg University, Heidelberg, 69120, Germany;

⁵National Ecological Observatory Network, Battelle, 1685 38th Street, Boulder, CO 80301, USA;

⁶University of Wisconsin-Madison, Dept. of Atmospheric and Oceanic Sciences, 1225 West Dayton Street, Madison, WI 53706, USA;

⁷Alfred Wegener Institute Helmholtz Centre for Polar and Marine Research, Am Handelshafen 12, 27570 Bremerhaven, Germany;

⁸Institute of Flight Guidance, TU Braunschweig, Hermann-Blenk-Str. 27, 38108 Braunschweig, Germany

Waterbodies in the arctic permafrost zone are considered a major source of the greenhouse gas methane (CH₄) in addition to CH₄ emissions from arctic wetlands. However, the spatio-temporal variability of CH₄ fluxes from waterbodies complicates spatial extrapolation of CH₄ measurements from single waterbodies. Therefore, their contribution to the CH₄ budget of the arctic permafrost zone is not yet well understood. Using the example of two study areas of 1,000 km² each in the Mackenzie Delta, Canada, we approach this issue

- (i) by analyzing correlations on the landscape scale between numerous waterbodies and CH₄ fluxes and
- (ii) by analyzing the influence of the spatial resolution of CH₄ flux data on the detected relationships [Kohnert et al., 2018].

A CH₄ flux map with a resolution of 100 m was derived from two aircraft eddy-covariance campaigns in the summers of 2012 and 2013. We combined the CH₄ flux map with high spatial resolution (2.5 m) waterbody maps from the Permafrost Region Pond and Lake Database based on TerraSAR-X data and

classified the waterbody depth based on Sentinel-1 SAR backscatter data. Subsequently, we reduced the resolution of the CH₄ flux map to analyze if different spatial resolutions of CH₄ flux data affected the detectability of relationships between waterbody coverage, number, depth, or size and the CH₄ flux. We did not find consistent correlations between waterbody characteristics and the CH₄ flux in the two study areas across the different resolutions. Our results indicate that waterbodies in permafrost landscapes, even if they seem to be emission hot spots on an individual basis or contain zones of above average emissions, do currently not necessarily translate into significant CH₄ emission hot spots on a regional scale, but their role might change in a warmer climate.

References

K. Kohnert, B. Juhls, S. Muster, S. Antonova, A. Serafimovich, S. Metzger, J. Hartmann, & T. Sachs [2018]: Toward understanding the contribution of waterbodies to the methane emissions of a permafrost landscape on a regional scale – A case study from the Mackenzie Delta, Canada. *Global Change Biology*. doi:10.1111/gcb.14289.



Decadal time-scale controls on catastrophic lake drainage in northern Alaska

M. J. Lara¹, B. M. Jones², & H. Genet³

¹*Department of Plant Biology, University of Illinois, Urbana, Illinois 61801, USA;*

²*Institute of Northern Engineering, Water and Environmental Research Center, University of Alaska Fairbanks, Fairbanks, Alaska 99701, USA;*

³*Institute of Arctic Biology, University of Alaska Fairbanks, Fairbanks, Alaska 99701, USA*

Observations of permafrost degradation have accelerated across the pan-Arctic, altering tundra surface morphology, hydrology, vegetation composition, biogeochemistry, and wildlife habitat. Our predictive understanding of the primary controlling factors facilitating landscape evolution in response to degrading permafrost is severely limited. Here, we advance our predictive understanding of catastrophic lake drainage in permafrost ecosystems by analyzing the spatiotemporal patterns of lake drainage occurring between 1975–2017 across $\approx 100,000$ lakes over $\approx 385,000$ km² of hillslope tundra in northern Alaska. We used a supervised support vector machine algorithm to extract lake area across northern Alaska every five years beginning in 1975, within the cloud-based geospatial parallel processing platform, Google Earth EngineTM API. An object based image analysis characterized the change in lake area between each time period. Greater than 25 static (i.e. vegetation type, soil texture, lake morphology, proximity to drainage gradient) and dynamic predictor variables (i.e. temperature, precipitation, fire occurrence) unique to each lake

were calculated. This robust dataset was used to develop a predictive model of catastrophic lake drainage using a machine learning algorithm, with lake drainage as a response variable and the static and dynamic variables as predictors. Our dataset identifies lake drainage to be regionally variable as colder regions with lower annual precipitation generally had higher rates of drainage than warmer and wetter regions, however these patterns varied over time. Our model identifies lakes highly vulnerable to drainage are small (<3 ha), round (<0.6 roundness), located in low elevation (<200 m.a.s.l.) wet sedge tundra with a probability of permafrost >0.7, where temperature and precipitation have increased. We estimate 2.2 % of lakes across the hillslope tundra of northern Alaska are currently highly vulnerable to drainage, which will notably increase over the coming decades. This work improves our ability to predict abrupt disturbances in response to permafrost degradation that may increase in arctic and subarctic regions with projected climate and environmental change.

Using Google Earth Engine to examine water and permafrost

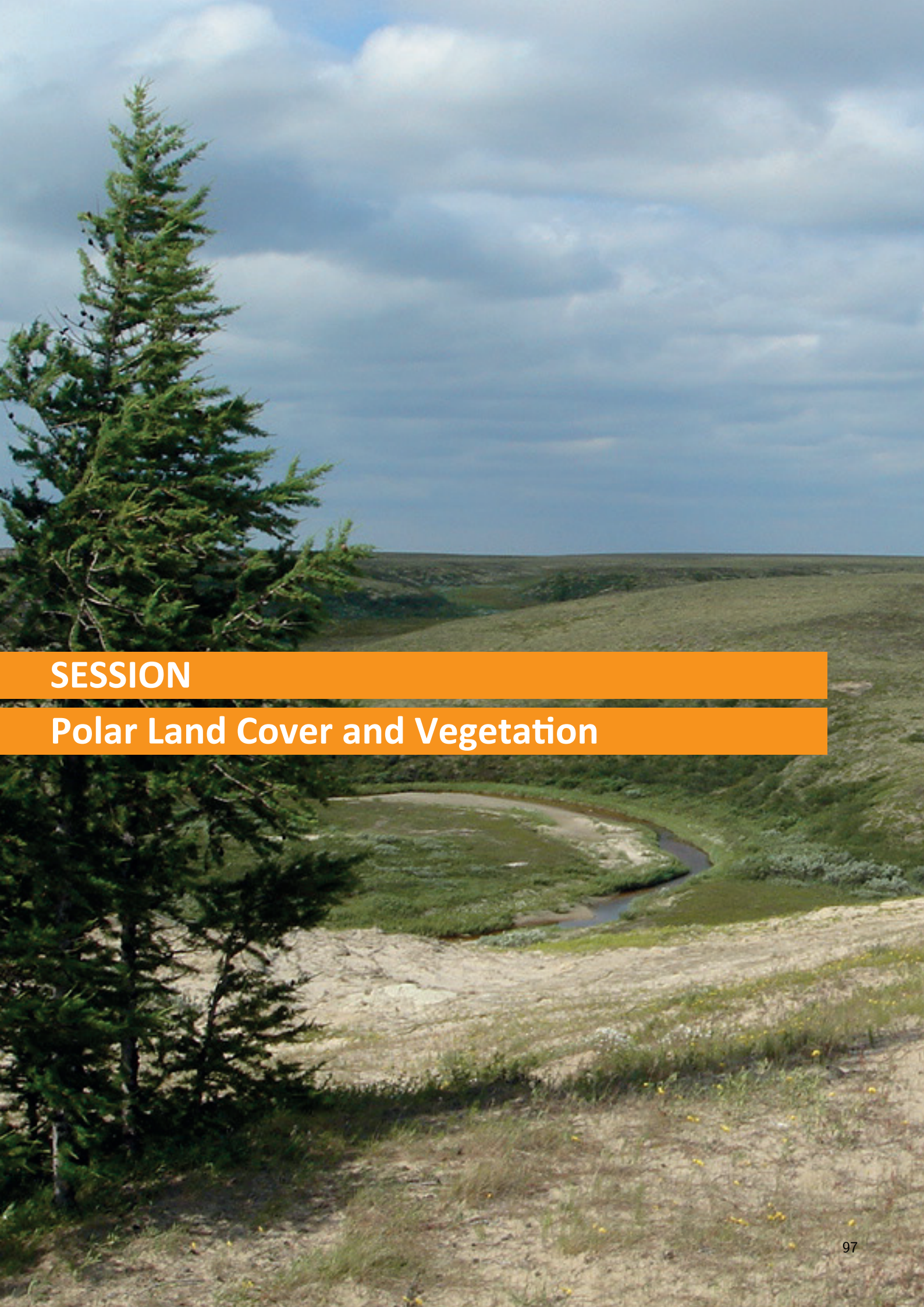
E. D. Trochim¹ & G. Donchyts²

¹*University of Alaska Fairbanks;*

²*Deltares*

Remote sensing applications globally are rapidly altering due to the availability of petabytes of remote sensing data via platforms offering high-performing computing services. In the Arctic, this approach offers significant advantages as there are large areas where observation networks are sparse. The interactions between vegetation, hydrology and the landscapes are complex as regional climatic regimes interact with cryosphere environments where frozen soil processes and glacial histories vary. Remote sensing of these environments is critical to understanding and quantifying past and current patterns and processes. By providing both a spatial and temporal understanding, this data is also crucial for validating models used to predict future scenarios. Platforms like Google Earth Engine offer the capacity to analyze data in a variety of ways including processing raw data from sensors like MODIS, Landsat and Sentinel to synthesizing existing methods and datasets. Starting with our area of expertise in surface water, we will begin by reviewing current global datasets that were used to synthesize trends for the northern hemisphere in comparison to permafrost. Next, we will review important considerations for potential projects interested in pursuing similar work. Our middle range propositions are that

data processing has become so powerful that researchers should now be coming at it with a new approach and comprehensive understanding of the gains and limitations to facilitate effective project management. In particular, an understanding of computational intensity, scaling and iteration for performance should be considered during the design phase to allow more efficient project management. Projects should weigh the value of using cutting edge techniques against the overall goals of the work. Deliberation should consider whether additional time and effort will result in appreciable gains in the final product. Data processing should be completed using current best practices. This often require personal interactions with the remote sensing and scientific community in both user forums and conferences in addition to methodologies published in peer-reviewed literature. Products and results should be conveyed using effective visualizations and by making code available to replicate the data and results. Finally, the process should be accessible to individuals from a variety of backgrounds and skill competencies. Care should be taken to consider how each team-member can add value and engage in an environment where data and techniques are rapidly evolving.



SESSION

Polar Land Cover and Vegetation

Estimation of forest properties in the treeline zone using TanDEM-X and airborne laser scanning data

Sofia Antonova^{1,2}, Christian Thiel³, Bernhard Höfle¹, Sabrina Marx¹, Katharina Anders¹, & Julia Boike^{2,4}

¹*Institute of Geography, Heidelberg University, Heidelberg, Germany;*

²*Alfred Wegener Institute Helmholtz Center for Polar and Marine Research, Potsdam, Germany;*

³*Institute of Geography, Friedrich-Schiller-University Jena, Jena, Germany;*

⁴*Department of Geography, Humboldt University of Berlin, Berlin, Germany*

Northward shift of the treeline is expected circum-Arctic and has been observed in a number of locations in response to Arctic warming. The transitional zone between forest and tundra is, therefore, a vulnerable region that requires systematic monitoring. Currently, radar remote sensing is hardly employed in the treeline zone. The unique constellation of the TanDEM-X satellites with its bistatic mode and unprecedented spatial resolution opens new opportunities for monitoring of the treeline zone. We focus on an area near the Trail Valley Creek research basin in the east of the Mackenzie Delta in the Northwest Territories, Canada. The area lies at the northern edge of the treeline zone. Erect vegetation there is characterised by deciduous shrubs up to 3 m in height and isolated patches of sparse coniferous forest. We evaluate the potential of TanDEM-X bistatic data to characterise the structural properties of the forest patches. The TanDEM-X data were acquired during the TanDEM-X Science Phase in 2015, when the effective baseline was large and constant (approximately 540 m). We employ interferometric coherence from multitemporal

bistatic pairs and compare it with standard vegetation metrics obtained from airborne LiDAR data. The full-waveform airborne LiDAR data were captured in September 2016, covering an area of about 20 km x 6 km with a point density of approximately 5 points per square meter. LiDAR metrics include vegetation height percentiles and vegetation ratio. The preliminary analysis shows a high agreement between TanDEM-X bistatic coherence and LiDAR vegetation metrics. The relation between coherence and LiDAR metrics, averaged for each forest patch, yields in a strong inverse correlation, varying from -0.81 to -0.88 for different LiDAR metrics. On sub-patch scale, spatial patterns of coherence and LiDAR metrics also show high inverse correspondence. Thus, a pixel-by-pixel comparison gives a first-shot correlation between tree height 99 percentile and coherence from -0.45 to -0.63 for different forest patches. Taking into account the global coverage of multiple bistatic TanDEM-X data acquired for the global digital elevation model, our results provide a basis for the quantification of the treeline properties circum-Arctic.

Evaluation of a Metop ASCAT derived surface soil moisture product in the Lena Delta

E. Högström^{1,2}, B. Heim³, A. Bartsch^{2,4}, H. Bergstedt⁵, & G. Pointner⁴

¹*Austrian Polar Research Institute, Vienna, Austria;*

²*Vienna University of Technology, Vienna, Austria;*

³*Alfred Wegener Institute Helmholtz Center for Polar and Marine Research, Potsdam, Germany;*

⁴*b.geos, Korneuburg, Austria;*

⁵*Department of Geoinformatics – Z_GIS, University Salzburg, Salzburg, Austria*

Coarse resolution soil moisture datasets are available globally. Their utilization in permafrost areas is however limited due to heterogeneity within the footprint. Validation across the Arctic does also not exist due to only very few monitoring sites which measure soil moisture. There is in addition the discrepancy between typical measurement depth and satellite data representativeness.

C-band scatterometer information is of specific interest in heterogeneous environments due to the availability of higher spatial resolution Synthetic Aperture Radar (SAR) data at this wavelength. The C-band scatterometer ASCAT (on board of several Metop platforms) provides operational data in near real time since 2007. The microwave backscatter variations are expected to correspond to soil moisture variations. Surface roughness and volume scattering, which also contribute to the backscatter signal, are parameterized or assumed to be constant under certain conditions. This provides the basis for a global near surface soil moisture product available through EUMETSAT.

We designed a monitoring set-up for measuring moisture very close to the surface in the Lena River

Delta, Siberia to specifically investigate Metop ASCAT derived surface soil moisture. Four sites have been covered representing two different ASCAT footprints and settings. Samoylov Island is dominated by a polygonal wet tundra landscape. The Yedoma landscape unit Kurungnakh is located only a few kilometres south from Samoylov Island. The measurement stations were installed in August 2013 on Kurungnakh and Samoylov and data were collected in August 2014. Three stations were placed on Kurungnakh and one on Samoylov. The Volumetric Water Content (VWC) and temperature sensors have been in the moss organic layer in order to account for the limited penetration depth of the signal. VWC measured at the different sites within the Lena Delta correlate well with each other. This indicates representativeness of single station records for ASCAT validation regarding temporal patterns. ASCAT backscatter variations are in general very small, in line with low variability of in situ VWC. Short term changes after complete thaw of the upper organic layer seem to be however mostly influenced by temperature.



Influence of litter and non-vascular components on the spatial aggregation of hyperspectral data in a low-Arctic ecosystem

A. Beamish¹, Maximilian Brell², Sabine Chabrillat², Nicholas Coops³, & Birgit Heim¹

¹*Alfred Wegener Institute Helmholtz Center for Polar and Marine Research, Permafrost Research, Telegrafenberg, A45, 14473 Potsdam, Germany;*

²*Helmholtz Centre Potsdam (GFZ), German Research Centre for Geosciences, Telegrafenberg A17, 14473 Potsdam, Germany;*

³*Integrated Remote Sensing Studio (IRSS) Faculty of Forestry, University of British Columbia, 2424 Main Mall, Vancouver, V6T1Z4 Canada*

Terrestrial Arctic ecosystems are spatially and temporally heterogeneous with high proportions of standing litter and non-vascular species as well as variable moisture conditions. These ecosystem characteristics create unique challenges for detailed remote sensing of Arctic tundra vegetation change. Recent research has shown that narrowband spectral data is superior for characterizing and monitoring terrestrial Arctic environments than wideband spectral data. At the vegetation however, little is known about how these data scale to the aerial and spaceborne scales. To better understand how the heterogeneity of Arctic tundra ecosystems scales from plot scale, to the ground and to satellite scale, ground-based, airborne and simulated satellite spectral data were compared in six dominant low-Arctic tundra vegetation communities. Next, a linear mixture analysis was used to explore the influence of litter, moss and water (dark) spectra on the convergence of the multi-scale data. The analysis was performed on 10 biophysically im-

portant wavelengths. Results show that litter was the most influential ecosystem component when data were spatially aggregated from the ground to airborne and spaceborne scale. Mixtures of up to 70 % and 75 % litter at the airborne and spaceborne scale resulted in the greatest convergence, respectively. Moss was influential at the airborne scale with mixtures of 70 % resulting in convergence while the water spectra showed no influence at any scale. The convergence varied by vegetation community but was greatest in the tussock sedge-shrub communities, which are dominant across the Arctic. The influence of litter has important implications for monitoring vegetation at satellite scales and the interpretation of biophysical parameters. With an increasing availability of hyperspectral remote sensing data, better characterization of non-vascular and non-photosynthetic ecosystem components will greatly improve our understanding of terrestrial Arctic ecosystem heterogeneity.

ArcticDEM terrain roughness and Structure from Motion for forest structure analysis and biomass quantification in the tundra-taiga ecotone (Siberia)

Frederic Brieger^{1,2}, Stefan Kruse¹, Birgit Heim¹, Bodo Bookhagen², Iulia Shevtsova¹, & Ulrike Herzs Schuh^{1,2}

¹Alfred Wegener Institute Helmholtz Centre for Polar and Marine Research, Potsdam, Germany;

²University of Potsdam, Institute of Earth and Environmental Science, Potsdam, Germany

The tundra-taiga interface is the world's largest ecotone and stretches for more than 6000 kilometers along Russia alone. It is defined as the zone between the densely forested southern taiga and treeless northern tundra. Its transitional character makes it sensitive to global warming, resulting in a higher productivity, a latitudinal northward and altitudinal upward shift [Kravtsova et al., 2012]. Monitoring it is important to understand past changes and future impacts regarding local vegetation dynamics and their implications on the regional and global carbon cycle.

In this study two different methods on different scales are used to analyze the spatial distribution and structure of tree populations in the remote study area in Chukotka, Russia. The ArcticDEM, an open access 2–5 m digital surface model of the circumpolar terrestrial domain, was used to identify tree patches. The Local Mean Absolute Plan Curvature (LMAPC) was utilized as a proxy for tree density, being a measurement of ups and downs perpendicular to the slope within an area. Most of the wrongly classified pixels occur in very rough and steep slopes, typically within unvegetated areas of higher elevation and can be filtered out with a NDVI based condition extracted from coarser resolution multispectral RapidEye data.

During field work this summer, high resolution multispectral imagery (in the blue, green, red and near infrared wavelengths) will be taken with a quadcopter and a 6 m stick mount and vegetation plots, including tree height, stem diameter and position measurements, will be created. We intend to derive structural information applying Structure from

Motion (SfM) on the acquired imagery using photogrammetry software. Previous studies have compared LiDAR- and SfM-based approaches to quantify biomass and concluded that the quality of the assessment is dependent on the quality of the DTM, since both methods deliver good DSMs. LiDAR has a much higher vegetation penetration and ground point density, but the method is more expensive. The fusion of SfM derived surface and terrain models with the in situ vegetation measurements should enable us to increase the quality of the DTM and therefore help to overcome the biggest disadvantage in comparison to LiDAR based studies, while being a low cost solution, contributing to more accurate biomass estimations and a better understanding of the local vegetation dynamics in the tundra-taiga ecotone.

References

- Valentina I. Kravtsova, Olga V. Tutubalina, & Annika Hofgaard [2012]: Aerospace Mapping of the Status and Position of Northern Forest Limit. *Geography*, 28. doi:[10.15356/2071-9388_03v05_2012_03](https://doi.org/10.15356/2071-9388_03v05_2012_03).
- Tetsuji Ota, Miyuki Ogawa, Katsuto Shimizu, Tsuyoshi Kajisa, Nobuya Mizoue, Shigejiro Yoshida, Gen Takao, Yasumasa Hirata, Naoyuki Furuya, Takio Sano, Heng Sokh, Vuthy Ma, Eriko Ito, Jumpei Toriyama, Yukako Monda, Hideki Saito, Yoshiyuki Kiyono, Sopal Chann, & Nang Ket [2015]: Aboveground Biomass Estimation Using Structure from Motion Approach with Aerial Photographs in a Seasonal Tropical Forest. *Forests*, 6, 3882–3898. doi:[10.3390/f6113882](https://doi.org/10.3390/f6113882).

Ecosystem functional diversity of the circumpolar arctic tundra

H. Epstein¹, A. Armstrong¹, D. Alcaraz-Segura², E. Montefiori², A. Castro³, M. Raynolds⁴ & Q. Yu⁵

¹University of Virginia;

²University of Granada;

³Idaho State University;

⁴University of Alaska Fairbanks;

⁵George Washington University

The Arctic is a region with a high degree of spatial variability in ecosystem functioning, but is also one that is changing dramatically over time due to dynamics in climate and land use. To assess the spatial and temporal heterogeneity of ecosystem functioning, we identify Ecosystem Functional Types (EFTs), patches of the land surface that process energy and matter in similar ways and potentially show coordinated responses to environmental factors. We classify EFTs circumpolarly through the use of satellite remote sens-

ing, using three key functional attributes derived from the seasonal dynamics of the MODIS Enhanced Vegetation Index (EVI) for the time period 2001–2017; these three attributes are the mean growing season EVI (Mean), the seasonality of the EVI, represented by the growing season coefficient of variation (SD), and the date of the maximum EVI (Dmax). We have done a preliminary analysis of the Ecosystem Functional Attributes and a classification of the Ecosystem Functional Types (Fig. 1).

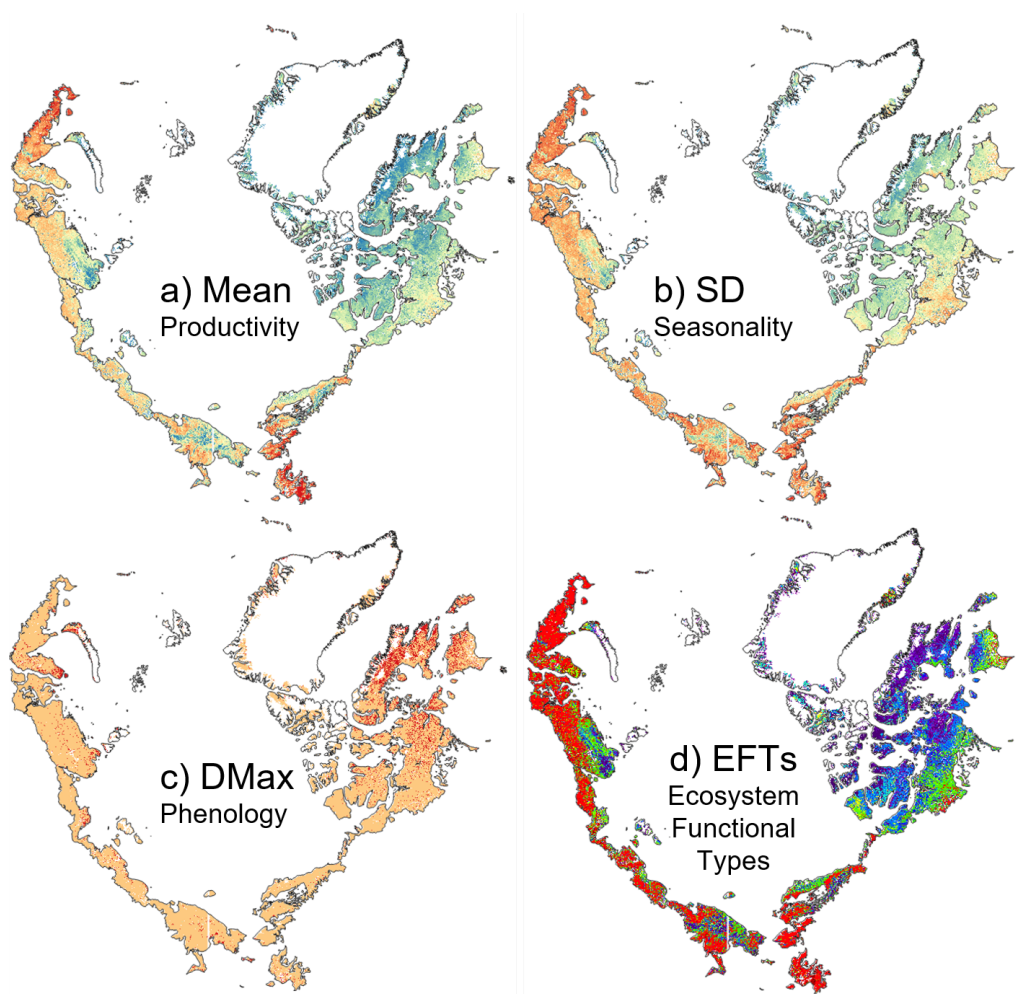


Figure 1: Ecosystem Functional Attributes (EFAs) and Ecosystem Functional Types (EFTs).



Ecosystem functional diversity can be represented by EFT richness (number of EFTs in a moving 8x8 pixel window) and EFT rarity (based on the fractional cover of the EFT). To determine the controls on EFT spatial distribution and EFT diversity variables, we will conduct a multivariate analysis (PCA) of several independent variables (climate, geology, land use) and analyze how the different EFTs are distributed throughout the multivariate space of the environmental variables. Using a new version of the Circumpolar Arctic Vegetation Map (CAVM), we will

assess the correspondence between vegetation structure and ecosystem functioning. Finally, we will assess which of the EFTs are most susceptible to change and to which other EFTs are they changing; we will identify areas that are either losing or gaining functional diversity. This functionally-based framework that we have begun to implement for the circumpolar Arctic tundra will allow us to identify “functional hotspots,” either regions that are functionally rich, or those that contain rare EFTs, as potential targets for conservation priority.

Retrospective remote sensing reveals accelerating rates of permafrost degradation on Alaska's Yukon-Kuskokwim Delta: Bellwether of the future Arctic, or black sheep?

G. V. Frost¹, Macander J. Macander¹, M. Torre Jorgenson², Matthew A. Whitley³, & Dorte Dissing¹

¹*ABR, Inc.—Environmental Research & Services, Fairbanks AK USA;*

²*Alaska Ecoscience, Fairbanks AK USA;*

³*University of Alaska Fairbanks, Fairbanks AK USA;*

The Yukon-Kuskokwim Delta (YKD) is among the most biologically productive areas of the tundra biome and supports one of the largest indigenous human populations in the Arctic. However, the YKD's relatively warm climate, proximity to the coast, and low elevation make the region highly vulnerable to rapid and persistent change following shifts about basic physical and thermal thresholds. Here we exploit disparate high-resolution datasets from long-established (optical) and newly developed (LiDAR) remote sensing technologies to examine degradation of permafrost plateaus on the YKD's central coast using a retrospective approach. Traditional optical datasets (airphotos, commercial satellite imagery) provide the longest period-of-record for examining landscape change. We photo-interpreted ecotypes using a point-intercept approach using a time-series of airphotos from circa 1953 and 1980, IKONOS satellite images from c. 2007, and WorldView satellite images from c. 2015. We found that ecotype classes changed 16.2 % (342 km²) overall during the ≈62-year timespan. Permafrost degradation was a dominant driver of ecotype changes since 1953, and rates of permafrost degradation increased dramatically during 2007–2015 (from 0.06

to 0.26 %/yr), coinciding with increasing storm frequency and air temperatures. Emerging technologies such as LiDAR now provide a means of mapping permafrost extent extremely well on the flat landscapes of the YKD, where ground-ice is the chief mechanism producing topography. Such maps provide a baseline for tracking permafrost dynamics and assessing risks to communities, subsistence resources, and wildlife habitats. Integrating field data with a high-resolution digital elevation model (DEM) from 2009 LiDAR supported a probabilistic mapping approach based on local surface elevation. Using a 0.9 predicted probability threshold yielded a permafrost map with 95 % accuracy (Fig. 1).

Recent “repeat“ LiDAR acquisition in 2016 permits precise modeling of changes in permafrost extent in both areal, and volumetric terms. Ongoing operation of legacy instruments, coupled with maturation of emerging remote technologies provide a powerful toolkit for detailed studies of high-latitude environmental change. We conclude with discussion of whether current dynamics on the YKD foretell changes likely to be seen in the future Arctic, or are unique to this corner of Beringia.

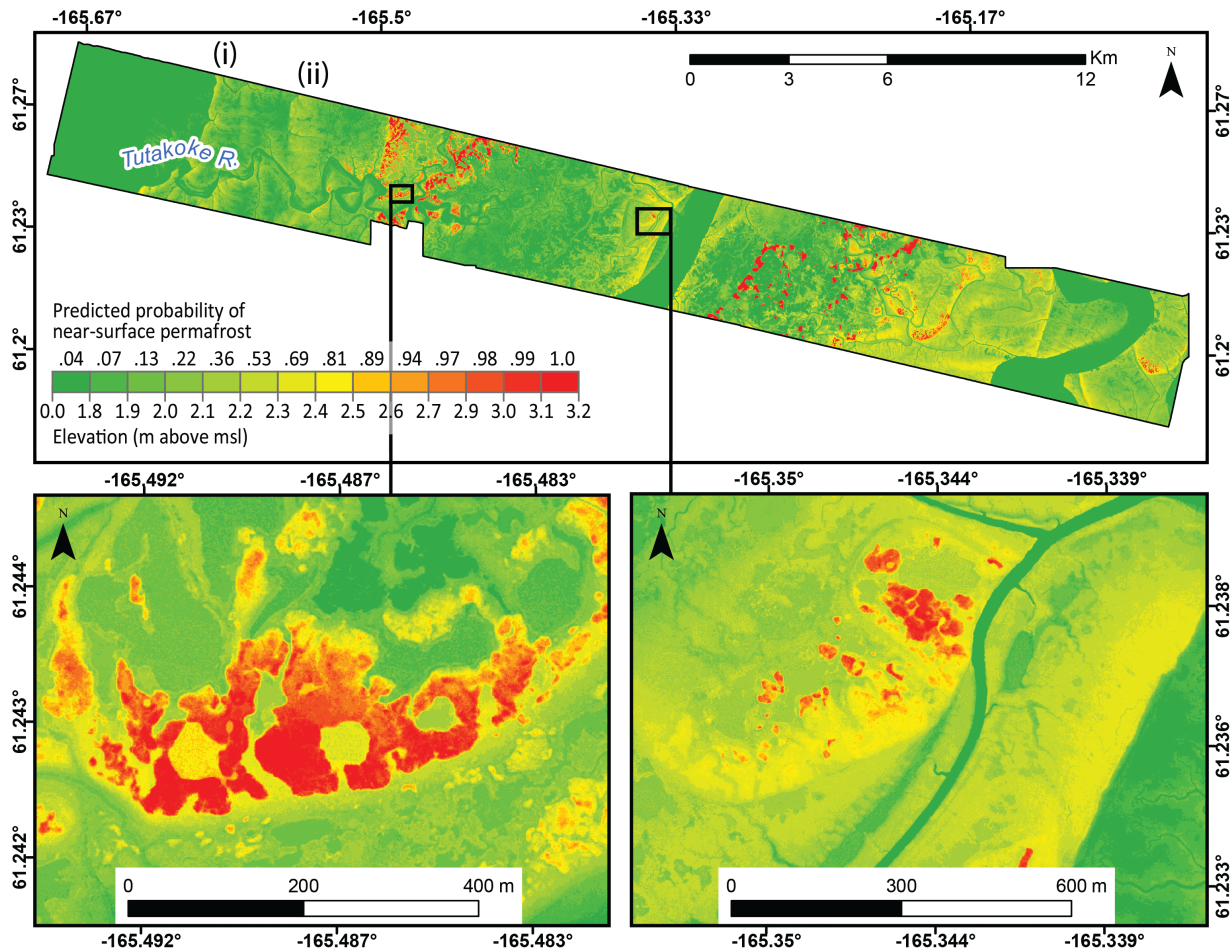


Figure 1: Map of the predicted near-surface permafrost probability calculated by 0.1 m elevation bins for permafrost plateau region on the central coast of the YKD, Alaska. The insets show more detail in areas of relative high elevation (left) and areas of relative low elevation (right). From [Whitley et al., 2018].

References

Matthew A. Whitley, Gerald V. Frost, M. Torre Jorgenson, Matthew J. Macander, Chris V. Maio & Samantha G. Winder [2016]: Assessment of LiDAR and spectral techniques for high-resolution mapping of sporadic permafrost on the Yukon-Kuskokwim Delta, Alaska. *Remote Sensing*, 10, 258. doi:[10.3390/rs10020258](https://doi.org/10.3390/rs10020258).

Analysis of permafrost taiga by means of X/C-Bands SAR imagery

S. Guillaso¹ & F. Garestier²

¹*Helmholtz Centre Potsdam, GFZ German Research Center for Geoscience, Potsdam, Germany;*

²*UMR 6143 M2C Morphodynamique Continentale et Côtière, CNRS, Caen, France*

Taiga, or boreal forest, is a biome that is mainly composed of coniferous trees, such as pines, spruces or larches. It is also composed of deciduous trees that seasonally shed their leaves like birch, alder, willow or poplar principally located in the most extreme winter cold region. In the southernmost part of the taiga, we can find trees like oak, maple, elm or lime. It is located in the high northern latitude, between 50°N and 70°N. The year temperature is varying from -54 °C to 30 °C (extreme temperature). The summers are generally short, warm and humid. The soil possesses 2 layers, one which is freezing/thawing, known as active layer, having a depth of some meters, and the second which remains constantly frozen. Due to the variation of the temperature during the year and according to the global warming change, the taiga properties are varying along the seasons and the years. The cycle freeze/thaw induces the conversion of soil organic carbon into the greenhouse gases carbon dioxide and methane that we need to know.

The use of polarimetric SAR time series is of importance in such region. Depending of the radar band, but also of the acquisition date, we can have access to the soil information through the volume defined by the trees. Moreover, SAR data are weather and illumination independent making possible to acquire periodically (up to 1 images every 6 days with the sentinel-1 A/B constellation) an image over a very large period covered by several years. We can thus follow the physical property changes corresponding to the different type of tree coverage. We observed in one site that the backscattering coefficient is strongly correlated with the ground temperature and the dom-

inant scattering mechanism is changing from a double bounce in winter to a volume diffusion in summer, which gives us an indication of the type of tree in the study area, here deciduous trees. After autumn, when the trees have lost their leaves, the electromagnetic wave is no longer reflected and can penetrate into the trees, resulting a double bounce (trunk-ground), while in summer, when leaves are present, we observe a volume diffusion.

Time series used for this study are constituted of X-band SAR (TerraSAR-X) dual polarization (HH-HV) data acquired every 11 days and of Sentinel-1 A/B, dual polarization (VV-VH) acquired every 6 days over two sites located 50 km east of Yakutsk (Central Siberia). The use of polarimetric data ensures a sensitivity to the vegetation dynamics and enables polarimetric optimization and the retrieval of polarimetric information of the dominant scatterer using ESPRIT method [Guillaso et al., 2005]. Furthermore, we use sentinel-2 multispectral data acquired over the same region, when possible, to analyze and determine type of vegetation using normalized indices. We concentrate our study over 5 typical East-Siberian environments: two alas (thermokarstic depressions) composed by grass and other herbaceous vegetation and lakes, and three other sites covered respectively by birch, larch and pine forests.

References

- S. Guillaso, A. Reigber, & L. Ferro-Famil [2005]: Evaluation of the ESPRIT approach in polarimetric interferometric SAR. *Proceedings of IGARSS'05*, Seoul, South Korea, 25–29 July 2005.

Spatial and temporal variability at the Toolik Lake vegetation grid (Alaska)

Birgit Heim¹, Alison Beamish¹, D. A. Walker², Howard E. Epstein³, Ulrike Herzsuh¹, Torsten Sachs⁴, Sabine Chabrillat⁴, Maximilian Brell⁴, Sebastian Rößler⁵, & Marcel Buchhorn^{6,1}

¹*Alfred Wegener Institute Helmholtz-Center for Polar and Marine Research AWI, Polar Terrestrial Ecosystems, Potsdam, Germany;*

²*University of Alaska Fairbanks, International Arctic Research Center, Institute of Arctic Biology, Fairbanks, United States;*

³*University of Virginia, Charlottesville, United States*

⁴*Deutsches GeoForschungsZentrum GFZ, Potsdam, Germany;*

⁵*FIELAX, Bremerhaven, Germany;*

⁶*VITO, Flemish Institute for Technological Research, Mol, Belgium*

Ground data for the validation of satellite-derived terrestrial Essential Climate Variables (ECVs) at high latitudes are sparse. Also for regional model evaluation of terrestrial variables we lack accurate ranges of terrestrial ground data and face the problem of a large mismatch in scale. Within the German research programs Regional Climate Change (REKLIM) and the Environmental Mapping and Analysis Program (EnMAP), we conducted a study on ground data representativeness for vegetation-related variables within a monitoring grid at the Toolik Lake LTE Research station in Alaska. The grid covers an area of $\approx 1 \text{ km}^2$ containing Eight five grid points spaced 100 meters

apart. Moist acidic tussock tundra is the most dominant vegetation type. Permanent 1 m^2 plots were also established to be representative of the individual gridpoints. During summer 2016, we conducted field spectrometry at selected plots during early, peak and late summer. We experimentally investigate more spatially extensive Elementary Sampling Units (ESUs) for the spatial representativeness of the permanent 1 m^2 plots and to map ESUs for various tundra types. We will present the first data analyses and maps of biophysically-focused ESUs for evaluation of the use of remote sensing data to estimate these ecosystem properties.

Viability of interferogram stacking for change detection in arctic environments using ESA Sentinel-1 Data

M. Hovemyr & I. A. Brown

Department of Physical Geography, Stockholm University, Stockholm, Sweden

The use of Small Baseline (SBAS) interferometric stacking for high precision calculation of displacement using Synthetic Aperture Radar (SAR) data has been successfully used in a wide range of applications. The Arctic, with its high seasonal variability in scattering behavior and low density of persistent scatterers presents an interesting but complicated environment for this type of analysis. In an effort to be able to reliably perform SBAS analysis in the Arctic, this study aimed to parameterize the application of the SBAS method over Arctic environments using Sentinel-1 C-band SAR.

Two main study areas in Sweden were chosen for this project, the Kiruna urban area and the Stordalen permafrost area close to Abisko. A third area, the Malmö greater metropolitan area was chosen as comparison and baseline due to absence of snow cover for the entire period. The data used was Sentinel-1A/B Single Look Complex (SLC) Interferometric Wide Swath (IW) co-polarized captures on a 6-day revisit time from mid-June to late December 2017.

To evaluate method behavior and thresholds in the context of data abundance and density as well as determining the effects of an increasing number of acquisitions with snow cover, a combination of stack thinning and moving stacks was used. The stack thinning consisted of iteratively re-running an initial stack of 22 images with 2 fewer images every iteration down to a final stack of 10 images, image pairs with

longest normal baseline removed first. The moving stack experiment was performed by keeping the stack length at 22 images while iteratively removing the two earliest acquisitions and adding two to the end of the stack thus creating a comparable but displaced temporal coverage.

The results of the stack thinning showed that while stack length greatly impacts displacement results, stacks of below the recommended number of images still retain the ability to describe the displacement process albeit with low precision in terms of displacement quantification. Furthermore, scatterer persistence proved vastly more important than image density for accurate displacement calculations.

The moving stack experiment yielded interesting results showing that when snow cover is introduced at the extremes of a stack, displacement calculations become erratic for the images in question, but as more images with snow cover are introduced, this erratic behavior subsides showing that the method is sensitive to poorly-distributed bi-modal image stacks. In conclusion, while higher stack density and acquisition abundance improves results, areas with a high fraction of persistent scatterers can still yield reliable results under below threshold conditions. Furthermore, the impact of snow cover shows a trend of high levels of noise in the results for a smaller presence of snow cover with noise effects decreasing as the fraction of snow covered images increase.

Morphostratigraphy investigation of alas on Kurungnakh Island (the Lena River Delta) by means of remote sensing UAV data and field studies

A. A. Kartoziia^{1,2,3}

¹*Novosibirsk State University;*

²*Sobolev Institute of Geology and Mineralogy Siberian Branch Russian Academy of Sciences;*

³*Trofimuk Institute of Petroleum Geology and Geophysics Siberian Branch Russian Academy of Sciences*

Our object of study (alas) is located on southeastern part of Kurungnakh Island. It is 25 m deep, 250 m in diameter with majorly isometric round shape thermokarst hollow. This depression has evolved in ice-rich permafrost deposits. We have applied analysis using ESRI ArcGIS 10.5 software package to perform the land unit recognition and study of its specific morphology features. The spatial data for the analysis of alas land units morphology includes: 1) aerial photo (resolution 0.05 m); 2) digital elevation model (DEM; horizontal rectangular grid with 0.5 m spacing and vertical resolution of 0.2 m); 3) derivative schemes of morphometric parameters (aspects, slopes, mean DEM (all mean schemes have moving window radius of 5 m), mean slopes, shaded relief, as well as drainage basin scheme (created with ArcGIS 10.5 Basin tools).

In the process of GIS spatial data analysis and field observations we revealed a number of land units, which differ among themselves in the angle of inclination, elevation, characteristics of ice-wedge polygons and others relief morphology parameters. Revealed land units are (1) ice complex uplands, (2) alas slopes, (3) slopes, (4) a 1st alas floor level, (5) a 2nd alas floor level, (6) a 3rd alas floor level, (7) a pingo, and (8) a brook valley.

After GIS analysis, we tried to determine the alas evolution steps by tracking relations between revealed land units, their morphology parameters, and deposit sedimentation history. Age estimations, alas deposit characteristics, and thermokarst intensity periods were taken from published data [Khazin et al., 2017, Morgenstern et al., 2013]. The first evolution step that we managed to sort out included ice complex thawing phase during the start of Holocene, the reception material from slopes, the sedimentation of alas lower Holocene deposits and the alluvial fan formation on the northeastern part of the alas bottom. The second step included movement of land units #4 and #5 in subaerial conditions after the alas drainage. Further, they were affected by thermal-contraction-cracks,

which later became ice wedges polygonal systems with unique morphology characteristics. At this moment, a pingo (7) also started to form, due to the permafrost reformation and talik freezing. The third step included residual lake development and its' degradation because of paludification process. Finally, during the fourth step, a brook dissected the alas bottom and formed the brook valley.

Thus, owing to the analysis of very high resolution remote sensing data using GIS, field observations and published core data we have managed to reconstruct the alas evolution steps. Moreover, high-resolution remote sensing UAV data allowed recognizing several land units and their morphology parameters with unprecedented accuracy. This study complements previous investigations of thermokarst evolution in East Siberia and shows further perspectives of using UAV data in morphostratigraphy studies.

This study was supported by state assignment project №0330-2016-0018.

References

- L. Khazin, I. Khazina, & O. Kuzmina [2017]: Micro-paleontological characteristic (Ostracods, Palynomorphs) of permafrost deposits in borehole on Kurungnakh Island (Lena Delta, Northeast Siberia). Novosibirsk: Intern. sci. Conf. "Use of subsurface. Mining. Directions and technologies of prospecting, exploration and development of mineral deposits. Economy. Geoecology.": Col. of materials in 4 t. T. 1, p. 7–11, (in Russian) <https://elibrary.ru/item.asp?id=29319422>.
- A. Morgenstern, M. Ulrich, F. Günther, S. Roessler, I. V. Fedorova, N. A. Rudaya, S. Wetterich, J. Boike & L. Schirrmeister [2008]: Evolution of thermokarst in East Siberian ice-rich permafrost: A case study. *Geomorphology*, 201, 363–379. doi:10.1016/j.geomorph.2013.07.011.

Progress towards pan-arctic shrub mapping using spectral, radar, and stereo metrics

M. J. Macander¹, G. V. Frost¹, P. M. Montesano², C. S. R. Neigh², & P. R. Nelson³

¹*ABR, Inc. – Environmental Research & Services;*

²*NASA Goddard Space Flight Center;*

³*University of Maine Fort Kent*

Changes in tundra shrub cover and height have well-documented ecosystem effects on snow distribution, soil temperature, wildlife habitat, and other landscape properties [Frost et al., 2018]. Local-scale studies have documented shrub expansion in upland and riparian systems in many parts of the Arctic. Here we present research on modeling modern tundra shrub cover, canopy height, and leaf habit (deciduous, evergreen) for large study areas (10^4 km² through 10^6 km²) at 30 m resolution. We developed machine learning regression models to predict:

- Total cover of low (50–150 cm) and tall (>150 cm) shrubs [Macander et al., 2017];
- Total cover of deciduous vs. evergreen shrubs [Macander et al., 2017]; and
- Mean height of woody vegetation.

We developed a calibration and validation dataset from detailed field plot measurements, airborne LiDAR including the Land, Vegetation, and Ice Sensor (LVIS), stereo models derived from commercial satellite imagery, and data products from Small Unmanned Aerial Systems (sUAS) RGB cameras.

Suites of predictors for modeling included:

- Spectral predictors (Landsat and Sentinel 2);
- Polarimetric C-band Synthetic Aperture Radar (SAR) predictors (Sentinel 1); and
- Texture and height metrics derived from high-resolution commercial satellite imagery stereo pairs.

We present results from the North Slope (Fig. 1) and an intensive study site on the Yukon River Delta. The best performance was achieved with models that combined all 3 suites of predictors. These predictor datasets, and the workflow used to analyze them are suitable for developing a modern (circa 2015–2018) snapshot of shrub cover and canopy properties for the entire tundra biome (10^7 km²). However, the radar and texture metrics are not available to support multi-temporal mapping for earlier epochs such as circa 2000. We discuss the feasibility and limitations of using globally available legacy data such as Landsat for mapping historical shrub cover.

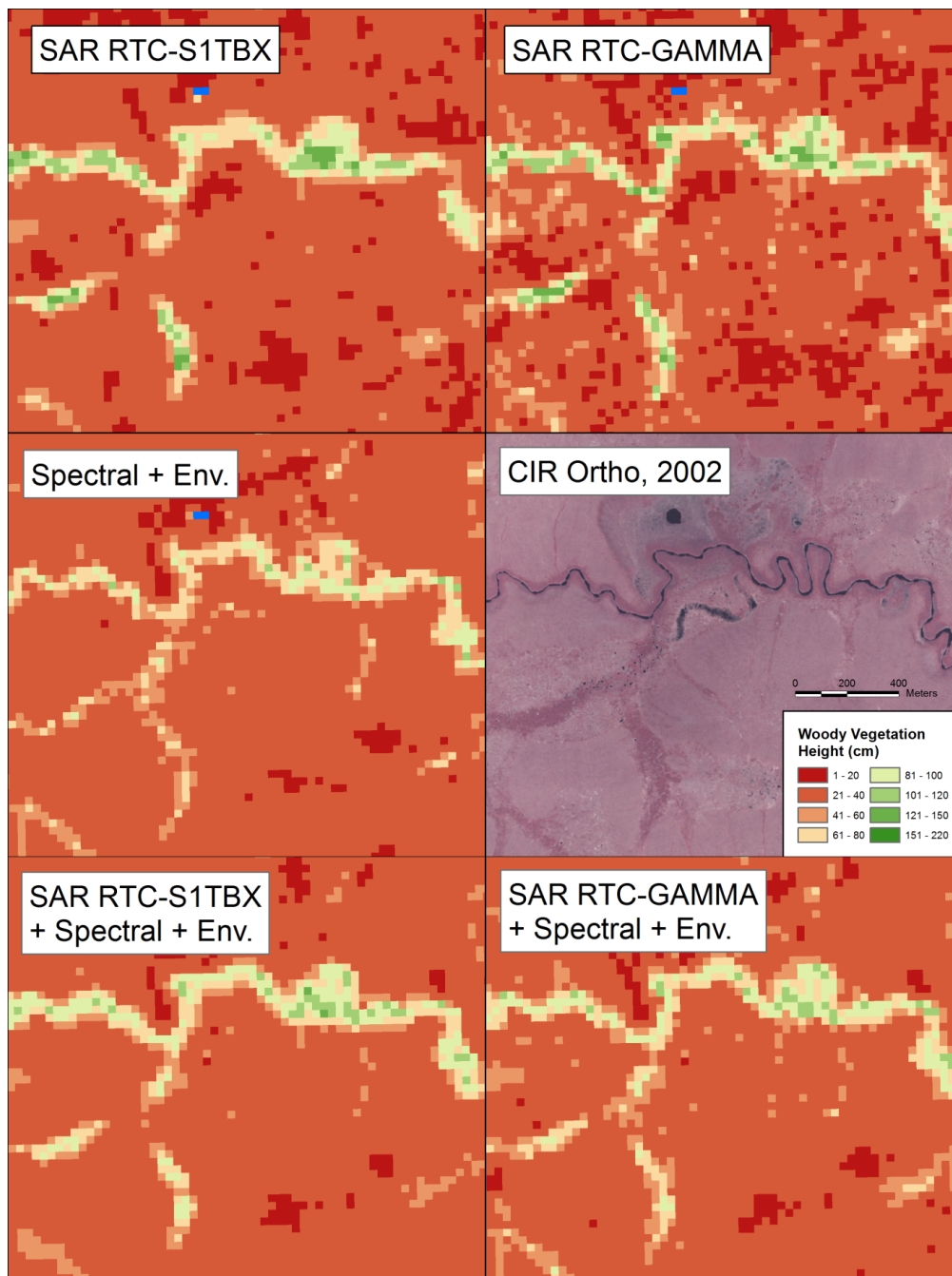


Figure 1: Map models of Woody Vegetation Height (cm) near a beaded stream based on different sets of radar and spectral predictors, North Slope, Alaska. Training data came from 188 vegetation point-intercept field plots sampled in 2012–2014.

References

- G.V. Frost, H.E. Epstein, D.A. Walker, G. Matyshak, and K. Ermokhina [2018]: Seasonal and long-term changes to active-layer temperatures after tall shrub expansion and succession in Arctic tundra. *Ecosystems*, 21, 507–520. doi:[10.1007/s10021-017-0165-5](https://doi.org/10.1007/s10021-017-0165-5).
- M.J. Macander, G.V. Frost, P.R. Nelson, and C.S. Swingley [2017]: Regional Quantitative Cover Mapping of Tundra Plant Functional Types in Arctic Alaska. *Remote Sensing*, 9, 26 pp. doi:[10.3390/rs9101024](https://doi.org/10.3390/rs9101024).

Urban heat island effects in the northern high latitudes as revealed by remote sensing

V. Miles & I. Esau

Nansen Environmental & Remote Sensing Center/ Bjercknes Centre for Climate Research, Bergen, Norway

The severe continental climate of the northern high latitudes is characterized by a generally negative surface heat balance and persistent strong static stability of the lower atmosphere. Such conditions favor localized surface temperature anomalies of large amplitude. It has been found that the locations of such anomalies correspond to urban areas, where artificial surfaces and anthropogenic heat raise air and surface temperatures – i.e., urban heat islands (UHIs). However, the magnitude and spatial extent of such anomalies – as well as the controlling factors in high latitudes – have not been well investigated. A recent advance using remote sensing is the identification of UHIs in 28 cities in northern West Siberia [Miles & Esau, 2017]. Here we present results focused on a few case studies. The analysis is based on the MODerate Resolution Imaging Spectro-radiometer (MODIS) data from Terra and Aqua satellite platforms. The 18 years (2000–2017) of MODIS Land Surface Temperature (LST) data reveal the geographical extent, seasonal and diurnal variations of the UHI. For some cities, the mean annual UHI magnitude is $>2.4\text{K}$. The apparent UHI area is larger than the urbanized area. It extends the influence of the positive temperature anomalies on the ecosystem around the city [Esau et al., 2016]. This magnitude corresponds to the thermal conditions within a climate zone which can be found hundreds of kilometers south of the city. The analysis of MODIS normalized difference vegetation index (NDVI) around urban areas reveals trends opposite to general background NDVI trends. For example, the decrease in vegetation around Surgut is lower than the general background trend for the middle taiga zone in northern West Siberia (NWS). Figure 1 shows high positive (or less negative) trends close to the city. For vegetation around the urban areas, intrazonal factors (or micro-climatic factors) have a large influence, together with zonal factors.

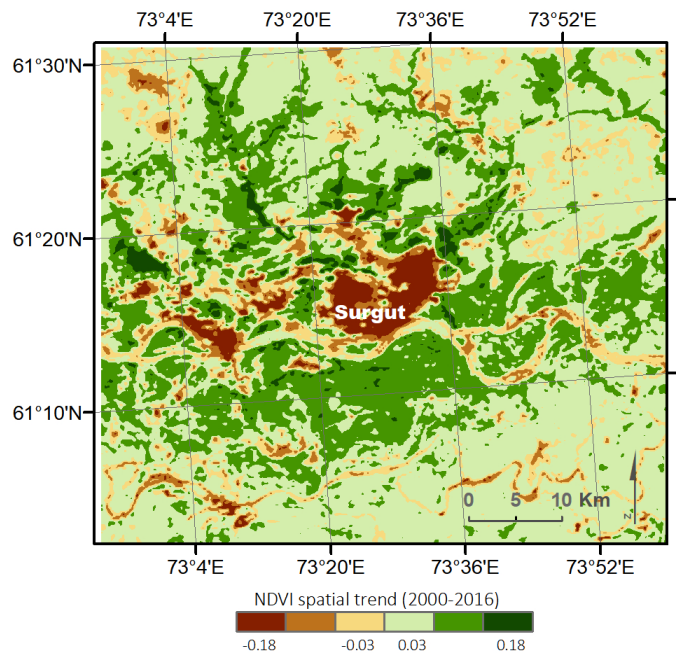


Figure 1: NDVI variability around Surgut, shown as local anomalies from the regional background extracted using trend surface analysis.

References

- Miles, V. V. and Esau, I. [2017]: : Seasonal and spatial characteristics of Urban Heat Islands (UHIs) in northern West Siberian Cities *Remote Sensing*, 9(10), doi:10.3390/rs91009-89.
- Esau, I., Miles, V.V., Davy, R., Miles, M.W., and Kurchatova, A [2016]: Trends in the normalized difference vegetation index (NDVI) associated with urban development of northern West Siberia. *Atmospheric Chemistry and Physics*, 16(15), doi:10.5194/acp-2016-51.



Quantifying patterns of forest structure across a circumpolar biome boundary

P. M. Montesano¹ & C. S. R. Neigh²

¹*Science Systems and Applications, Inc.;*

²*NASA Goddard Space Flight Center*

Interactions between broad-scale climate, local-scale site factors and disturbance history have produced a range of forest cover patterns in the taiga (boreal) – tundra ecotone (TTE). These patterns, indicative of a biome boundary, both influence and reflect ecological processes and can be captured by satellites at a range of scales. The goal of this work was to update our understanding of the extent of the TTE, and capture differences in its structure across the entire circumpolar domain. We used a dataset of

tree canopy cover based primarily on the Landsat 7 and 8 archive from 2010 – 2015 that was calibrated and validated for boreal forest tree canopy cover. With these data we refined the delineation of this circumpolar biome boundary, classified tree cover to map the extent of the ecotone, and quantified ecotone structure patterns. The patterns of ecotone structure will help distinguish the differences in this biome boundary across the circumpolar domain and provide a basis for examining differences in dynamics.



3D satellite observations North American boreal forest growth

Christopher S. R. Neigh¹, Paul M. Montesano², Joseph O. Sexton³, Min Feng³, Saurabh Channan³, Nuno Carvalhais⁴, Mathias Forkel⁵, Leonardo Calle⁶, & Ben Poulter¹

¹NASA GSFC, Greenbelt, MD USA;

²Science Systems Applications Inc. Lanham MD USA;

³University of Maryland, College Park, MD USA;

⁴Max Planck Institute for Biogeochemistry, Jena, Germany;

⁵TU Wien, Vienna, Austria;

⁶Montana State University, Bozeman, MT USA

Keywords: Forests, Growth, Stereo, Landsat, WorldView

We are studying the growth, disturbance and carbon (C) storage of North American boreal forests to improve understanding of Arctic/Boreal terrestrial ecosystems that may be approaching a potential tipping point of C release. At continental scales, climate change is altering vegetation productivity and C sequestration. These impacts can be observed in vegetation canopy structure (cover and height) which varies across the landscape. Currently a need exists to understand environmental constraints on site-scale canopy structure and to predict impacts of environmental change on vegetation cover and C-stock/flux. Dynamic Global Vegetation Models (DGVMs) thus

far have found large increases in productivity and C-flux. However, turnover rates in these models have a large source of divergence between them. Site Index (SI) is a parameter widely used in forestry to describe the potential height-growth of trees in a particular location or 'site.' SI knowledge will reduce uncertainty of live C turnover into soil C pools. We have successfully estimated boreal forest SI by pairing Landsat estimates of forest disturbance with spaceborne LiDAR and spaceborne commercial sub-meter resolution stereo canopy height models. In this talk, approaches for calculating SI from remote sensing will be presented along with estimated rates of carbon accumulation.

Mapping vegetation in a north-boreal fen in very-high and ultra-high spatial resolution

A. Räsänen, S. Juutinen, & T. Virtanen

Ecosystems and Environment Research Programme, Faculty of Biological and Environmental Sciences, and Helsinki Institute of Sustainability Science (HELSUS), P.O Box 65, FI-00014 University of Helsinki, Finland

Very-high spatial resolution (VHSR) and ultra-high spatial resolution (UHSR) remote sensing data allow detailed mapping of vegetation such as plant community types and leaf-area index (LAI), which are necessary e.g. when analyzing ecosystem-atmosphere exchange of carbon and water. We analyze

- the usability of UHSR drone data and
- data type requirements in mapping vegetation patterns in a patterned fen.

We mapped land cover, plant communities, biomass and LAI at two spatial scales in a fen (69° 08' 25" N, 27° 16' 11" E) and a larger catchment in Kaamanen, northern Finland. The 0.4 km² fen site is characterized by strings dominated by dwarf shrubs and flarks with little emergent vegetation. We combined 5 cm resolution drone RGB image, vegetation height model and digital elevation model (DEM) with VHSR (0.5–3 m spatial resolution) optical images (WorldView-2 image, aerial image and four Planetscope images) and airborne laser scanning point cloud, canopy height model and DEM. We mapped the 33 km² catchment in 2 m resolution with VHSR data. The main land cover types in the catchment include pine and birch forests as well as bogs and fens, while elevation ranges from 153 to 212 m.

We utilized object-based methodology by combining full lambda schedule segmentation with random forest classification and regression. For each segment, we calculated multiple features characterizing spectral,

textural, topographic, and vegetation height patterns. In land cover type classification, we ended to classes in the fen and to ten classes in the whole catchment. Overall classification accuracy was 72 % at both scales. We used species and plant functional type specific presence-absence data in configuring plant communities with fuzzy c-means clustering. We delineated five fuzzy plant community clusters and modeled membership values of each cluster to vegetation plots. We then modeled the spatial patterns of the cluster membership values with remote sensing data and regression models with varying success (R² values from 0.25 to 0.67). We built regression models for estimating biomass and LAI using harvested biomass and LAI measurements as response variables and remote sensing data as explanatory variables. The R² values in the fen were 0.52 for both biomass and LAI. In the whole catchment, we mapped also tree biomass and LAI, with R² values ranging between 0.29 and 0.47 for different biomass and LAI components.

UHSR data allows detailed mapping of plant community and land cover types which cannot be distinguished at all with VHSR data in a patchy fen, but the use of UHSR data is hampered e.g. by more demanding data processing. Furthermore, optical data should be combined with data about topography and vegetation height both in UHSR and VHSR. To further facilitate detailed mapping of fen vegetation, we will carry out vegetation survey and fly a drone with a hyperspectral camera during summer 2018. Initial results will be shown in the conference.

Comparing spectral characteristics of Landsat-8 and Sentinel-2 data for Arctic permafrost regions

A. Runge^{1,2} & G. Grosse^{1,2},

¹Alfred Wegener Institute for Polar and Marine Research, Telegrafenberg A45, 14473 Potsdam, Germany;

²Institute of Earth and Environmental Sciences, University of Potsdam, 14469 Potsdam, Germany

Optical remote sensing in the Arctic is highly restricted by frequent cloud cover and low illumination angles, which decreases the amount of useable images during the short vegetation period considerably. As a result, even the more than 30-year long and continuous Landsat mission archive only contains few suitable images for a summer season per year. With the start of the ESA Copernicus Sentinel-2 mission in 2015 and enhanced data availability from its two satellites (S-2A, S-2B) the revisit time, combining data of the two Sentinel-2 and the Landsat-8 satellites, is shortened to less than five days in high latitude regions. The dramatic increase in the number of images per summer season enhances the opportunity for cloud-free image acquisitions considerably. Hence, assessing the spectral compatibility of multispectral Landsat-8 and Sentinel-2 images for a combined application in time-series analysis of multispectral properties to monitor vegetation and landscape dynamics in the Arctic is particularly important. This increase in image availability of the Arctic facilitates the possibility of creating dense time series, which improves mapping vegetation and biomass and monitoring their changes in a rapidly warming Arctic. An advantage is to be able to detect landscape dynamics and to differentiate between rapid and gradual changes, and therefore describing permafrost region disturbances better [Stow et al., 2004]. In general, the multispectral Landsat-8 Operational Land Imager (OLI) and the Sentinel-2 Multispectral Imager (MSI) sensors are comparable: they feature several roughly corresponding bands and similar spatial resolutions. While both global and regional assessments of Landsat-8 and Sentinel-2 datasets already describe the combined usability of the two, they also underline the necessity of regional studies to capture the landscape specific responses of both sensors before any combined application. Therefore, before a linked use in time series analysis of high latitude tundra regions the comparability of sensor-signal responses for both systems needs to be tested and analysed in detail for specific target surfaces. The aim of this

study in progress is to assess spectral characteristics of Landsat-8 and Sentinel-2 same-day acquisition images from the Arctic Lena Delta in North Siberia in summer 2016. We assess image pairs corrected to surface reflectance and cloud masked based on single band comparisons, multispectral indices (e.g. normalized difference vegetation index (NDVI)) and the sensor responses over a summer period by land cover type. Our focus areas are especially areas with wet sedge- and moss-dominated tundra, moist grass- and moss-dominated tundra, moist to dry dwarf shrub-dominated tundra as well as dry moss-, sedge- and dwarf shrub-dominated tundra areas in the central Lena Delta [Schneider et al., 2009]. While we hypothesize that both sensors show the same spectral properties, we expect that the specific signal responses may systematically differ. Therefore, in certain analysis contexts, the joint use of Landsat-8 and Sentinel-2 imagery requires the application of spectral adjustment. The land cover specific analysis will likely indicate the range of differing signal responses of Landsat-8 and Sentinel-2 images.

References

- Schneider, J., Grosse, G. and Wagner, D. [2009]: Land cover classification of tundra environments in the Arctic Lena Delta based on Landsat 7 ETM+ data and its application for upscaling of methane emissions. *Remote Sensing of Environment*, 113(2): 380–391 doi:[10.1016/j.rse.2008.10.013](https://doi.org/10.1016/j.rse.2008.10.013).
- Stow, D.A., Hope, A., McGuire, D., Verbyla, D., Gamon, J., Huemmrich, F., Houston, S., Racine, C., Sturm, M., Tape, K., Hinzman, L., Yoshikawa, K., Tweedie, C., Noyle, B., Silapaswan, C., Douglas, D., Griffith, B., Jia, G., Epstein, H., Walker, D., Daeschner, S., Petersen, A., Zhou, L. and Myneni, R. [2004]: Remote sensing of vegetation and land-cover change in Arctic Tundra Ecosystems. *Remote Sensing of Environment*, 89(3): 281–308 doi:[10.1016/j.rse.2003.10.018](https://doi.org/10.1016/j.rse.2003.10.018).

Changes in land cover classes of north-eastern Siberia between 2001 and 2016 inferred from combining field data with Landsat spectral ratio indices

Iuliia Shevtsova, Birgit Heim, Stefan Kruse, & Ulrike Herzschuh

Alfred Wegener Institute Helmholtz Centre for Polar and Marine Research, Research Unit Potsdam, Potsdam, Germany

Vegetation is sensitive to recent climate warming which is particularly strong in Arctic regions. Changes in vegetation are reflected by satellites sensor data however interpretation of inferred changes is difficult. We combined vegetation cover data (58 sites, 4 locations from N65.90 to N67.82 and from E163.38 to E168.71) from the field expedition July 2016 to North-Eastern Siberia [Overduin et al., 2017] and remote sensing information (vegetation indices calculated from cloudless peak-summer acquisitions Landsat imagery). With this data an RDA-model was built and used for k-means classification and prediction of the land cover classes for modern time (2016–2017 years) and in the past (2001–2002 years). The best results for RDA-model were gained from using spectral indices of Landsat-8 OLI: from 8 indices only three chosen as the best predictors describing coverage field data variance:

$$VegHT = NDVI + NDMI + NDWI,$$

VegHT – Hellinger transformed vegetation data,
Normalized Difference Vegetation Index:

$$NDVI = \frac{NIR - RED}{NIR + RED}$$

Normalized Difference Moisture Index:

$$NDMI = \frac{NIR - SWIR1}{NIR + SWIR1}$$

Normalized Difference Water Index:

$$NDWI = \frac{Green - NIR}{Green + NIR}$$

The k-means classification was based on 2 RDA-axes with 4 classes for reasonable representation of vegetation types according to biomass:

1. high biomass (predominantly dense forest)
2. sparse forest and scrublands,
3. open tundra (hummock, grasslands),
4. very low biomass (Dryas-lichens-mosses associations on rocks).

Despite the appropriate results of Landsat-8 OLI classification (Fig. 1), direct comparison with Landsat-7 ETM+ and classification itself using above described model for this sensor data is not possible since the spectral band response of the different Landsat missions sensors differ from each other. For this described classification method high consistency between the spectral bands of different Landsat missions is required. The standard corrections between Landsat-8 OLI and Landsat-7 ETM+ spectral bands [Roy et al., 2016] were still not sufficient and a significant bias remained between the 2 sensors when we applied the sensor transformation. Therefore, it was important to optimize the transformation between Landsat-7 ETM+ and Landsat-8 OLI. For this purpose Landsat-7 ETM+ and Landsat-8 OLI cloudless images with 2 days difference were taken for sampling and making models for each band using Local polynomial regression fitting (*loess* function in R).

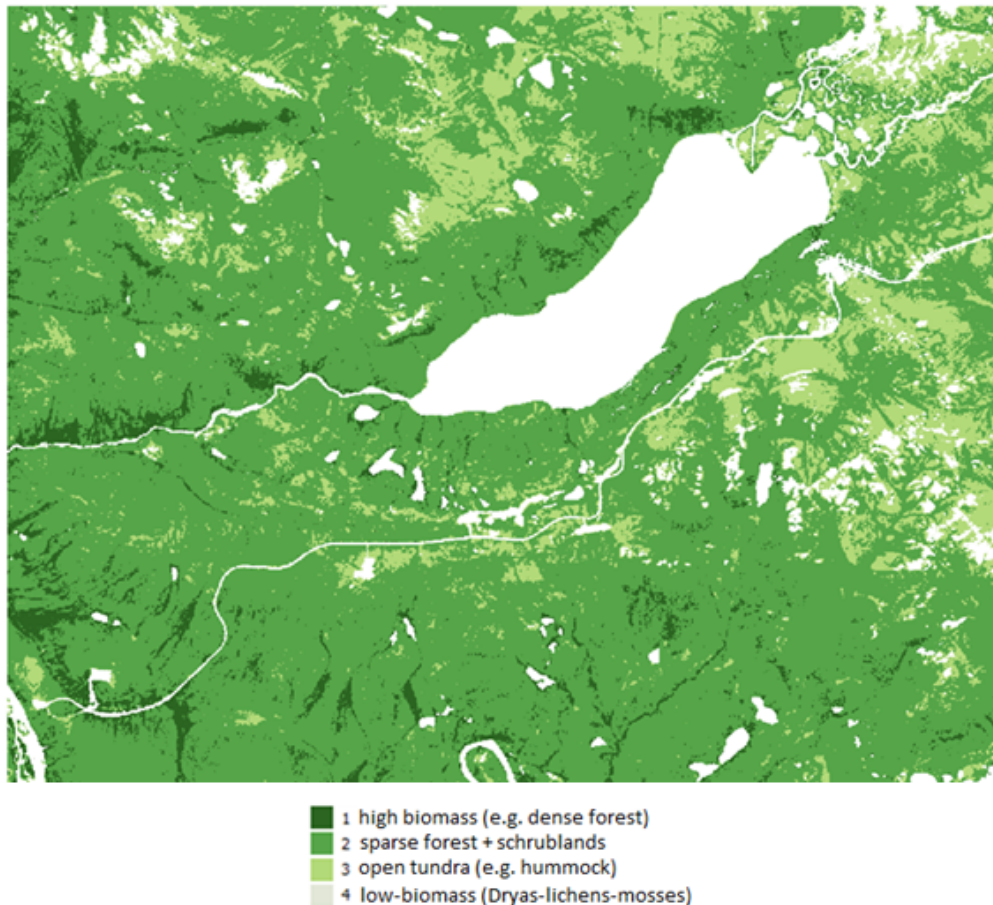


Figure 1: Results of Landsat-8 classification of one of the field locations – Lake Illerney

References

Overduin, P. , Blender, F. , Bolshiyarov, D. Y. , Grigoriev, M. N. , Morgenstern, A. and Meyer, H. (eds.) [2017]: Russian-German Cooperation: Expeditions to Siberia in 2016. *Reports on Polar and Marine Research*, 709, Bremerhaven, Alfred Wegener Institute for Polar and Marine Research, 295 p.

Roy, D. P., V. Kovalskyy, H.K. Zhang, E. F. Vermote, L. Yan, S.S. Kumar, and A. Egorov [2016]: Characterization of Landsat-7 to Landsat- 8 reflective wavelength and normalized difference vegetation index continuity. *Remote Sensing of Environment*, 185: 57–70. doi:[10.1016/j.rse.2015.12.024](https://doi.org/10.1016/j.rse.2015.12.024).

Zackenbergl Valley seen by TerraSAR-X – land cover and moisture conditions

Jennifer Sobiech-Wolf¹, Tobias Ullmann², Achim Roth³, & Wolfgang Dierking¹

¹Alfred-Wegener-Institut, Bremerhaven, Germany;

²University of Würzburg, Germany;

³DLR Oberpfaffenhofen, Germany

Radar remote sensing is an important tool for regular environmental monitoring as it works independent from sunlight and radar waves are able to penetrate clouds. This makes it especially useful for regions such as the Arctic, where the applicability of optical sensors is limited and ground based observations are costly and need immense logistics. However, radar data are not easy to interpret and need thus good evaluation as a first step. In this study, we test the potential of the active Synthetic Aperture Radar TerraSAR-X to monitor soil moisture variations in a high Arctic Tundra landscape and tested their use in land cover classification.

Our investigation area is Zackenberg valley in NE Greenland at 74°30'N and 20°30'W. The area is underlain by permafrost and covered by low Tundra vegetation. The valley is a key site for research due to its accessibility via the Zackenberg research station and ongoing permanent environmental monitoring programs by Aarhus University, Denmark. In summers 2013 and 2014, we performed extensive soil moisture measurements, determined the water content of the above ground biomass and mapped the land cover. Soil moisture was measured manually by use of a Hydrosense HS2 with 12cm rods. In total, 5966 measurements were done in 2013 and 4518 measurements in 2014. In parallel to our fieldwork, the German radar satellite TerraSAR-X recorded several images from the valley in dual-pol Spotlight mode (HH / VV) with a spatial resolution of 3.4 meters after multi-looking and further processing. We used 17 images from summer 2013 and 15 images from

summer 2014 for our analysis.

Statistical analyses of the relationship of the backscatter and soil moisture values showed no significant correlation ($R^2 = 0.1$). As radar backscatter in general depends on soil moisture and is sensitive to moisture variations, we conclude that the main reflection of the radar waves is from the surface and the vegetation layer on top of the soils and that the surface roughness is the dominant factor, with influence of the vegetation structure.

Inside Zackenberg valley, seven main land cover classes are present. To analyse the land cover separability by TerraSAR-X, polarimetric features were processed from the dual-pol images. A Kennaugh Matrix Decomposition was performed and the features dual-pol entropy, alpha, double bounce and surface scattering were processed. As reference, a land cover map and own in-field observations were used. The transformed divergence was used as a metric to indicate the separability of land cover classes. A Maximum Likelihood and a Random Forest classification showed similar classification results with low overall accuracy of about 44%. Water bodies and fan areas could be separated best from their surroundings, whereas lowest classification performance was found for heath and salix formations.

From our analyses, we conclude that TerraSAR-X is valuable to separate land, water, and fen areas in this high arctic tundra landscape, while soil moisture monitoring and further land cover analysis require data from radar sensors operating with longer wavelength.

More lightning in the high latitudes: implications for fire and carbon

Sander Veraverbeke¹, Yang Chen², Brendan M. Rogers³, Mike L. Goulden², Randi R. Jandt⁴, Charles E. Miller⁵, Elizabeth B. Wiggins², & James T. Randerson²

¹Faculty of Science, Vrije Universiteit Amsterdam, the Netherlands;

²Department of Earth System Science, University of California, Irvine, CA, USA;

³Woods Hole Research Center, Falmouth, MA, USA;

⁴Alaska Fire Science Consortium, University of Alaska, Fairbanks, AK, USA;

⁵NASA Jet Propulsion Laboratory, California Institute of Technology, Pasadena, CA, USA

The boreal forest and arctic tundra store more than 35 % of the global soil carbon and lightning fires are the main landscape disturbance in these biomes. Using satellite fire and lightning network data, we found that record number of lightning ignitions drove two recent extreme fire seasons in boreal North America, Northwest Territories 2014 and Alaska 2015. We also found that, in these regions, lightning ignitions are on the rise with between 2 and 5 % since 1975. Exceptional high levels of burning also occurred near the northern treeline.

We then used global lightning observations from

the Optical Transient Detector in combination with climate variables from reanalysis (temperature, convective precipitation and convective available energy) to model contemporary and future lightning in the high latitudes. Our model predicts increases in lightning of more than 200 % in the world's boreal forest, and more than 300 % in arctic tundra by the end of the century. This suggests that there will be more fire in the high latitudes, which may accelerate carbon losses from organic soils. This represents a new mechanism and positive feedback loop between climate, fire and carbon emissions.

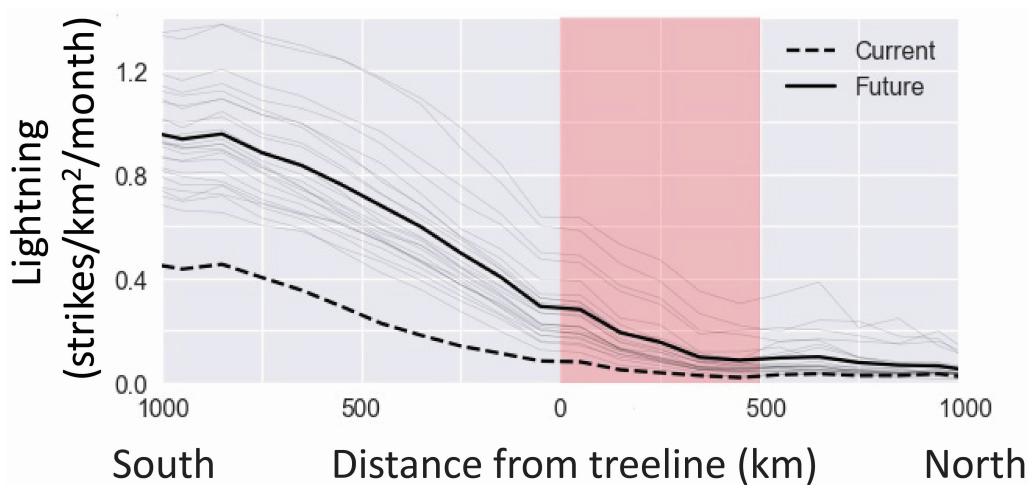


Figure 1: Increases in future (2100) lightning in the treeline ecotone.



SESSION

Remote Sensing of the Polar Atmosphere

A new algorithm for cloud identification over the Arctic using AATSR/SLSTR and its application for ACLOUD/PASCAL campaigns

S. Jafariserajehlou, L. Mei, M. Vountas, V. V. Rozanov, & J. P. Burrows

Institute of Environmental Physics, University of Bremen, Otto-Hahn-Allee 1, 28359 Bremen, Germany

The remoteness of the Arctic region has led to limited number and marginal coverage of ground-based measurements of geophysical parameters in this region and highlighted the role of space-borne observations to investigate parameters and feedback mechanisms which contribute to Arctic research. However, clouds represent one of the major sources of error in satellite-based retrievals of snow properties, aerosol, trace gases as well as cloud properties and etc. In fact, a precise cloud detection method as a prerequisite in satellite-based retrievals plays an important role in reliability of final results and could hamper the usage of them for further analyses.

In this study, a new cloud detection algorithm based on time-series measurements is developed and applied to Advanced Along-Track Scanning Radiometer (AATSR), one payload on the European Environmental Satellite (Envisat). Furthermore, the developed algorithm is successfully applied to the Sea and Land Surface Temperature Radiometer (SLSTR) onboard the Sentinel-3 platforms to estimate cloud properties during ACLOUD/PASCAL campaigns [Wendisch et al., 2018].

The main idea behind this method is that clouds have larger spatial variability and less stability compared to cloud free conditions. Therefore, the stability of ground scenarios in cloud-free conditions is characterized by Pearson Correlation Coefficient (PCC) values, calculated between the last measurement and time-series data.

One central aim of this work is cloud masking for aerosol retrieval over the Arctic. To avoid misclassification of heavy aerosol loadings with cloud, PCC analysis has been designed for a wavelength which is affected little by aerosol particles, whereas the Top Of Atmosphere (TOA) reflectance is affected by clouds. Furthermore, additional information from thermal infrared channels of the above mentioned instruments

has been utilized to separate cloudy and cloud-free pixels to produce a cloud mask with $1 \times 1 \text{ km}^2$ spatial resolution. Moreover, a simple land classification step is added to derive five surface types: snow, land, ice, cloud and ocean.

The results of applying this algorithm to case studies over the Arctic region and the validation against

1. European Space Agency (ESA) standard cloud product from AATSR L2 nadir cloud flag,
2. One of existing methods based on clear-snow spectral shape,
3. Surface synoptic observations (SYNOP),
4. Moderate Resolution Imaging Spectroradiometer (MODIS) are presented.

Acknowledgements

This work was supported by the SFB/TR 172 “Arctic Amplification: Climate Relevant Atmospheric and Surface Processes, and Feedback Mechanism (AC)3” funded by the German Research Foundation (DFG, Deutsche Forschungsgemeinschaft: 40101200).

References

- M. Wendisch, et al. [2018]: The Arctic cloud Puzzle: Using ACLOUD/PASCAL Multi-Platform Observations to Unravel the Role of clouds and aerosol particles in Arctic Amplification. *to be submitted to Bull. Am. Meteorol. Soc.*
- S. Jafariserajehlou, L. Mei, M. Vountas, V. V. Rozanov, J. P. Burrows [2018]: Cloud identification algorithm for aerosol retrieval over the Arctic using AATSR/SLSTR time series measurements. *to be submitted to Atmos. Meas. Tech.*



Understanding of polar atmospheric dynamics by measurements of surface air pressure using O₂-band differential absorption radar

Bing Lin¹, Qilong Min², Steve Harrah¹, Yongxiang Hu¹, & Roland (Wes) Lawrence³

¹NASA Langley Research Center, Hampton, VA 23681, USA;

²State University of New York at Albany, Albany, NY 12222, USA;

³National Institute of Aerospace, Hampton, VA 23666, USA

Polar regions have very high sensitivities on global environmental variations and could enhance extreme weather conditions in middle latitudes, which would significantly affect people's daily life and public safety. Continuous monitoring polar weather conditions is a key in understanding polar dynamics, improving weather predictions, and minimizing polar impacts. Although many major meteorological variables have been measured over the regions from space, the key atmospheric dynamic variable, air pressure, can only be observed in very limited surface stations. There is a significant gap in the measurement of air pressure in various spatiotemporal scales: from small, local to regional and large and from hourly, daily to weekly and even longer ones. There is no operational space capability available for direct air pressure remote sensing over polar regions. This effort tries to develop a feasible active microwave approach that measures surface air pressure from space using a Differential-absorption BARometric Radar (DiBAR) operating at 50-55 GHz O₂ absorption band for weather forecasts. The measured data will enable numerical weather prediction models constraining their assimilated dynamic fields close to actual meteorological conditions and improving the weather forecasts of not only polar re-

gions but also the globe. For example, this approach will increase our knowledge on polar vortex dynamics, monitor their changes and variations in real-time, and predict their impacts accurately. Analyses show that with the proposed space DiBAR the errors in instantaneous (averaged) pressure estimates can be as low as $\approx 4\text{mb}$ ($\approx 1\text{mb}$) under all weather conditions.

NASA Langley research team has made substantial progresses in advancing the DiBAR concept and technology since it developed a decade ago. The feasibility assessment clearly shows the potential of surface barometry using existing radar technologies. The team has also developed a DiBAR system design, fabricated a Prototype-DiBAR (P-DiBAR) for proof-of-concept, conducted laboratory, ground and airborne P-DiBAR tests. The flight test results are consistent with the instrumentation goals. Observational system simulation experiments (OSSEs) for space DiBAR performance based on the existing DiBAR technology and capability show substantial improvements in weather predictions. Satellite DiBAR measurements will provide an unprecedented level of the prediction and knowledge on polar and global weather conditions. The development of the DiBAR concept will be presented.

Characteristics and genesis conditions of January polar lows: Microwave satellites, radiative transfer simulations and arctic system reanalysis

A. Radovan¹, S. Crewell¹, M. Mech¹, & A. Rinke²

¹University of Cologne, Institute of Geophysics and Meteorology, Pohligstr. 3, 50969 Cologne, Germany;

²Alfred Wegener Institute, Helmholtz Centre for Polar and Marine Research, Telegrafenberg A43, 14473 Potsdam, Germany

Polar lows (PLs), often called “hurricanes of the Arctic” are intense, high-latitude maritime cyclones that bring heavy precipitation, (mostly in the form of snow), and whose winds are above gale force. Their intense winds combined with large amounts of snow, can cause significant infrastructural damage to coastal communities and disruption of shipping routes. However, their small horizontal scale (less than 1000 km) and short life time (sometimes only 3 h) makes them hard to predict. Therefore, improved understanding and prediction is of high importance. Satellite observations in the microwave range that have a good coverage of the Arctic region offer high potential due to their sensitivity to snow. In this study, two such satellite instruments, namely Advanced Microwave Sounding Unit –B (AMSU-B) and Microwave Humidity Sounder (MHS) have been used. The investigation of PLs is done for the period of 12 years (January, 2000–December, 2011) over which 33 January cases were reported. Arctic System Reanalysis version 1 (ASRv1) is used for the analysis of atmospheric gen-

esis conditions of PLs and compared with AMSU-B and MHS observations. For the latter, radiative transfer simulator called PAMTRA (Passive and Active Microwave Radiative Transfer Model) that is able to simulate microwave brightness temperatures (TB) in the 1–800 GHz range has been employed. We found that AMSU-B and MHS are performing well in representing the PLs, where channels around strong water vapour line, namely 183.31, ± 1 , ± 3 , ± 7 and 190.31 GHz, are showing strong depression in PL convective cores. The depression at times can be more than 40 K for the 183.31 ± 7 and 190 GHz channels. Generally, simulations show good agreement with the AMSU-B and MHS observations, though not all cores of multi-low PL are resolved. Possible explanation for that could be coarser resolution of the ASR as well as the parameterization of the precipitation processes. Furthermore, we investigate PL cases originating in different geographical area and the amount of snowfall they bring.



SESSION

Snow Trends

Quantifying spring snow cover evolution on Kurungnakh Island, North Siberia

T. Hainbach^{1,2}, A. Morgenstern², & B. Heim

¹University of Potsdam;

²Alfred Wegener Institute Helmholtz Centre for Polar and Marine Research, Potsdam, Germany

Snow plays a key role in the thermal regime of permafrost, as well as for the supply of water for vegetation and for erosional processes. Besides areal coverage, snow depth and snow water equivalent are the most important parameters for snow cover investigations as they define the insulation properties and the amount of stored water, respectively. Across arctic lowlands, however, the snow cover is very heterogeneous reaching from a few centimeters on flat elevated areas to several meters in local depressions or valleys (Fig. 1). This leads to greatly varying water content within the snow cover. Furthermore, snow cover and its properties develop differently throughout the spring snow-melt period in different landscape units and relief settings. Standard remote-sensing products like NDSI (Normalized Difference Snow Index)-based snow cover of multispectral satellite imagery lack the temporal continuity needed for short time scale observations such as snow melt. Therefore, a higher temporal resolution is needed for the spatial analysis of seasonal snow cover evolution. Additional ground-based image acquisitions such as using time-lapse cameras can help to close the gaps in-between consecutive satellite images. Our study aims at quantifying snow cover properties and its evolution at an ice-rich per-

mafrost site affected by thermal erosion. We installed 10 time-lapse cameras at several key sites covering different relief settings on Kurungnakh Island, North Siberia, i.e. different types of thermo-erosional valleys (Fig. 1) and flat terrain of Yedoma uplands. We applied recently developed methods tested for mountainous regions to this high arctic lowland site for extracting snow cover maps from RGB-images captured with the time-lapse cameras. This information was used as ground truth data to improve NDSI-based snow cover products. Additionally, we conducted snow water equivalent, snow height and high-precision relief measurements in the field to estimate the amount of stored water. We found that time lapse images display valuable ground truth data. By using a combination of supervised classifications methods and field measurements, we show that snow cover distribution and snow melt is primarily driven by wind and slope exposure. Especially narrow thermo-erosional valleys can accumulate significant amounts of snow which in turn enhance further permafrost degradation. This study provides a toolset to describe snow cover evolution in a quantifiable manner and gives evidence for key characteristics how snow may influence permafrost degradation.



Figure 1: Two installed time lapse cameras on Kurungnakh Island facing different slopes of a thermo-erosional valley. Heterogenous snow cover height is clearly visible, ranging from a few centimeters around the camera pole to several meters high cornices in the background.

Fractional snow cover area from terrestrial photography in Svalbard Islands (Norway)

R. Salzano & R. Salvatori

Institute of Atmospheric Pollution Research, National Research Council of Italy

The availability of different webcam in Svalbard islands (Norway) offers the opportunity to network different data sources useful for preparing new snow cover products. The fraction of snow cover is a critical essential variable that is of interest especially in polar areas where remotely sensed data are not continuous. This topic is particularly important in climate change studies and it is included in the iCupe project, where different information at different spatial and time resolutions will be combined in order to develop knowledge about the Arctic region. The presented activity is aimed to network different cameras at the ground, with different field of view and formats, and the final outcome is the preparation of a dataset about the fraction of snow cover. This data source will be aimed to support the estimation of parameters that characterize the cryosphere using remotely sensed data, with a particular attention to data obtained in the framework of the Copernicus program. The availability of this dataset in a “natural” laboratory such as Svalbard islands will support the reduction of the gap between remotely sensed data and modeling activities. This added value will be very important considering the higher spatial resolution of the sensors recently deployed. The dataset will be

based on re-using data obtained from public repositories such as the digital elevation model of Svalbard, the available webcam imagery in Svalbard and satellite products from different missions/sensors (Landsat, Sentinel and MODIS). All the available data will be integrated in order to estimate the fraction of snow cover, at different spatial resolutions, for each satellite mission. These estimations, computed at different sites in Svalbard islands, will offer the opportunity to better integrate results obtained by remote sensing with modeling and air-snow interactions studies.

References

- R. Salvatori, P. Plini, M. Giusto, M. Valt, R. Salzano, M. Montagnoli, A. Cagnati, G. Crepaz & D. Sigismondi [2011]: Snow cover monitoring with images from digital camera systems. *Ital. J. Remote Sens.*, p. 137–145 doi:[10.5721/ItJRS201143211](https://doi.org/10.5721/ItJRS201143211).
- A.N. Arslan, C.M. Tanis, S. Metsämäki, M. Aurela, K. Böttcher, M. Linkosalmi & M. Peltoniemi [2017]: Automated Webcam Monitoring of Fractional Snow Cover in Northern Boreal Conditions. *Geosciences*, 7, 55. doi:[10.3390/geosciences7030055](https://doi.org/10.3390/geosciences7030055).



Local and regional trends in snow cover from a 34-year time series of satellite observations

Rune Solberg¹, Øystein Rudjord¹, Arnt-Børre Salberg¹, Mari Anne Killie², Steinar Eastwood², & Lars-Anders Breivik²

¹Norwegian Computing Center;

²Norwegian Meteorological Institute

Changes in the seasonal snow cover over time are a sensitive indicator of climate change at the global, continental and local scale. The Arctic region is warming faster than the Earth in general, and the corresponding part of the cryosphere is significantly affected. This includes the seasonal snow cover resulting in shorter snow seasons.

Trying to quantify the changes in snow cover regionally and hemispherically, we developed a snow cover extent (SCE) product (www.cryoclim.net) of 5 km spatial resolution based on algorithms processing optical and passive microwave radiometer (PMR) data. From 1982 onwards, most of the planet is covered daily by a combination of the sensors AVHRR and SMMR or SSM/I. To compensate for lack of sunlight during winter at high latitudes, and lack of observations with optical sensors under cloudy conditions, we developed a sensor-fusion approach combining optical and PMR data in a time series for estimating the most likely snow cover each day, given all the observations by both sensor types within the current snow season.

The fusion algorithm is based on a hidden Markov model (HMM) simulating the snow states based on the satellite observations. The basic idea is to simulate the states the snow surface goes through during the snow season with a state model. The model is described by the different states and the possible transitions between these states. The states are given by probability density functions and the transitions by transition probabilities. The transition probabilities

depend on the current time within the season. The states are not directly observable, but the remote sensing observations give data describing the snow conditions, which are related to the snow states. A Viterbi algorithm is used to find the most likely snow cover sequence throughout the hydrological year at a given location. The HMM solution represents not only a multi-sensor model but also a multi-temporal model.

For validation of the snow cover product we have used time series of *in situ* observations. From the four datasets GHCN-D, HSDSD, FSUHSS and RHIMI we obtain total accuracies of 91.7 %, 94.0 %, 94.9 % and 92.9 %, respectively. We found somewhat lower accuracy in October and November, and to some degree also in April. This is likely due to thin and wet snow (affecting PMR) combined with darkness (affecting optical) in the autumn and patchy and wet snow cover in the spring (affecting both sensors).

The first version (version 1) of the snow products was made available in 2013. The algorithms have been improved in 2016–2018, and an extended time series covering 34 years is now produced with the updated algorithms (version 2.0). We will use this version for regional and local trend analysis of snow cover in the circumpolar regions over the period 1982–2015.

The presentation will describe the algorithm, validation and results from the trend analysis regionally and for both hemispheres.

TerraSAR-X time series fills a gap in high spatiotemporal monitoring of snowmelt in small Arctic catchments

Samuel Stettner¹, H. Lantuit^{1,2}, B. Heim¹, B. Rabus³, J. Eppler³, A. Roth⁴, & A. Bartsch⁵

¹Alfred Wegener Institute Helmholtz Centre for Polar and Marine Research, Permafrost Research Section, Telegrafenberg A45, 14473 Potsdam, Germany;

²Institute of Earth and Environmental Science, University of Potsdam, Karl-Liebknecht-Str. 24-25, 14476 Potsdam-Golm, Germany;

³Synthetic Aperture Radar Laboratory, Simon Fraser University, 8888 University Dr. Burnaby, BC, V5A 1S6, Canada;

⁴Department Land Surfaces, German Aerospace Center Oberpfaffenhofen, 82234 Weßling, Germany;

⁵b.geos, Industriestrasse 1, 2100 Korneuburg, Austria

The timing of snowmelt is an important turning point in the seasonal cycle of small Arctic catchments. The TerraSAR-X (TSX) satellite mission has high potential to improve our understanding of the high spatiotemporal variability of snow cover extent (SCE) and fractional snow cover (FSC) on the catchment scale. TSX provides a combined spatial and temporal resolution not offered by operational optical and other microwave missions. We investigated the performance of multi-polarized and multi-pass TSX in mapping SCE in small catchments of Qikiqtaruk Island (Herschel Island) at the Yukon Coast, western Canadian Arctic compared to Landsat 8 derived SCE. Additionally, we analyzed the spatiotemporal dynamics of FSC from TSX and *in-situ* time lapse cameras from 2015 to 2017. Results showed that the performance of TSX X-Band data was strongly influenced by polar-

ization but not by incidence angle. We observed the highest mean overall accuracy of 0.80 ± 0.27 when using VH polarized images, compared to a mean overall accuracy of 0.71 ± 0.19 and 0.66 ± 0.22 for HH and VV polarized images, respectively. TSX derived FSC time series captured snow melt dynamics similar to those measured by the *in-situ* time lapse cameras. Diurnal temperature variations in early snowmelt season had an impact on capabilities of TSX to detect wet snow highlighting the importance of acquisition time for mission planning. We conclude that multi-orbit and multi-pass TSX snowmelt monitoring performs well for catchment based analysis when the VH polarization is used and together with Landsat 8 draws a complete picture of snowmelt dynamics in small Arctic catchments.



Author Index

- Abdullahi, S., 37
Alcaraz-Segura, D., 102
Aleksyutina, D., 21
Anders, K., 98
Antoine, D., 88, 89
Antonova, A., 94
Antonova, S., iii, 52*, 98*
Ardelean, F., 53
Armstrong, A., 102
Arp, C. D., 19
Arslan, A. N., 39*
- Babkina, E. A., 70
Baranskaya, A. V., 16, 21
Barnes, D. K. A., 25
Bartsch, A., iii, 23, 40*, 54*, 69, 71, 92, 99, 129
Baughman, C. A., 19
Bax, N., 25
Beamish, A., iii, 100*, 107
Belova, N., 21
Belova, N. G., 16*
Berger, S., 34*
Bergstedt, H., 23*, 69, 99
Bernhard, P., 55*
Boike, J., 52, 58, 93, 98
Bolch, T., 7*
Bondurants, A., 19
Bookhagen, B., iii, 36, 101
Bornemann, N., 52
Boss, E., 85
Brönnner, M., 35
Bracher, A., iii, 80*, 85–87
Brauchle, J., 42
Braun, M., iii
Breivik, L.-A., 128
Brell, M., 100, 107
Brieger, F., 101*
Brown, I. A., 108
Bucher, T., 41, 42*
Buchhorn, M., 107
Bull, D. L., 19
Burke, E. J., 58
Burrows, J. P., 86, 122
Buzard, R. M., 19
Calle, L., 114
Carvalhais, N., 114
Castro, A., 102, 104
Chabrillat, S., 100, 107
Chang, J., 58
Channan, S., 114
Chase, A., 85
Chen, R. H., 76
Chen, Y., 120
Ciais, P., 58
Coops, N., 100
Crewell, S., 124
Dörr, N., 34
Dallimore, S., 19
Desyatkin, R., 59
Dinter, T., 80, 86, 87
Dissing, D., 104
Dolan, W., 24*
Donchyts, G., 96
Downey, R., 25
Drews, R., 34
Dugay, C., 40
Duguay, C., 23
Dumais, M.-A., 35*
Dvornikov, Yu. A., 70, 92*
Eastwood, S., 128
Eisen, O., 34
El Kassar, J. R., 82*
Elger, K., 45
Eppler, J., 129
Epstein, H., 102*
Epstein, H. E., 107
Esau, I., 112
Fanara, L., 57*
Fedorova, I., 92
Fell, F., 84
Feng, M., 114
Feuster, A., iii
Fischer, C., 41*
Fischer, J., 82, 83
Fleming, A., 25
Forkel, M., 114
Frederick, J. M., 19
Fricke, A., 62
Frost, G., iii
Frost, G. V., 104*, 110
Fuchs, M., iii, 17*, 60
Gädeke, A., 58*
Günther, F., iii, 0*, 19, 20, 60, 62*, 63, 66, 74
Garestier, F., 59*, 106
Genet, H., 95
Gibbs, A., 19
Goetz, S. J., 12
Gonçalves-Araujo, I., 80
Gordon, R. R., 18
Goulden, M. L., 120
Griffith, P. C., 12
Grosfeld, K., 135
Grosse, G., i, iii, 0*, 17, 19, 40, 43, 45, 57, 60*, 62, 65, 66, 74, 93, 116
Gubarkov, A., 54, 92
Guillaso, S., 59, 61*, 106*
Gwinner, K., 57
H. Haghghi, M., 62, 63*
Hansch, R., 57
Höfle, B., 98
Högström, E., 99*
Hölemann, J., 87
Haas, A., iii, 40, 43*, 45
Haas, C., 26, 29
Hainbach, T., 126*
Hajsek, I., 8*, 55
Halle, W., 41
Hansen, C., 12
Hantson, W., 64*, 65
Harrah, S., 123
Hartmann, J., 94
Hauber, E., 57



- Hayes, D. J., [iii](#), [64](#), [65*](#)
Heim, B., [iii](#), [40](#), [43](#), [45](#), [47](#), [52](#), [63](#),
[84](#), [87](#), [92](#), [99–101](#), [107*](#),
[117](#), [126](#), [129](#), [135](#)
Held, C., [25*](#)
Hellmann, S., [87](#)
Helm, V., [34](#)
Hendricks, S., [26*](#)
Henning, T., [66*](#)
Herzschuh, U., [92](#), [101](#), [107](#), [117](#)
Hodkinson, D., [12](#)
Hofton, M., [12](#)
Hood, M., [iii](#)
Hovemyr, M., [108*](#)
Hoy, L., [12](#)
Hu, Y., [78](#), [123](#)
Huber, M., [37](#)
Humbert, A., [iii](#)
Huntemann, M., [27*](#)

Immerz, A., [43](#)
Irrgang, A. M., [iii](#), [18*](#)
Irrgang, C., [44*](#)
Iwahana, G., [19](#)

Jacobi, S., [68](#)
Jafariserajehlou, S., [122*](#)
Jandt, R. R., [120](#)
Janout, M. A., [87](#)
Jones, B. M., [i](#), [iii](#), [0*](#), [19*](#), [23](#),
[60](#), [65](#), [93](#), [95](#)
Jones, C., [19](#)
Jong, D. J., [84](#)
Jorgenson, M. T., [104](#)
Juhls, B., [iii](#), [82](#), [83*](#), [94](#)
Juutinen, S., [115](#)

Kääb, A., [40](#), [52](#), [71](#)
Kaiser, S., [iii](#), [68*](#)
Kanevskiy, M., [19](#)
Kartozia, A. A., [109*](#)
Kasischke, E. S., [12](#)
Kasper, J. L., [19](#)
Kennedy, R. E., [65](#)
Khairullin, R. R., [70](#)
Khomutov, A. V., [54](#), [70](#), [92](#)
Kilbride, J., [64](#)
Killie, M. A., [128](#)
Kimball, J. S., [76](#)
Kizyakov, A. I., [20*](#), [62](#), [66](#), [70](#),
[74](#)
Klein, K. P., [84*](#)

Kohnert, K., [iii](#), [94*](#)
Komarov, A., [29](#)
Korpelainen, P., [73](#)
Kouraev, A., [59](#)
Kroisleitner, C., [69*](#)
Kruppen, T., [10*](#)
Kruse, S., [101](#), [117](#)
Kumpula, T., [73](#)

López-Martínez, J., [61](#)
Laboor, S., [iii](#), [40](#), [43](#), [45*](#)
Landy, J., [29*](#)
Langer, M., [52](#), [58](#), [68](#)
Lantuit, H., [18](#), [84](#), [129](#)
Lara, M. J., [95*](#)
Larson, E., [12](#)
Lawrence, R., [123](#)
Leibman, M. O., [54](#), [70*](#), [92](#)
Leichtle, T., [37](#)
Lin, B., [123*](#)
Liu, L., [78](#)
Liu, Y., [80](#), [85*](#)
Losa, S. N., [86](#), [87](#)

Müller-Schmied, H., [58](#)
Macander, M. J., [104](#), [110*](#)
Maio, C., [19](#)
Mann, D. H., [19](#)
Manson, G. K., [18](#)
Margolis, H. A., [12](#)
Martynov, F., [87](#)
Marx, S., [98](#)
Maslakov, A., [21](#)
Matsuoka, A., [11*](#)
Maximov, G. T., [62](#)
McCubbin, I., [12](#)
McLennan, D., [50](#)
Mech, M., [124](#)
Mei, L., [122](#)
Metzger, S., [94](#)
Miles, V., [112*](#)
Miller, C. E., [12*](#), [76](#), [120](#)
Min, Q., [123](#)
Moghaddam, M., [76](#)
Mommertz, R., [68](#)
Montefiori, E., [102](#)
Montesano, P. M., [110](#), [113*](#), [114](#)
Moreau, C., [25](#)
Moreno, B., [25](#)
Morgenstern, A., [57](#), [126](#)
Mota, A., [19](#)

Motagh, M., [63](#)
Moutier, W., [88](#), [89](#)
Muetting, A., [36*](#)
Mullanurov, D., [54](#)
Muster, S., [40](#), [43](#), [45](#), [94](#)

Nöthig, E., [85](#)
Neckel, N., [34](#)
Neigh, C. S. R., [110](#), [113](#), [114*](#)
Nelson, P. R., [110](#)
Nitze, I., [iii](#), [17](#), [19](#), [40](#), [45](#), [60](#),
[93*](#)
Novikova, A. V., [16](#), [21*](#)

Oberst, J., [57](#)
Obu, J., [40](#), [71*](#)
Oelker, J., [86*](#)
Ogorodov, S. A., [16](#), [21](#)
Onaca, A., [53](#)
Ostberg, S., [58](#)
Overduin, P. P., [83](#)

Pan, Y., [85](#)
Pattyn, F., [34](#)
Paul, S., [26](#)
Paulsen, M., [25](#)
Pavelsky, T., [24](#)
Peeken, I., [80](#)
Pefanis, V., [87*](#)
Peltoniemi, M., [39](#)
Petereit, J., [44](#)
Pinto, N., [12](#)
Piskor, A., [18](#)
Pointner, G., [99](#)
Poulter, B., [114](#)
Precht, E., [47](#)
Preusker, R., [82](#)

Räsänen, A., [115*](#)
Rößler, S., [92](#), [107](#)
Rabenstein, L., [47](#)
Rabus, B., [129](#)
Radovan, A., [124*](#)
Randerson, J. T., [120](#)
Raynolds, M. A., [13*](#), [102](#)
Richmond, B., [19](#)
Richter, A., [86](#)
Ricker, R., [26](#)
Rinke, A., [124](#)
Roberts, J., [19](#)
Robinson, C. M., [88](#), [89*](#)
Rogers, B. M., [120](#)



- Romanovsky, V. E., 19, 93
Roth, A., iii, 37, 129
Rozanov, V. V., 86, 87, 122
Runge, A., iii, 60, 116*
Ryan-Keogh, T. J., 88, 89
- Säuberlich, T., 41
Sîrbu, F., 53*
Sachs, T., iii, 19, 94, 107, 135
Salberg, A.-B., 128
Salvatori, R., 127
Salzano, R., 127*
Sands, C. J., 25
Sauter, E. J., 47*
Saynisch, J., 44
Schäfer-Neth, C., 43, 45
Schüller, L., 49*
Schaphoff, S., 58
Scheidemann, D., iii
Schlaffer, G., iii
Schmid, T., 43, 61
Schneider von Deimling, T., 68
Schuback, N., 88, 89
Seifert, F. M., 40, 43
Seneviratne, S., 58
Serafimovich, A., 94
Serbin, S., 64, 65
Sexton, J. O., 114
Shabanov, P., 31
Shabanova, N. N., 16, 21, 31*
Shevtsova, I., 101, 117*
- Singha, S., 32*, 119*
Skorospekhova, T., 92
Smith, T., 36
Solberg, R., 128*
Sonyushkin, A. V., 20
Soppa, M. A., 86, 87
Spreen, G., 27
Steinhage, T., 42
Stettner, S., 129*
Stolpmann, L., iii
Strozzi, T., 40, 52, 54
Sudhaus, H., 52
- Tanis, C. M., 39
Teshebaeva, K., 72*
Thiel, C., 98
Thiery, W., 58
Thomalla, S. J., 88, 89
Thomas, M., 19, 44
Thonicke, K., 58
Thorpe, A., 12
Treffeisen, R., 135
Trochim, E. D., 96*
Tweedie, C., 19
- van Huissteden, Ko J., 72
Veraverbeke, S., 120*
Verdonen, M., 73*
Veremeeva, A. A., 60, 62, 74*
Virtanen, T., 115
Vonk, J. E., 84
- Vountas, M., 122
- Wagner, J., 50*
Walker, D. A., 13, 107
Walter, A., 43
Wessel, B., 37
Westermann, S., 40, 60, 71
Wetterich, S., 20
Whalen, M., iii
Whitley, M. A., 104
Widhalm, B., 40, 54, 92
Wiegmann, S., 85
Wiesmann, A., 40
Wiggins, E. B., 120
Wohlfahrt, C., 37*
Wolter, J., 60
Woods, J., 12
- Xi, H., 85
Xiao, M., 19
- Yang, X., 24
Yi, Y., 76*
Yu, Q., 102
- Zakharova, E., 59
Zelenin, E., 21
Zhang, J., 78*
Zhang, S., 24
Zimin, M. V., 20, 70
Zwieback, S., 52, 55

Picture Credits

- Titlepage and abstract wallpaper: Aurora Borealis, by Noel Bauza, pixabay.com
- “Ice Shelf” (p. 3): NASA MODIS Aqua image, Western Ross Shelf Ice on October 21, 2012.
- “Ice Berg” (p. 4): Ice berg near the Antarctic Peninsula, by Robert Ricker, <http://multimedia.awi.de/>
- “Ice Floe” (p. 5): Ice floes in the Arctic Ocean, by Mario Hoppmann, <http://multimedia.awi.de/>
- “Ice Crystal” (p. 6): Ice crystals on a lake in Fairbanks, Alaska, by Guido Grosse.
- “Polar Coasts and Deltas” (p. 15): Olenyok Delta, Siberia, Sentinel-2, July 26, 2018, by B. Juhls.
- “Floating Ice” (p. 22): Lake ice on Devil Mountain Mar Lakes, Alaska, by Guido Grosse.
- “Glaciers and Ice Sheets” (p. 33): Dzhau Khat Glacier, Central Caucasus, by Frank Günther.
- “New Sensors and Operational Services” (p. 38): International Space Station, pixabay.com
- “Permafrost State and Changes” (p. 51): Ice wedge polygons, Alaska North Slope, by F. Günther.
- “Oceanography of Polar Seas” (p. 79): Gotland, Baltic Sea, Sentinel-2, July 27, 2018, by B. Juhls.
- “Polar Lake Dynamics” (p. 91): Thermokarst lakes, Kobuk Valley, Alaska, by Guido Grosse.
- “Land Cover” (p. 97): Forest tundra margin, Tazovskiy Peninsula, West Siberia, by F. Günther.
- “Polar Atmosphere” (p. 121): LiDAR laser beam over Ny Ålesund, Svalbard, <https://blogs.helmholtz.de>
- “Snow Trends” (p. 125): Snow pit, Elbrus, Central Caucasus, by Frank Günther, AWI



Appendix

Helmholtz Climate Initiative Regional Climate Change (REKLIM) –

www.reklim.de



REKLIM

Helmholtz-Verbund
Regionale Klimaänderungen

Since October 2009 experts of nine German Centres of the Helmholtz Association, most of them in the research field “Earth and Environment”, have been working together on eight interdisciplinary research topics. In cooperation with nine university partners, the Helmholtz Centres combine their expertise in regional climate change research. Regional observations and process studies coupled with model simulations aim at improving regional and global climate models, providing a more solid basis for climate-related decision support. Hence, REKLIM is contributing to the strengthening of multidisciplinary regional climate research. More information on REKLIM: www.reklim.de/en/

The ability to project climate change on the global scale and its potential impacts under different repres-

entative concentration pathways (equivalent to future anthropogenic greenhouse gas emissions) has significantly increased in recent years. Nevertheless, one of the remaining great challenges is to understand and project the regional and local patterns of global climate change, and especially to assess societal impacts and consequences. This is what the Helmholtz Climate Initiative REKLIM (Regional Climate Change) focuses on. REKLIM is contributing to strengthen multidisciplinary regional climate research in Germany and internationally.

Among the [eight research topics](#) especially one topic focuses on the Arctic and its permafrost regions: “Regional climate change in the Arctic”. The massive and deep reaching permafrost layers contain a large reservoir of organic carbon, which could be mobilized and turned into a significant greenhouse gas source as the Arctic continues to warm. Research key questions are:

- What are the effects of climate change on the Arctic Ocean, sea ice and permafrost regions?
- What are the interactions between cryosphere, land, ocean and atmosphere?
- Can our understanding of those climate relevant processes at high latitudes be improved by advancing new technologies and methods?

Answering these questions remote sensing, field observations and modelling efforts are used. REKLIM intends to advance technologies and methods for improving observations and multi-scale work and to get new constraints, evaluation and forcing data for regional models of the Arctic region.

Furthermore, REKLIM especially focuses on two areas that are vital to modern research: knowledge transfer, and dialogue processes with society at large. In this context, the goal of knowledge transfer is to achieve an open dialogue between the scientific community and society with regard to the findings produced by REKLIM, and to provide the best available scientific evidence so that it can be used as the basis for societal actors’ decision-making processes.

Accordingly, the scientific outcomes of REKLIM will be contextualised, tailored to the needs of the respective actors, and made available in a broad range of formats, channels, instruments and activities. Special emphasis will be placed on working together with the scientific community to jointly develop and implement new ideas. Another important aspect: this process is bound to yield new research questions, which will inform and enrich the REKLIM network's own research efforts.

Moreover, REKLIM is exploring new forms of dialogue and new ways of conveying its research content. These include [multimedia](#), [interactive](#) and [filmic interpretations](#), which can help transport the issue of climate change into the day-to-day lives of the “young generation”, raise awareness for the need to take action, and make researchers' work and findings available to a broader audience in a concise and journalistic/ artistic form. As an example in this context a Social Media project, jointly organised by the Helmholtz Climate Initiative REKLIM and DEKRA University of Applied Sciences in Berlin to accompany the [International Conference on Permafrost \(ICOP\)](#)

2016 in Potsdam, was intended to promote innovative cooperation between the scientific community and students from the media sciences (Fig. 1). One week long, the students accompanied the conference and used various Social Media channels to report – in the form of interviews, background-information reports, image galleries and “Best of Day” videos – on the latest permafrost findings presented at the conference. With this Social Media project, REKLIM made a valuable contribution, by encouraging not only the public but also (and especially) the young students involved to address the topic of permafrost, and by raising awareness for the importance of regional climate changes.

Contacts:

- coordination office: [Dr Klaus Grosfeld](#)
- knowledge transfer: [Dr Renate Treffeisen](#), [Dr. Klaus Grosfeld](#)
- Topic 3: [Dr Birgit Heim](#), [Prof Torsten Sachs](#)

More information

<http://icop2016.org/media/reklim-dekra-social-media-project.html>;

<https://www.reklim.de/en/news-activities/reklim-events/social-media-projekt-auf-icop-2016/>



Figure 1: Left: In the media room of the editorial team at the ICOP-Conference (photo: Renate Treffeisen/AWI). Right: Members of the Social Media Team during an interview at the ICOP Conference (Photo: Marietta Weigelt/AWI).

References

Grosfeld, K., Lemke, P., Braesicke, P., Brauer, A., Dethloff, K., Kunz, M., Latif, M., Ratter, B. M., Sachs, T., Schmidt, H. P., Treffeisen, R. and Schwarze, R. [2016]: The Helmholtz Regional Climate Initiative REKLIM from a Polar Perspective – a Preface. *Polarforschung*, Bremerhaven, Alfred Wegener Institute for Polar and Marine Research & German Society of Polar Research, 85 (2), pp. 65–68. doi:[10.2312/polfor.2016.001](https://doi.org/10.2312/polfor.2016.001).



IEEE Geoscience and Remote Sensing Society



Fields of Interest

The fields of interest of the IEEE Geoscience and Remote Sensing Society are the theory, concepts, and techniques of science and engineering as they apply to the remote sensing of the earth, oceans, atmosphere, and space, as well as the processing, interpretation and dissemination of this information.

Interdisciplinary Nature of GRSS

Members of GRSS come from both engineering and scientific disciplinary backgrounds. Those with engineering backgrounds often support geoscientific investigations with the design and development of hardware and data processing techniques, thereby requiring of them familiarity in areas such as geophysics, geology, hydrology, meteorology, etc. Conversely, discipline scientists find in GRSS a forum for the dissemination and evaluation of remote sensing related work in these areas. This fusion of geoscientific and engineering disciplines gives GRSS a unique interdisciplinary character and an exciting role in furthering remote sensing science and technology.

History

The Society was first known as the Geoscience Electronics Group, formed in 1962. It then became the Geoscience Electronics Society in January 1978. Two years later, the name of the Society was changed to the Geoscience and Remote Sensing Society (GRSS), as it is currently known, to more accurately reflect the broad scope of its interests and activities. Since 1981 it has sponsored the highly successful International Geoscience and Remote Sensing Symposium (IGARSS) series in the USA, Canada, Europe, and Asia. This prestigious meeting has become the reference international focus of remote sensing programs

and activities, each year drawing hundreds of scientists and engineers from around the world to hear papers and discuss instruments, techniques, models and programs of global interest.

Benefits of GRSS Membership / Affiliation

Direct technical exchange with the foremost experts in the field and exposure to new programs and cutting edge technology are available to you through participation in GRSS sponsored conferences, workshops, seminars and Chapter meetings. You also have the opportunity to associate with a large, international group of people with shared interests in geoscience and remote sensing. In addition, all GRSS members have access to:

- Publications: IEEE Transaction on Geoscience and Remote Sensing, IEEE Geoscience and Remote Sensing Letters, IEEE Journal on Selected Topics on Applied Remote Sensing, the Geoscience and remote Sensing Magazine, and the GRSS e-Newsletter
- Significant price break on registration to annual IGARSS meeting
- Sizable discounts on purchase of symposium digests
- Participation in Technical Committees, local chapters, and networking opportunities...

For more information:

<http://www.grss-ieee.org/>

To join IEEE GRSS:

<https://www.ieee.org/membership/index.html>



EUMETSAT



careers.eumetsat.int

FROM HERE.

RECENT GRADUATES LAUNCH THEIR LEGACY

We know it takes the world's leading thinkers to help us develop the best ideas for the future monitoring of our planet. That is why we are always on the lookout for young, inquisitive team players with the ambition and passion to improve the world we live in and the organisation they work with.



